

ESI for:

Tin(II) Cations Stabilized by Non-symmetric N,N',O-chelating Ligands: Synthesis and Stability

Miroslav Novák,* Jan Turek,* Yaroslava Milasheuskaya, Miriam Syková, Jesse Stalmans,
Zdeňka Růžičková, Klaus Jurkschat and Roman Jambor

Table of contents:

Crystallographic data for 1 (Table S1)	S2
Crystallographic data for 2 (Table S2)	S3
Crystallographic data for 3 (Table S3)	S4
Crystallographic data for 4 (Table S4)	S5
Crystallographic data for 9 (Table S5)	S6
Crystallographic data for 10 (Table S6)	S7
Crystallographic data for 12 (Table S7)	S8
Computational details	S9-S10
Optimized geometries of the cationic part of the complexes 1 – 6 (Figure S1)	S11
Optimized geometries of 7 – 9 (Figure S2)	S12
Optimized geometries of 10 – 13 (Figure S3)	S13
Relevant NBOs involving Sn atom in 1, 7 and 10 . (Figure S4)	S14
Gibbs free energy differences for the formation of 1 – 13 (Table S8)	S15
Computed % V_{Bur} for the ligands L ^{1–6} in the cationic part of complexes 1 – 6 (Table S9)	S16
Energy decomposition analysis for 1 – 9 (Table S10)	S17
Selected Wiberg bond indices and NPA atomic charges for 1 – 13 (Table S11)	S18
Selected NBO second-order perturbation energies for 1 – 13 (Table S12)	S19
Computed FIA for cationic complexes 1⁺ – 6⁺ (Table S13)	S20
NMR spectra of studied compounds (Figures S5 – S73)	S21-S89
References	S90-S91

Table S1. Crystallographic data for **1**

Crystal data	
Chemical formula	C ₃₀ H ₃₁ ClN ₂ OPSn·Cl ₃ Sn
M _r	845.72
Crystal system, space group	Triclinic, <i>P</i> -1
Temperature (K)	150
<i>a</i> , <i>b</i> , <i>c</i> (Å)	8.6557 (5), 13.0223 (7), 16.2740 (8)
α, β, γ (°)	73.940 (2), 82.797 (2), 72.263 (2)
<i>V</i> (Å ³)	1677.28 (16)
<i>Z</i>	2
Radiation type	Mo <i>K</i> α
μ (mm ⁻¹)	1.88
Crystal size (mm)	0.59 × 0.17 × 0.12
Data collection	
Diffractometer	Bruker D8 - Venture
Absorption correction	Multi-scan <i>SADABS2016/2</i> - Bruker AXS area detector scaling and absorption correction
<i>T</i> _{min} , <i>T</i> _{max}	0.319, 0.746
No. of measured, independent and observed [<i>I</i> > 2σ(<i>I</i>)] reflections	53897, 7715, 6699
<i>R</i> _{int}	0.045
(sin θ/λ) _{max} (Å ⁻¹)	0.651
Refinement	
<i>R</i> [<i>F</i> ² > 2σ(<i>F</i> ²)], <i>wR</i> (<i>F</i> ²), <i>S</i>	0.024, 0.058, 1.07
No. of reflections	7715
No. of parameters	365
No. of restraints	330
H-atom treatment	H-atom parameters constrained
Δρ _{max} , Δρ _{min} (e Å ⁻³)	0.43, -0.86

Computer programs: Bruker Instrument Service vV6.2.3, *APEX3* v2016.5-0 (Bruker AXS), *SAINT* V8.37A (Bruker AXS Inc., 2015), *XT*, VERSION 2014/5, *SHELXL2014/7* (Sheldrick, 2014), *PLATON* (Spek, 2009).

Table S2. Crystallographic data for **2·CH₂Cl₂**

Crystal data

Chemical formula	C ₃₁ H ₃₃ ClN ₂ OPSn·Cl ₃ Sn·CH ₂ Cl ₂
M _r	944.67
Crystal system, space group	Triclinic, <i>P</i> -1
Temperature (K)	150
<i>a</i> , <i>b</i> , <i>c</i> (Å)	12.0479 (6), 12.0989 (6), 13.7729 (7)
α, β, γ (°)	87.484 (2), 68.313 (2), 78.076 (2)
<i>V</i> (Å ³)	1824.10 (16)
<i>Z</i>	2
Radiation type	Mo <i>K</i> α
μ (mm ⁻¹)	1.88
Crystal size (mm)	0.40 × 0.37 × 0.12

Data collection

Diffractometer	Bruker D8 - Venture
Absorption correction	Multi-scan <i>SADABS2016/2</i> - Bruker AXS area detector scaling and absorption correction
<i>T</i> _{min} , <i>T</i> _{max}	0.563, 0.746
No. of measured, independent and observed [<i>I</i> > 2σ(<i>I</i>)] reflections	57933, 8437, 7022
<i>R</i> _{int}	0.052
(sin θ/λ) _{max} (Å ⁻¹)	0.652

Refinement

<i>R</i> [<i>F</i> ² > 2σ(<i>F</i> ²)], <i>wR</i> (<i>F</i> ²), <i>S</i>	0.027, 0.061, 1.06
No. of reflections	8437
No. of parameters	402
No. of restraints	348
H-atom treatment	H-atom parameters constrained
Δρ _{max} , Δρ _{min} (e Å ⁻³)	0.74, -0.84

Computer programs: Bruker Instrument Service vV6.2.3, *APEX3* v2016.5-0 (Bruker AXS), *SAINT* V8.37A (Bruker AXS Inc., 2015), *XT*, VERSION 2014/5, *SHELXL2014/7* (Sheldrick, 2014), *PLATON* (Spek, 2009).

Table S3. Crystallographic data for **3**

Crystal data	
Chemical formula	C ₂₆ H ₃₁ ClN ₂ O ₂ PSn·Cl ₃ Sn
M _r	813.68
Crystal system, space group	Triclinic, <i>P</i> -1
Temperature (K)	150
<i>a</i> , <i>b</i> , <i>c</i> (Å)	8.8688 (11), 12.8162 (16), 15.329 (2)
α, β, γ (°)	76.435 (6), 85.256 (6), 73.499 (6)
<i>V</i> (Å ³)	1623.8 (4)
<i>Z</i>	2
Radiation type	Mo <i>K</i> α
μ (mm ⁻¹)	1.94
Crystal size (mm)	0.59 × 0.23 × 0.04
Data collection	
Diffractometer	Bruker D8 - Venture
Absorption correction	Multi-scan <i>SADABS2016/2</i> - Bruker AXS area detector scaling and absorption correction
<i>T</i> _{min} , <i>T</i> _{max}	0.554, 0.746
No. of measured, independent and observed [<i>I</i> > 2σ(<i>I</i>)] reflections	27085, 6239, 4883
<i>R</i> _{int}	0.068
(sin θ/λ) _{max} (Å ⁻¹)	0.617
Refinement	
<i>R</i> [<i>F</i> ² > 2σ(<i>F</i> ²)], <i>wR</i> (<i>F</i> ²), <i>S</i>	0.067, 0.159, 1.15
No. of reflections	6239
No. of parameters	342
No. of restraints	312
H-atom treatment	H-atom parameters constrained <i>w</i> = 1/[σ ² (<i>F</i> _o ²) + 30.0796 <i>P</i>] where <i>P</i> = (<i>F</i> _o ² + 2 <i>F</i> _c ²)/3
Δρ _{max} , Δρ _{min} (e Å ⁻³)	1.30, -1.33

Computer programs: Bruker Instrument Service vV6.2.3, *APEX3* v2016.5-0 (Bruker AXS), *SAINT* V8.37A (Bruker AXS Inc., 2015), *XT, VERSION 2014/5*, *SHELXL2014/7* (Sheldrick, 2014), *PLATON* (Spek, 2009).

Table S4. Crystallographic data for **4·CH₂Cl₂**

Crystal data	
Chemical formula	C ₂₇ H ₃₃ ClN ₂ O ₂ PSn·Cl ₃ Sn·CH ₂ Cl ₂
M _r	912.63
Crystal system, space group	Triclinic, <i>P</i> -1
Temperature (K)	150
<i>a</i> , <i>b</i> , <i>c</i> (Å)	8.6259 (4), 12.4009 (5), 17.2050 (8)
α, β, γ (°)	81.057 (2), 86.640 (2), 75.835 (2)
<i>V</i> (Å ³)	1762.34 (14)
<i>Z</i>	2
Radiation type	Mo <i>K</i> α
μ (mm ⁻¹)	1.95
Crystal size (mm)	0.35 × 0.27 × 0.04
Data collection	
Diffractometer	Bruker D8 - Venture
Absorption correction	Multi-scan <i>SADABS2016/2</i> - Bruker AXS area detector scaling and absorption correction
<i>T</i> _{min} , <i>T</i> _{max}	0.542, 0.747
No. of measured, independent and observed [<i>I</i> > 2σ(<i>I</i>)] reflections	54631, 6208, 5317
<i>R</i> _{int}	0.250
(sin θ/λ) _{max} (Å ⁻¹)	0.594
Refinement	
<i>R</i> [<i>F</i> ² > 2σ(<i>F</i> ²)], <i>wR</i> (<i>F</i> ²), <i>S</i>	0.052, 0.141, 1.06
No. of reflections	6208
No. of parameters	376
No. of restraints	318
H-atom treatment	H-atom parameters constrained
Δρ _{max} , Δρ _{min} (e Å ⁻³)	1.98, -2.34

Computer programs: Bruker Instrument Service vV6.2.3, *APEX3* v2016.5-0 (Bruker AXS), *SAINT* V8.37A (Bruker AXS Inc., 2015), *XT*, VERSION 2014/5, *SHELXL2014/7* (Sheldrick, 2014), *PLATON* (Spek, 2009).

Table S5. Crystallographic data for **9**

Crystal data	
Chemical formula	C ₂₆ H ₃₉ F ₃ N ₂ O ₇ PSSn·CF ₃ O ₃ S
M _r	922.47
Crystal system, space group	Orthorhombic, <i>Pbcn</i>
Temperature (K)	150
<i>a</i> , <i>b</i> , <i>c</i> (Å)	24.7026 (10), 16.5078 (6), 18.7687 (7)
<i>V</i> (Å ³)	7653.6 (5)
<i>Z</i>	8
Radiation type	Mo <i>Kα</i>
μ (mm ⁻¹)	0.90
Crystal size (mm)	0.35 × 0.22 × 0.18
Data collection	
Diffractometer	Bruker D8 - Venture
Absorption correction	Multi-scan <i>SADABS2016/2</i> - Bruker AXS area detector scaling and absorption correction
<i>T</i> _{min} , <i>T</i> _{max}	0.660, 0.746
No. of measured, independent and observed [<i>I</i> > 2σ(<i>I</i>)] reflections	50179, 6731, 4755
<i>R</i> _{int}	0.117
(sin θ/λ) _{max} (Å ⁻¹)	0.595
Refinement	
<i>R</i> [<i>F</i> ² > 2σ(<i>F</i> ²)], <i>wR</i> (<i>F</i> ²), <i>S</i>	0.039, 0.089, 1.05
No. of reflections	6731
No. of parameters	458
No. of restraints	398
H-atom treatment	H atoms treated by a mixture of independent and constrained refinement
Δρ _{max} , Δρ _{min} (e Å ⁻³)	0.50, -0.46

Computer programs: Bruker Instrument Service vV6.2.3, *APEX3* v2016.5-0 (Bruker AXS), *SAINT* V8.37A (Bruker AXS Inc., 2015), *XT*, VERSION 2014/5, *SHELXL2014/7* (Sheldrick, 2014), *PLATON* (Spek, 2009).

Table S6. Crystallographic data for **10·0.5C₇H₈**

Crystal data	
Chemical formula	2(C ₂₄ H ₂₆ Cl ₃ N ₂ O ₂ PSn ₂)·C ₇ H ₈
M_r	1590.47
Crystal system, space group	Triclinic, <i>P</i> -1
Temperature (K)	150
<i>a</i> , <i>b</i> , <i>c</i> (Å)	13.2768 (4), 15.5938 (6), 15.9485 (6)
α , β , γ (°)	85.119 (2), 79.741 (1), 77.525 (1)
<i>V</i> (Å ³)	3168.7 (2)
<i>Z</i>	2
Radiation type	Mo <i>K</i> α
μ (mm ⁻¹)	1.91
Crystal size (mm)	0.39 × 0.26 × 0.16
Data collection	
Diffractometer	Bruker D8 - Venture
Absorption correction	Multi-scan <i>SADABS2016/2</i> - Bruker AXS area detector scaling and absorption correction
<i>T</i> _{min} , <i>T</i> _{max}	0.505, 0.746
No. of measured, independent and observed [<i>I</i> > 2σ(<i>I</i>)] reflections	112517, 14671, 12036
<i>R</i> _{int}	0.059
(sin θ/λ) _{max} (Å ⁻¹)	0.652
Refinement	
<i>R</i> [<i>F</i> ² > 2σ(<i>F</i> ²)], <i>wR</i> (<i>F</i> ²), <i>S</i>	0.026, 0.051, 1.05
No. of reflections	14671
No. of parameters	685
No. of restraints	627
H-atom treatment	H-atom parameters constrained
Δρ _{max} , Δρ _{min} (e Å ⁻³)	0.52, -0.59

Computer programs: Bruker Instrument Service vV6.2.3, *APEX3* v2016.5-0 (Bruker AXS), *SAINT* V8.37A (Bruker AXS Inc., 2015), *XT*, VERSION 2014/5, *SHELXL2014/7* (Sheldrick, 2014), *PLATON* (Spek, 2009).

Table S7. Crystallographic data for **12·CH₂Cl₂**

Crystal data	
Chemical formula	C ₂₁ H ₂₈ Cl ₃ N ₂ O ₃ PSn ₂ ·CH ₂ Cl ₂
M _r	816.08
Crystal system, space group	Triclinic, <i>P</i> -1
Temperature (K)	150
<i>a</i> , <i>b</i> , <i>c</i> (Å)	8.9021 (5), 12.8588 (5), 13.7649 (5)
α, β, γ (°)	91.567 (2), 97.803 (1), 108.514 (2)
<i>V</i> (Å ³)	1476.12 (12)
<i>Z</i>	2
Radiation type	Mo <i>K</i> α
μ (mm ⁻¹)	2.23
Crystal size (mm)	0.41 × 0.15 × 0.05
Data collection	
Diffractometer	Bruker D8 - Venture
Absorption correction	Multi-scan <i>SADABS2016/2</i> - Bruker AXS area detector scaling and absorption correction
<i>T</i> _{min} , <i>T</i> _{max}	0.541, 0.746
No. of measured, independent and observed [<i>I</i> > 2σ(<i>I</i>)] reflections	47685, 6807, 5192
<i>R</i> _{int}	0.080
(sin θ/λ) _{max} (Å ⁻¹)	0.652
Refinement	
<i>R</i> [<i>F</i> ² > 2σ(<i>F</i> ²)], <i>wR</i> (<i>F</i> ²), <i>S</i>	0.050, 0.144, 1.01
No. of reflections	6807
No. of parameters	342
No. of restraints	322
H-atom treatment	H-atom parameters constrained
Δρ _{max} , Δρ _{min} (e Å ⁻³)	1.26, -2.19

Computer programs: Bruker Instrument Service vV6.2.3, *APEX3* v2016.5-0 (Bruker AXS), *SAINT* V8.37A (Bruker AXS Inc., 2015), XT, VERSION 2014/5, *SHELXL2014/7* (Sheldrick, 2014), *PLATON* (Spek, 2009).

Computational details

All calculations were carried out by using DFT as implemented in the Gaussian16 quantum chemistry program.^[S1] Geometry optimizations were performed at the M06-2X^[S2]/cc-pVDZ^[S3] level of theory (cc-pVDZ-PP^[S4] basis set including small-core relativistic pseudopotentials that account also for relativistic effects was used for Ga and Ge). The electronic energies of the optimized structures were re-evaluated by additional single-point calculations on each of the optimized geometries by using the triple- ζ quality cc-pVTZ(-PP) basis set.^[S3,S4] Analytical vibrational frequencies within the harmonic approximation were computed with the cc-pVDZ(-PP) basis set to confirm a proper convergence to well-defined minima or saddle points on the potential energy surface. The Gibbs free energies G^{solv} (cc-pVTZ) used to calculate the energy differences reported in this article were computed by using Equations (1) – (4)

$$G^{\text{solv}}(\text{cc-pVTZ}) = G(\text{cc-pVTZ}) + \text{SC} \quad (1)$$

$$G(\text{cc-pVTZ}) = E(\text{cc-pVTZ}) + \text{TC} \quad (2)$$

$$\text{TC} = G(\text{cc-pVDZ}) - E(\text{cc-pVDZ}) \quad (3)$$

$$\text{SC} = E^{\text{solv}}(\text{cc-pVDZ}) - E(\text{cc-pVDZ}) \quad (4)$$

in which $E(x)$ is the self-consistent field electronic energy derived from the cc-pVDZ or cc-pVTZ basis sets, TC is the thermal correction to the energy calculated with the cc-pVDZ basis set, $G(\text{cc-pVDZ})$ is the free energy at 298.15 K for the double- ζ quality basis set, and SC is the solvent correction for $E^{\text{solv}}(\text{cc-pVDZ})$, which is the self-consistent field energy in the implicit Solvation Model based on Density (SMD)^[S5] using tetrahydrofuran ($\epsilon = 7.4257$) as solvent, calculated with the cc-pVDZ basis set.

The natural bond orbital (NBO) analysis^[S6] and calculations of the Wiberg bond indices^[S7] were performed using NBO 7.0 program^[S8] package at the M06-2X^[S2]/cc-pVTZ(-PP)^[S3,S4] level of theory.

The Ziegler-Rauk energy decomposition analysis^[S9] was carried out on the optimized structures at the ZORA^[S10]/M06-2X^[S2]/TZ2P^[S11] level of theory using Amsterdam Modeling Suite (AMS2020; ADF engine).^[S12] The interaction energy ΔE_{int} between two fragments can be decomposed into physically meaningful terms within Kohn–Sham MO theory [Equation (5)],

$$\Delta E_{\text{int}} = \Delta E_{\text{Pauli}} + \Delta V_{\text{elst}} + \Delta E_{\text{oi}} \quad (5)$$

where ΔE_{Pauli} , ΔV_{elst} , and ΔE_{oi} are the Pauli repulsion, electrostatic interaction, and orbital interaction between fragments, respectively. The Pauli repulsion is the result of the steric repulsion between fragments, caused by the destabilizing interaction between electrons with identical spin. ΔV_{elst} represents the quasi-classical electrostatic interaction between the unperturbed charge distributions of the two fragments. The ΔE_{oi} term originates from orbital interactions, charge transfer, and polarization.

The web application SambVca 2.1^[S13] was used to calculate the percentage buried volume (% V_{Bur}), which quantifies the fraction of the first coordination sphere around the metal centre occupied by the ligand.

Fluoride ion affinities (FIAs) were calculated at the PW6B95-D3BJ^[S14]/def2-QZVPP^[S15] level of theory according to the procedure suggested by Greb using the TMS-system as an anchor point for the FIA computations *via* (pseudo-)isodesmic reactions.^[S16]

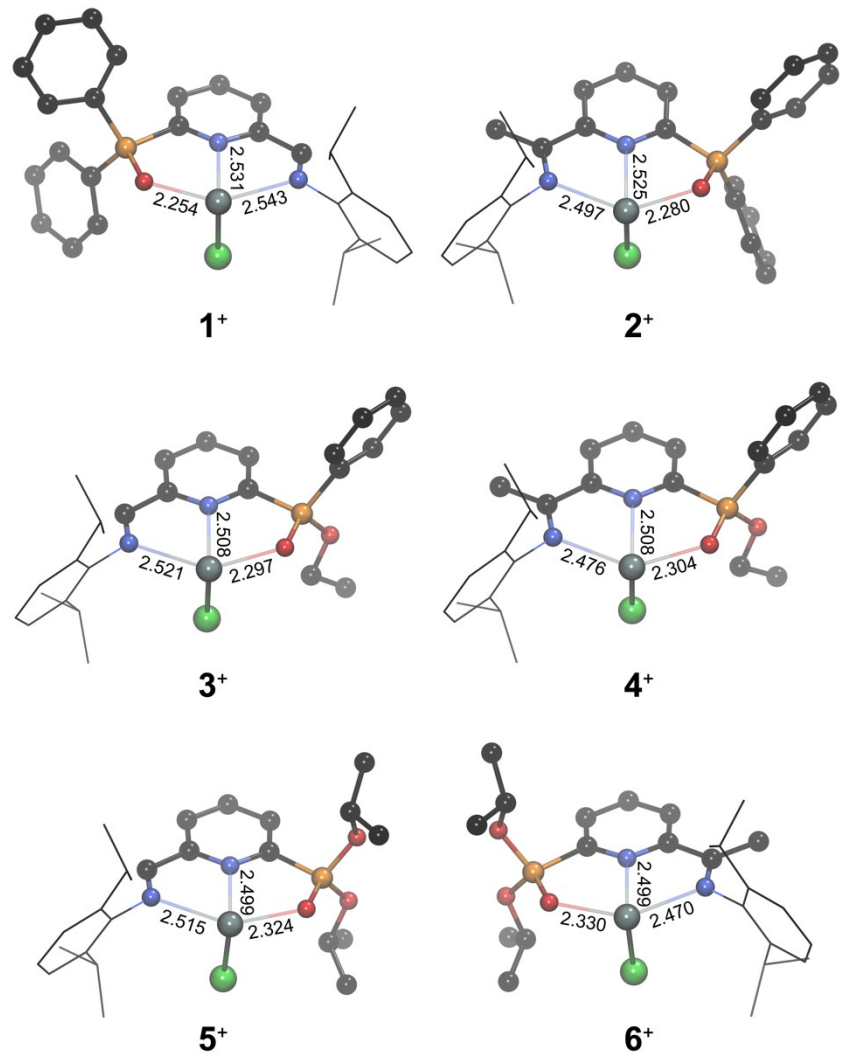


Figure S1. Optimized geometries of the cationic part of the complexes **1 – 6** along with selected interatomic distances (in Å). Hydrogen atoms are omitted for clarity.

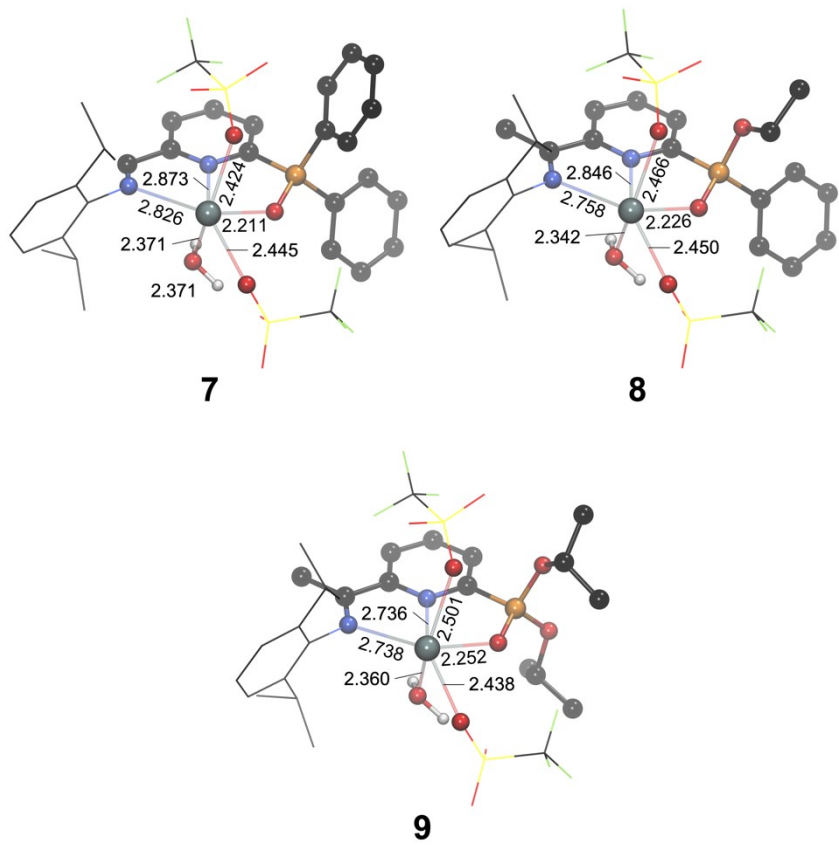


Figure S2. Optimized geometries of **7 – 9** along with selected interatomic distances (in Å).
Hydrogen atoms are omitted for clarity.

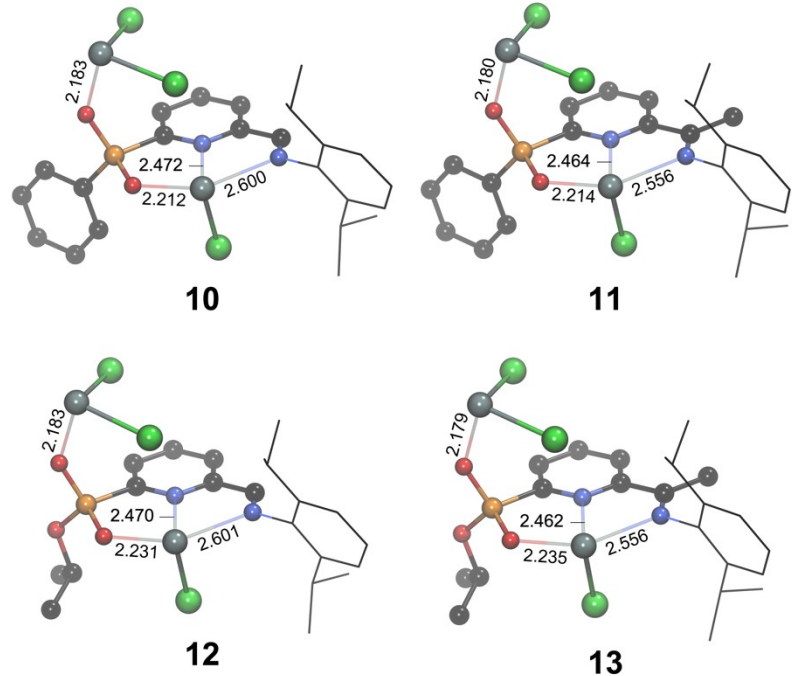


Figure S3. Optimized geometries of **10 – 13** along with selected interatomic distances (in Å).
Hydrogen atoms are omitted for clarity.

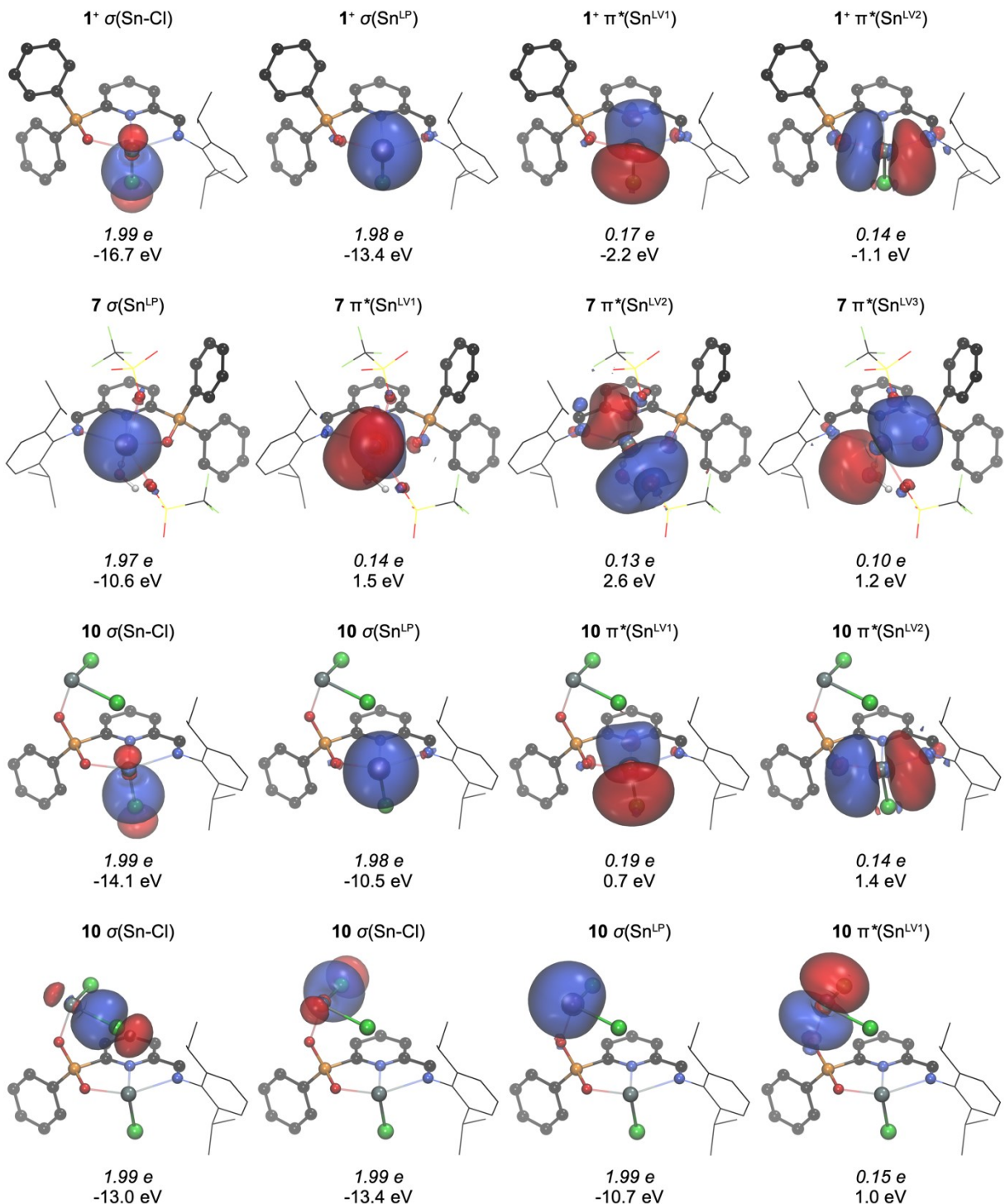


Figure S4. Relevant NBOs (isosurface 0.03 a.u.) involving Sn atom in **1**, **7** and **10**. NBO populations and orbital energies are also displayed.

Table S8. Gibbs free energy differences (ΔG ; in kcal mol⁻¹) for the formation of **1 – 13**.

	$\Delta G(\text{DZ})^{[\text{a}]}$	$\Delta G(\text{TZ})^{[\text{b}]}$	$\Delta G^{\text{solv}}(\text{TZ})^{[\text{c}]}$
$\text{L}^1 + 2 \text{SnCl}_2 \rightarrow [\text{L}^1\text{SnCl}][\text{SnCl}_3]$ (1)	24.9	22.5	-31.5
$\text{L}^2 + 2 \text{SnCl}_2 \rightarrow [\text{L}^2\text{SnCl}][\text{SnCl}_3]$ (2)	24.1	21.9	-31.5
$\text{L}^3 + 2 \text{SnCl}_2 \rightarrow [\text{L}^3\text{SnCl}][\text{SnCl}_3]$ (3)	26.0	23.7	-29.8
$\text{L}^4 + 2 \text{SnCl}_2 \rightarrow [\text{L}^4\text{SnCl}][\text{SnCl}_3]$ (4)	23.6	21.2	-31.4
$\text{L}^5 + 2 \text{SnCl}_2 \rightarrow [\text{L}^5\text{SnCl}][\text{SnCl}_3]$ (5)	27.5	24.7	-29.9
$\text{L}^6 + 2 \text{SnCl}_2 \rightarrow [\text{L}^6\text{SnCl}][\text{SnCl}_3]$ (6)	25.1	22.4	-31.4
$\text{L}^1 + \text{Sn(OTf)}_2 + \text{H}_2\text{O} \rightarrow [\text{L}^1\text{Sn}(\text{H}_2\text{O})][\text{OTf}]_2$ (7)	-33.8	-30.4	-27.8
$\text{L}^4 + \text{Sn(OTf)}_2 + \text{H}_2\text{O} \rightarrow [\text{L}^4\text{Sn}(\text{H}_2\text{O})][\text{OTf}]_2$ (8)	-37.0	-33.1	-28.8
$\text{L}^6 + \text{Sn(OTf)}_2 + \text{H}_2\text{O} \rightarrow [\text{L}^6\text{Sn}(\text{H}_2\text{O})][\text{OTf}]_2$ (9)	-38.1	-34.2	-29.8
$[\text{L}^3\text{SnCl}][\text{SnCl}_3]$ (3) $\rightarrow \text{10} + \text{EtCl}$	-78.3	-85.0	-19.1
$[\text{L}^4\text{SnCl}][\text{SnCl}_3]$ (4) $\rightarrow \text{11} + \text{EtCl}$	-77.3	-84.1	-19.0
$[\text{L}^5\text{SnCl}][\text{SnCl}_3]$ (5) $\rightarrow \text{12} + \text{iPrCl}$	-79.1	-85.6	-19.3
$[\text{L}^6\text{SnCl}][\text{SnCl}_3]$ (6) $\rightarrow \text{10} + \text{iPrCl}$	-78.5	-84.9	-19.4

^[a]Calculated at the M06-2X/cc-pVDZ-PP level of theory; ^[b]Calculated at the M06-2X /cc-pVTZ-PP level of theory; ^[c]Calculated at the M06-2X /cc-pVTZ-PP level of theory in THF.

Table S9. Computed $\%V_{\text{Bur}}$ for the ligands L^{1-6} in the cationic part of complexes **1 – 6**.

	1⁺	2⁺	3⁺	4⁺	5⁺	6⁺
$\%V_{\text{Bur}}$	41.5	43.7	42	43.5	42.5	44.1

Table S10. Energy decomposition analysis (EDA) for **1 – 9**. (All energies are in kcal mol⁻¹).^[a]

	ΔE_{int}	ΔE_{Pauli}	ΔE_{oi}	ΔV_{elstat}
1^[b]	-124.3	128.1	-104.6 (41)	-147.8 (59)
2^[b]	-125.9	130.9	-105.9 (41)	-150.8 (59)
3^[b]	-119.5	125.9	-101.5 (41)	-143.9 (59)
4^[b]	-123.0	130.7	-105.2 (41)	-148.4 (59)
5^[b]	-116.2	123.7	-99.7 (42)	-140.1 (58)
6^[b]	-119.3	128.6	-103.1 (42)	-144.8 (58)
7^[c]	-93.0	114.0	-77.8 (38)	-129.2 (62)
8^[c]	-94.3	115.1	-77.7 (37)	-131.7 (63)
9^[c]	-91.2	116.3	-76.7 (37)	-130.8 (63)

^[a]Values written in parentheses represent the relative contribution (in %) of the orbital interaction energy and the electrostatic energy with respect to the total stabilization component of the interaction energy;

^[b][L^{1–6}] and [SnCl]⁺ fragments; ^[c][L^{1,4,6}] and [Sn(H₂O)(OTf)₂] fragments.

Table S11. Selected Wiberg bond indices (WBI) and NPA atomic charges (q ; in e) for **1 – 13**.

	WBI _{O-Sn}	WBI _{N(Im)-Sn}	WBI _{N(Py)-Sn}	WBI _{P-O}	q_{Sn}	q_{P}	q_{O}
1⁺	0.194	0.141	0.159	0.974	1.39	1.94	-1.18
2⁺	0.188	0.147	0.156	0.983	1.38	1.94	-1.18
3⁺	0.174	0.147	0.165	1.022 0.775 ^[d]	1.39	2.21	-1.17 -0.83 ^[f]
4⁺	0.172	0.152	0.161	1.026 0.774 ^[d]	1.39	2.21	-1.17 -0.84 ^[f]
5⁺	0.161	0.149	0.166	1.031 0.788 ^[e] 0.803 ^[e]	1.39	2.46	-1.18 -0.84 ^[g] -0.84 ^[g]
6⁺	0.159	0.153	0.162	1.035 0.784 ^[e] 0.802 ^[e]	1.39	2.45	-1.18 -0.84 ^[g] -0.84 ^[g]
7	0.163 0.127 ^[a] 0.108 ^[b] 0.116 ^[b]	0.071	0.065	0.953	1.64	1.97	-1.22 -1.03 ^[h] -1.10 ^[i] -1.06 ^[i]
8	0.157 0.130 ^[a] 0.105 ^[b] 0.115 ^[b]	0.076	0.070	0.989 0.765 ^[d]	1.64	2.24	-1.21 -0.84 ^[f] -1.04 ^[h] -1.10 ^[i] -1.05 ^[i]
9	0.147 0.124 ^[a] 0.099 ^[b] 0.117 ^[b]	0.076	0.082	1.002 0.750 ^[e] 0.804 ^[e]	1.64	2.48	-1.21 -0.85 ^[g] -0.85 ^[g] -1.04 ^[h] -1.09 ^[i] -1.06 ^[i]
10	0.202 0.244 ^[c]	0.118	0.166	0.953 0.912	1.40 1.28	2.23	-1.20 -1.21
11	0.201 0.245 ^[c]	0.120	0.166	0.955 0.909	1.40 1.28	2.23	-1.20 -1.21
12	0.190 0.241 ^[c]	0.118	0.163	0.961 0.942 0.745 ^[e]	1.40 1.29	2.47	-1.21 -1.20 -0.84 ^[g]
13	0.188 0.243 ^[c]	0.120	0.163	0.965 0.939 0.743 ^[e]	1.41 1.29	2.47	-1.21 -1.20 -0.84 ^[g]

^[a]O^{H2O}→Sn bond; ^[b]O^{OTf}→Sn bond; ^[c]O→SnCl₂ bond; ^[d]P–O^{OEt} bond; ^[e]P–O^{OiPr} bond; ^[f]O^{OEt} atom;
^[g]O^{OiPr} atom; ^[h]O^{H2O} atom; ^[i]O^{OTf} atom.

Table S12. Selected NBO second-order perturbation energies ($E^{(2)}$; in kcal mol⁻¹) for **1 – 13**.

$E^{(2)}$	O→Sn ^[a]	N(Im)→Sn ^[b]	N(Py)→Sn ^[c]	O→P ^[d]
1⁺	62.6	31.7	39.1	52.3
2⁺	59.1	34.3	39.1	51.5
3⁺	58.6	34.2	40.7	58.5
4⁺	57.4	36.3	40.2	59.3
5⁺	52.8	34.9	41.0	63.3
6⁺	51.7	36.8	40.4	63.7
7	59.3 33.4 ^[e] 35.9 ^[f] 31.2 ^[f]	14.8	15.5	48.9
8	57.0 35.2 ^[e] 35.9 ^[f] 30.2 ^[f]	16.1	16.9	56.2
9	52.7 34.0 ^[e] 36.1 ^[f] 29.2 ^[f]	16.2	20.0	60.6
10	70.1 81.3 ^[g]	26.2	43.5	50.9 46.3
11	70.0 81.8 ^[g]	27.4	44.0	51.2 46.0
12	66.7 82.4 ^[g]	26.3	43.0	54.7 50.2
13	65.7 83.3 ^[g]	27.5	43.3	55.3 50.0

^[a]n_O→π*_{Sn} interaction; ^[b]n_{N(Imine)}→π*_{Sn}; ^[c]n_{N(Pyridine)}→π*_{Sn}; ^[d]n_O→σ*_{P-R} ^[e]O^{H2O}→Sn bond; ^[f]O^{OTf}→Sn bond;
^[g]O→SnCl₂ bond.

Table S13. Computed FIA (in kJ mol⁻¹) for cationic complexes **1**⁺ – **6**⁺ along with the FIA value of SbF₅ as a reference.

	1 ⁺	2 ⁺	3 ⁺	4 ⁺	5 ⁺	6 ⁺	SbF₅
FIA ^[a]	536	535	555	546	563	551	496

^[a]calculated at the M06-2X/cc-pVDZ-PP//PW6B95-D3BJ/def2-QZVPP level of theory.

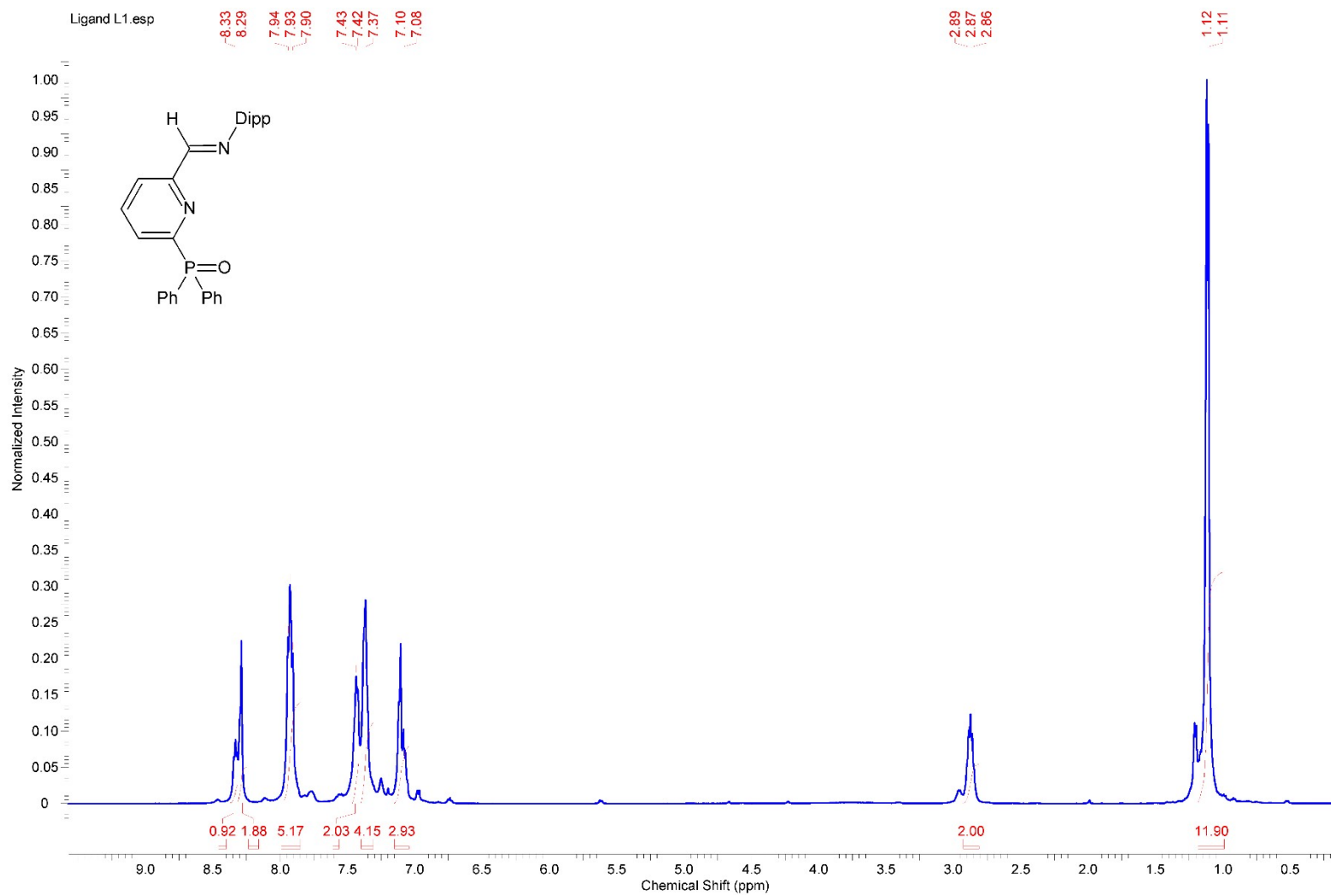


Figure S5. ^1H NMR spectrum of \mathbf{L}^1 in CDCl_3

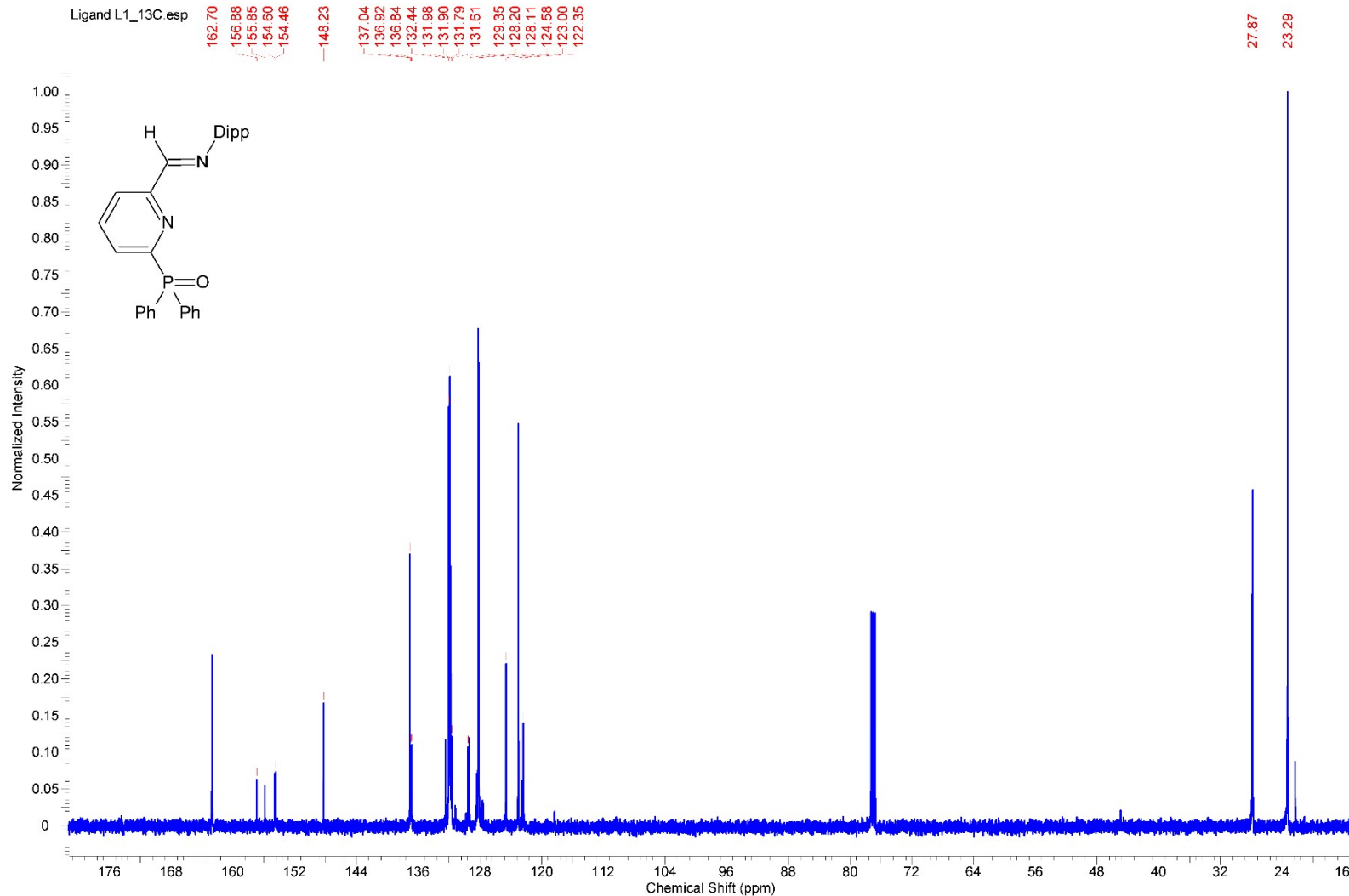


Figure S6. $^{13}\text{C}\{^1\text{H}\}$ NMR spectrum of **L¹** in CDCl_3

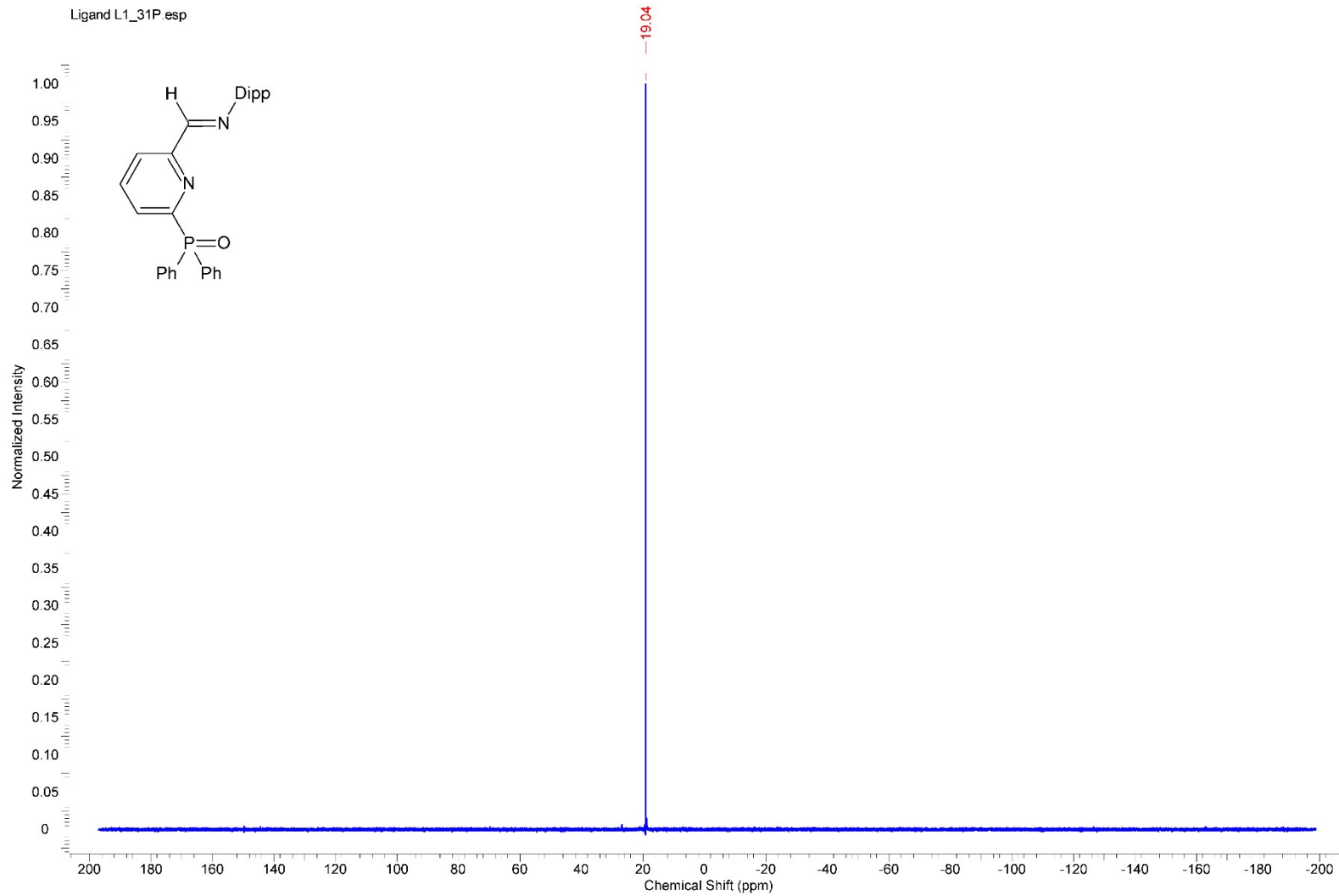


Figure S7. ^{31}P NMR spectrum of \mathbf{L}^1 in CDCl_3

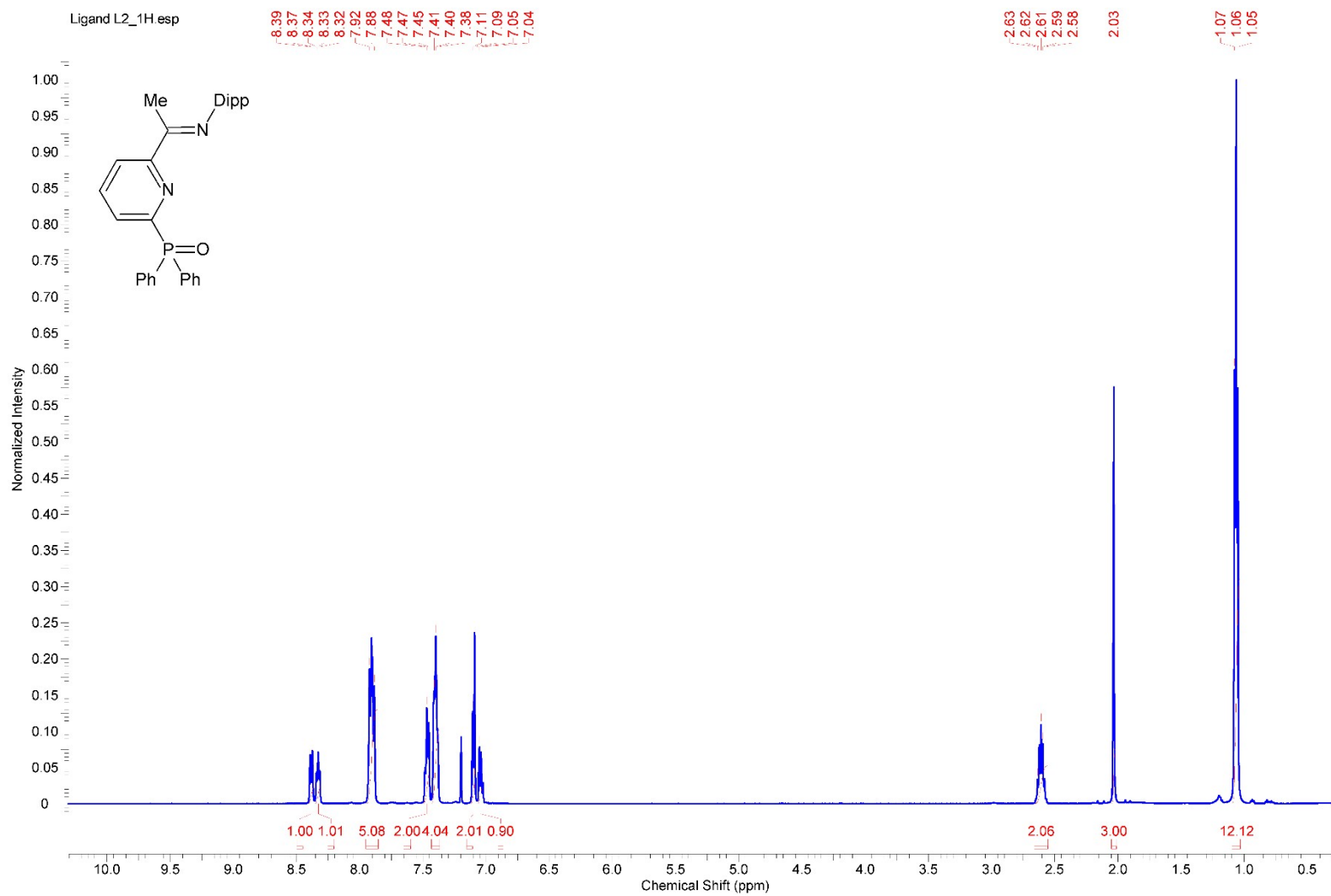


Figure S8. ^1H NMR spectrum of L^2 in CDCl_3

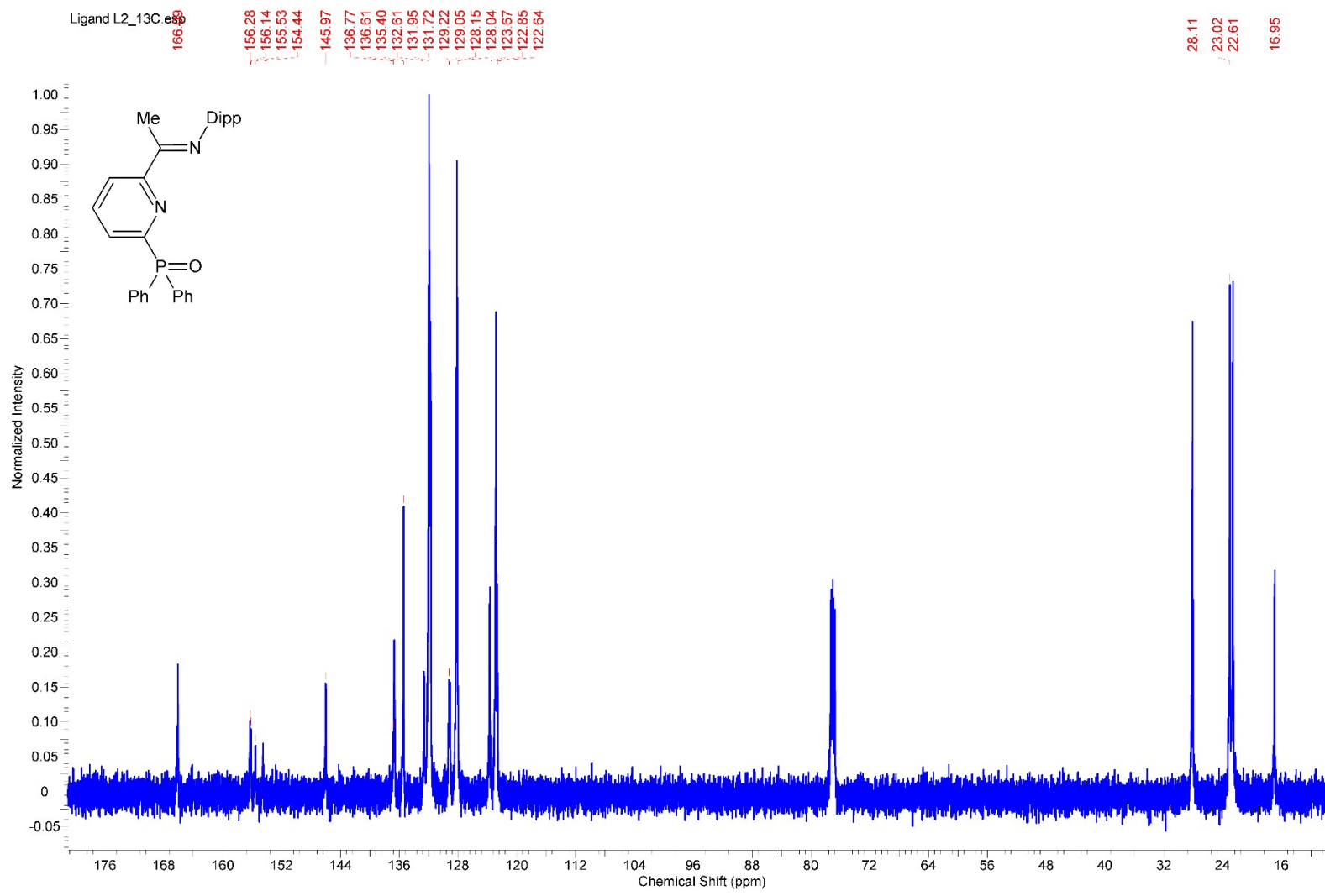


Figure S9. $^{13}\text{C}\{^1\text{H}\}$ NMR spectrum of \mathbf{L}^2 in CDCl_3

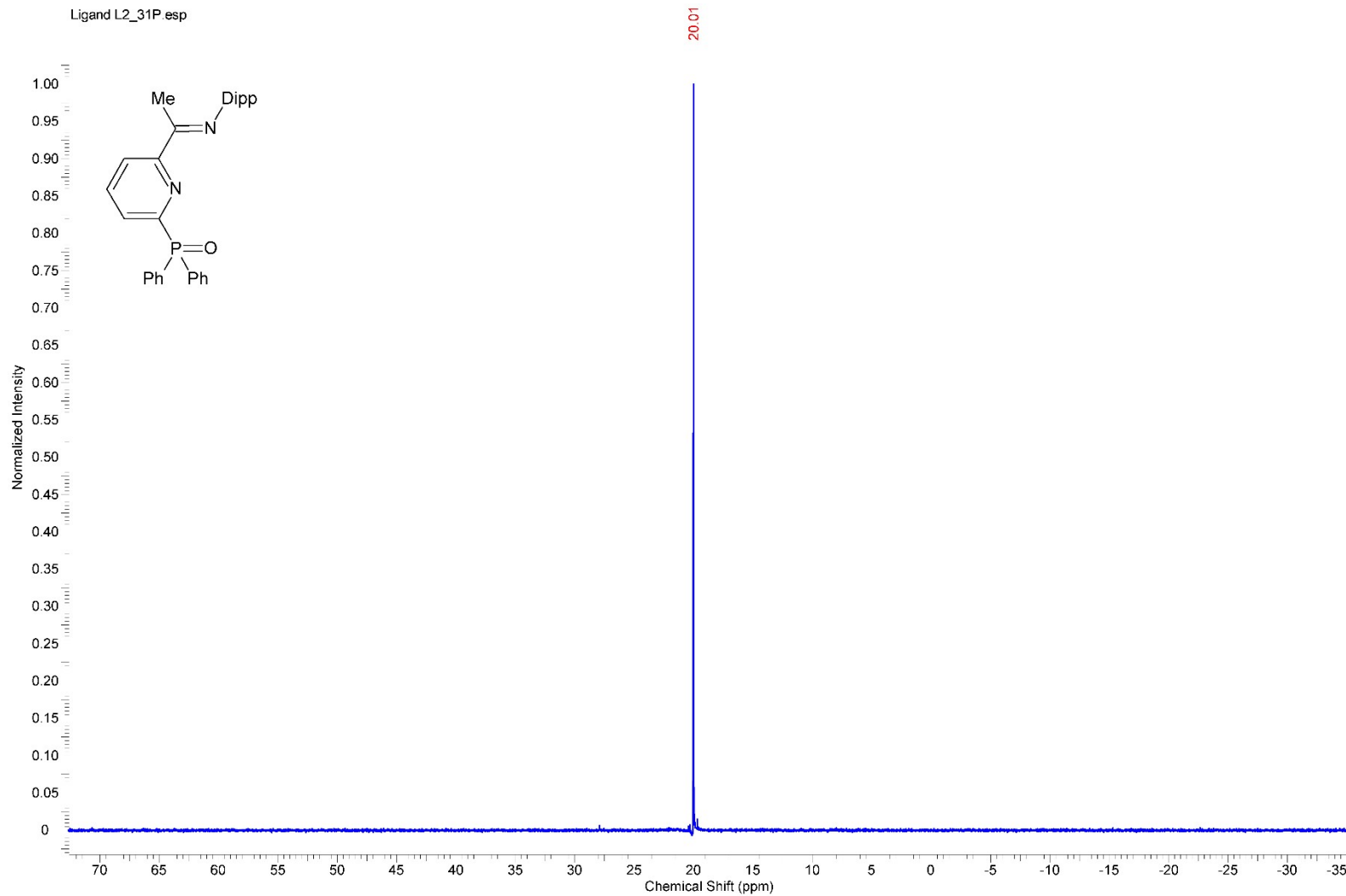


Figure S10. ^{31}P NMR spectrum of \mathbf{L}^2 in CDCl_3

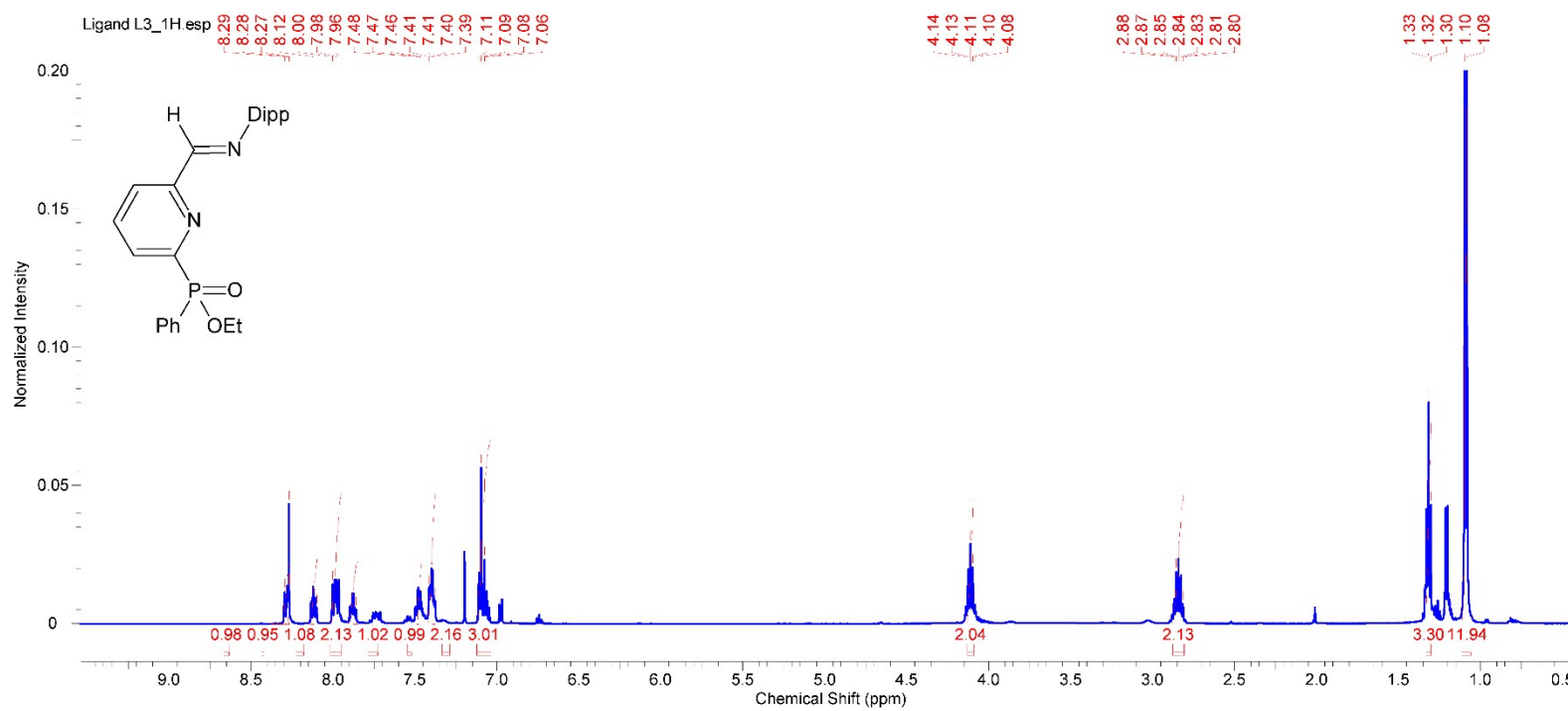


Figure S11. ^1H NMR spectrum of L^3 in CDCl_3

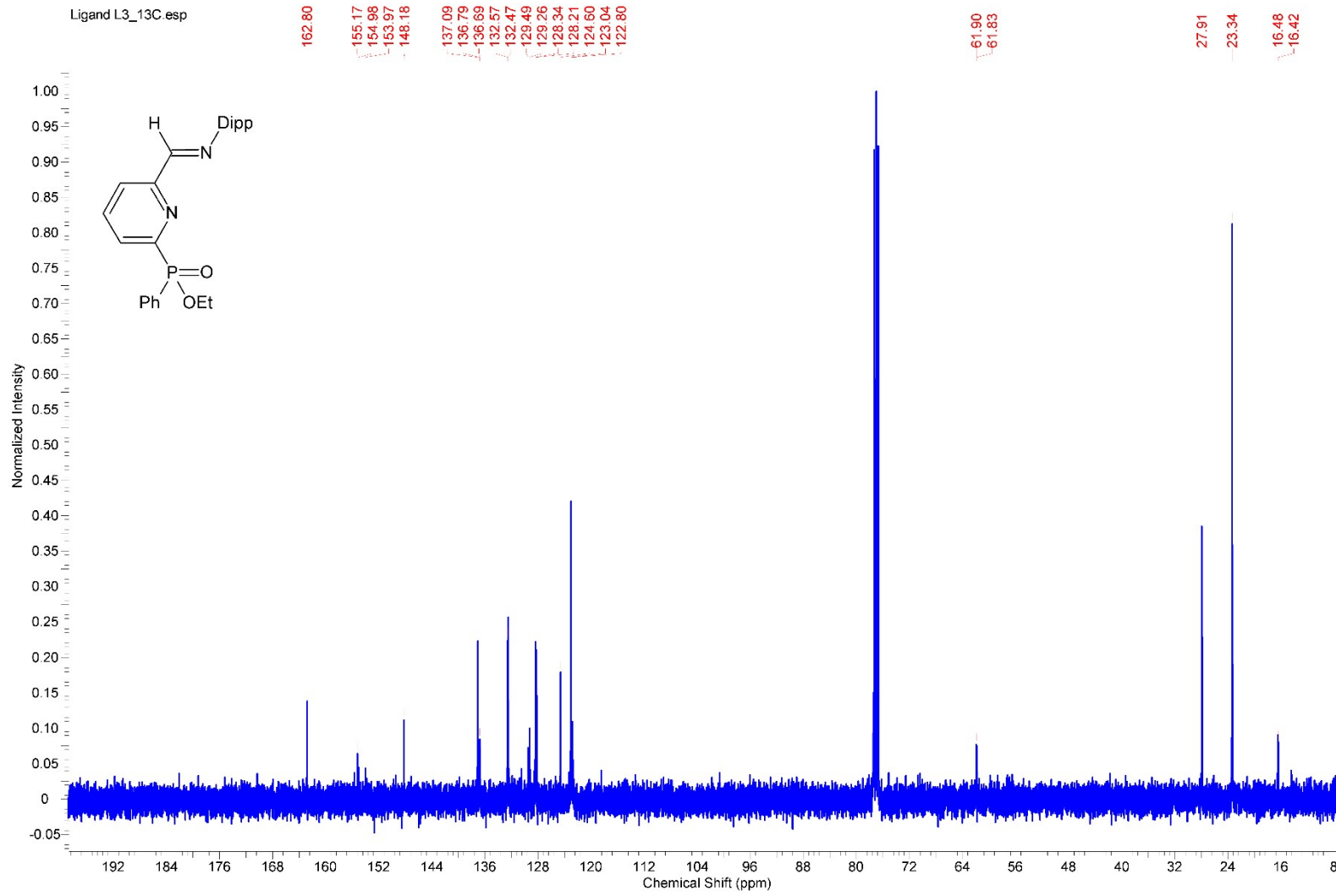


Figure S12. $^{13}\text{C}\{^1\text{H}\}$ NMR spectrum of L^3 in CDCl_3

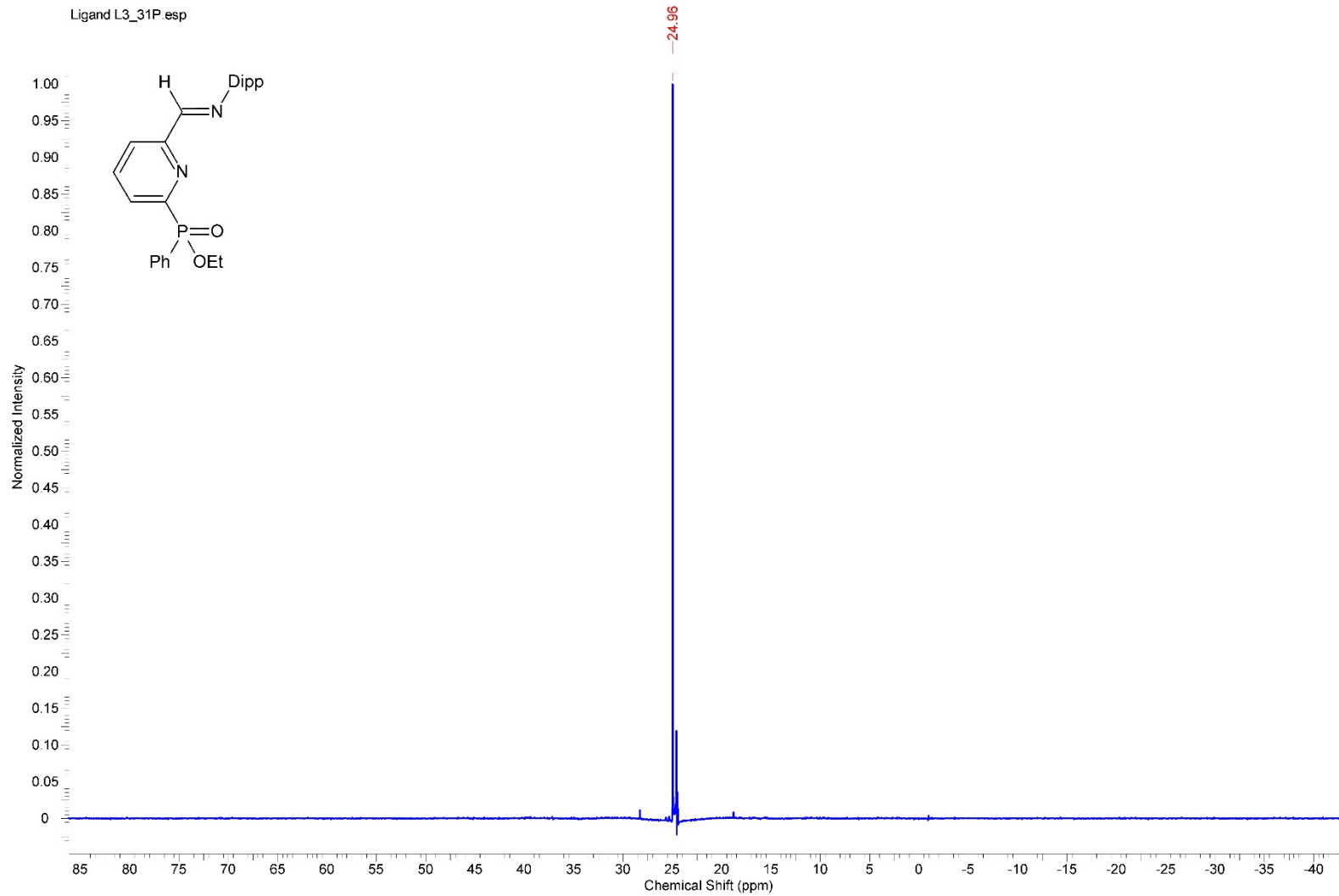


Figure S13. ^{31}P NMR spectrum of L^3 in CDCl_3

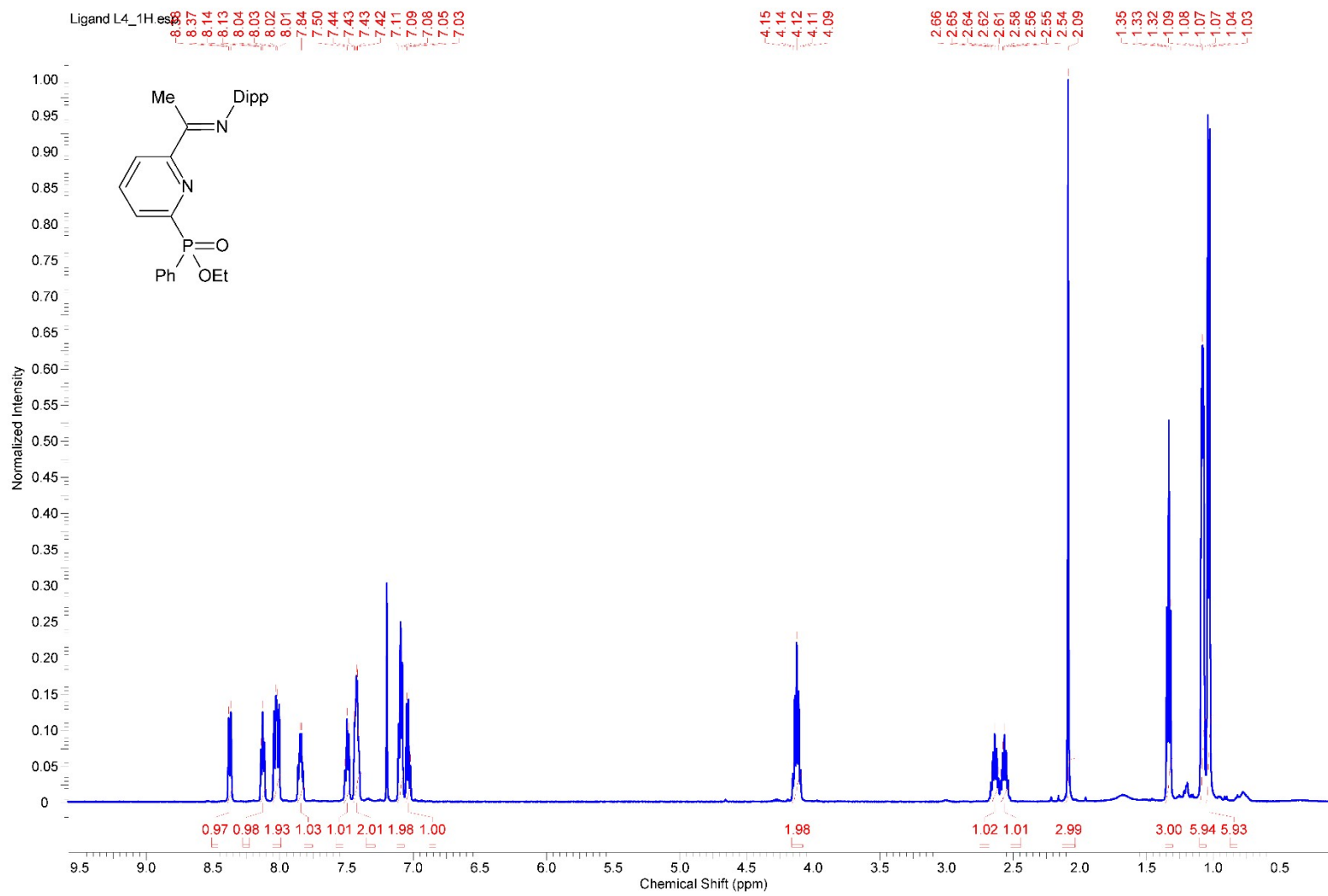


Figure S14. ^1H NMR spectrum of L⁴ in CDCl_3

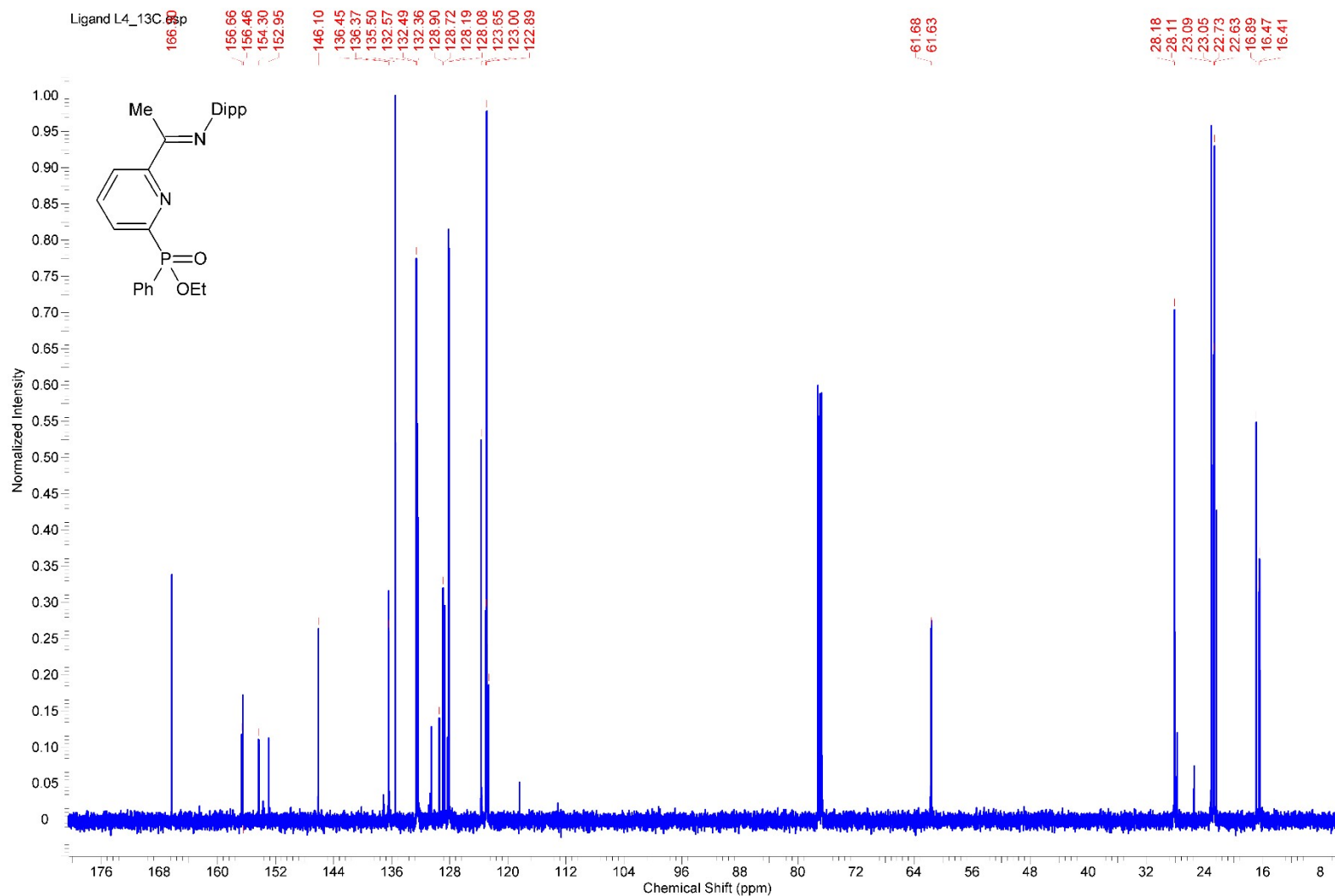


Figure S15. $^{13}\text{C}\{\text{H}\}$ NMR spectrum of \mathbf{L}^4 in CDCl_3

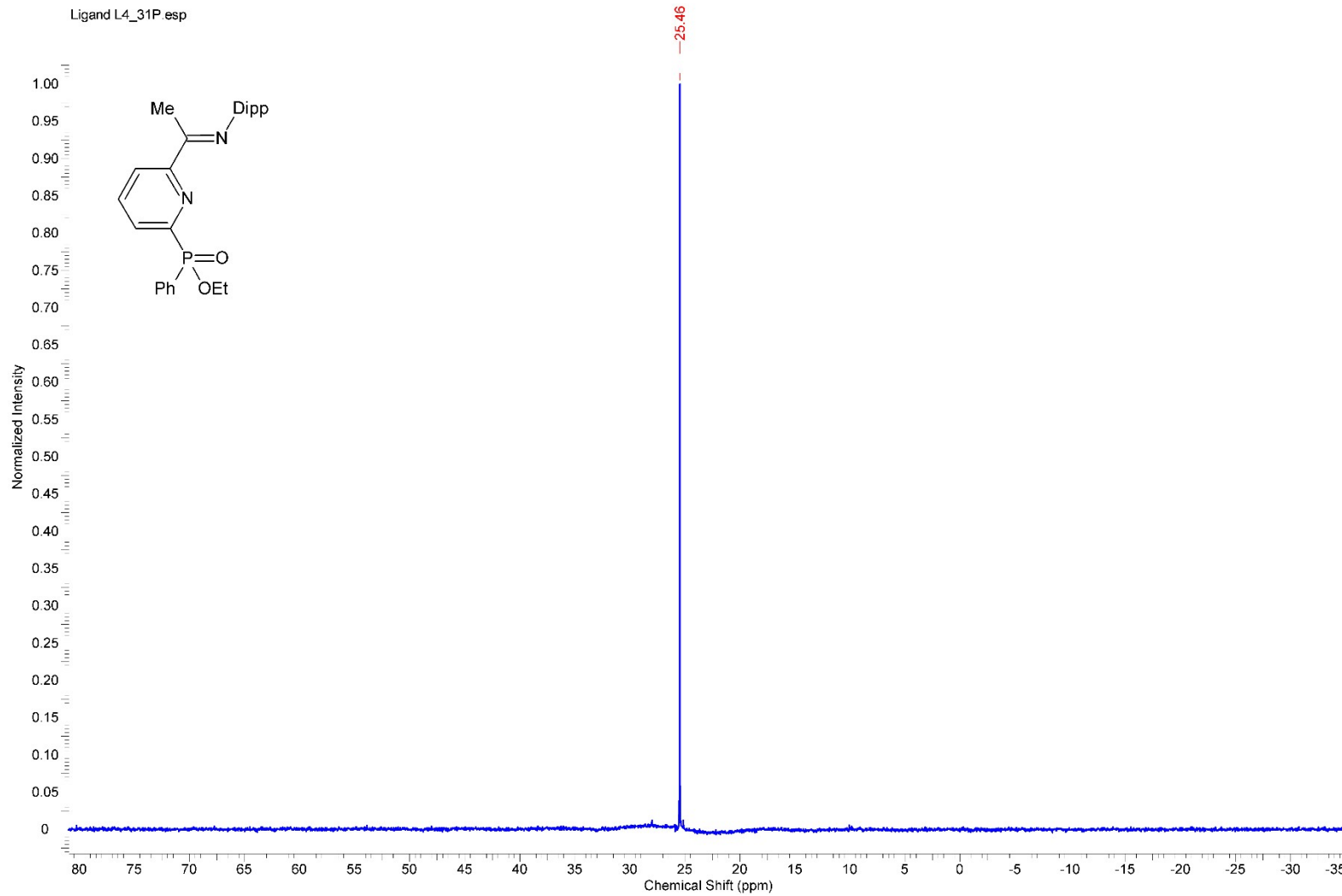


Figure S16. ^{31}P NMR spectrum of L^4 in CDCl_3

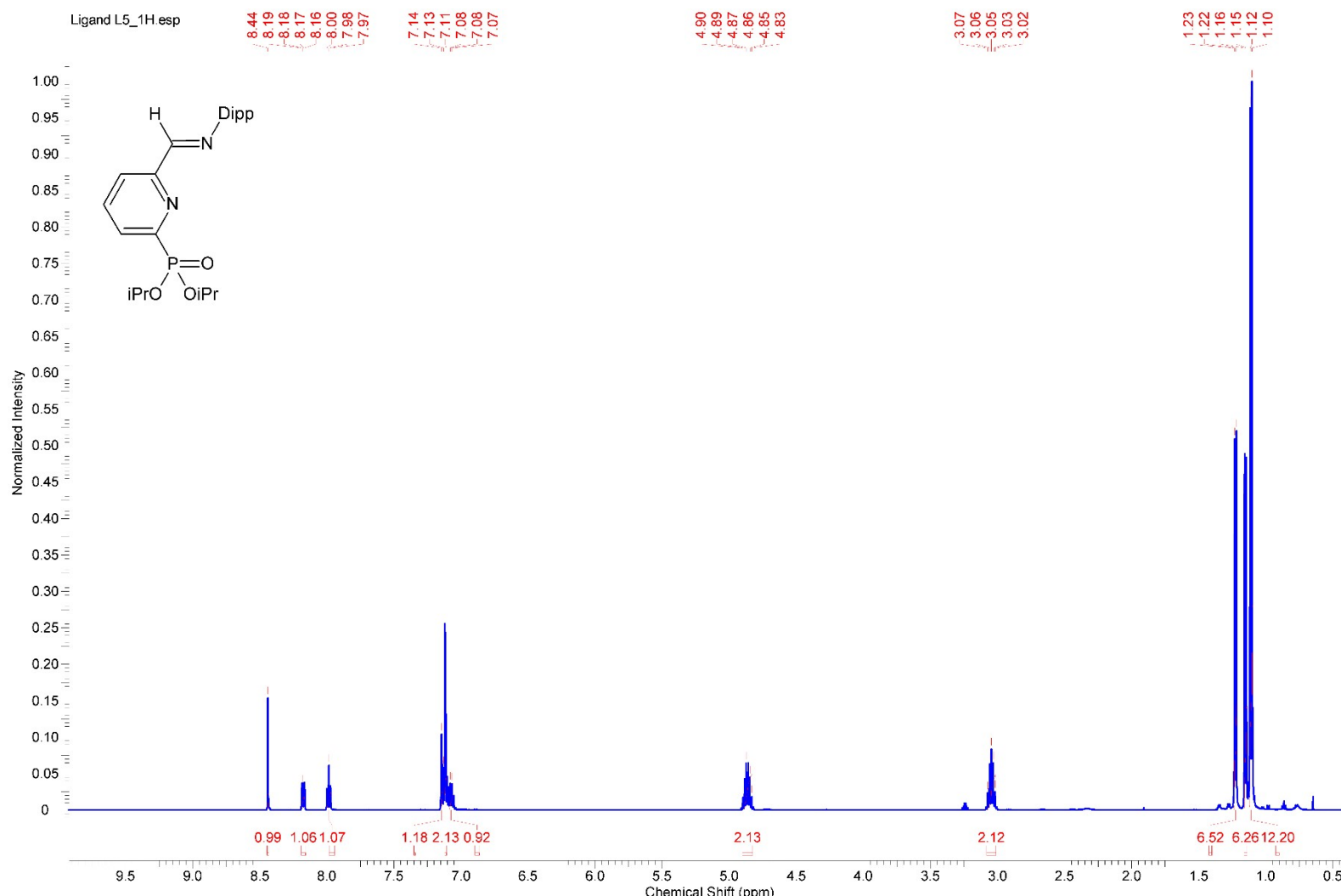


Figure S17. ¹H NMR spectrum of L⁵ in CDCl₃

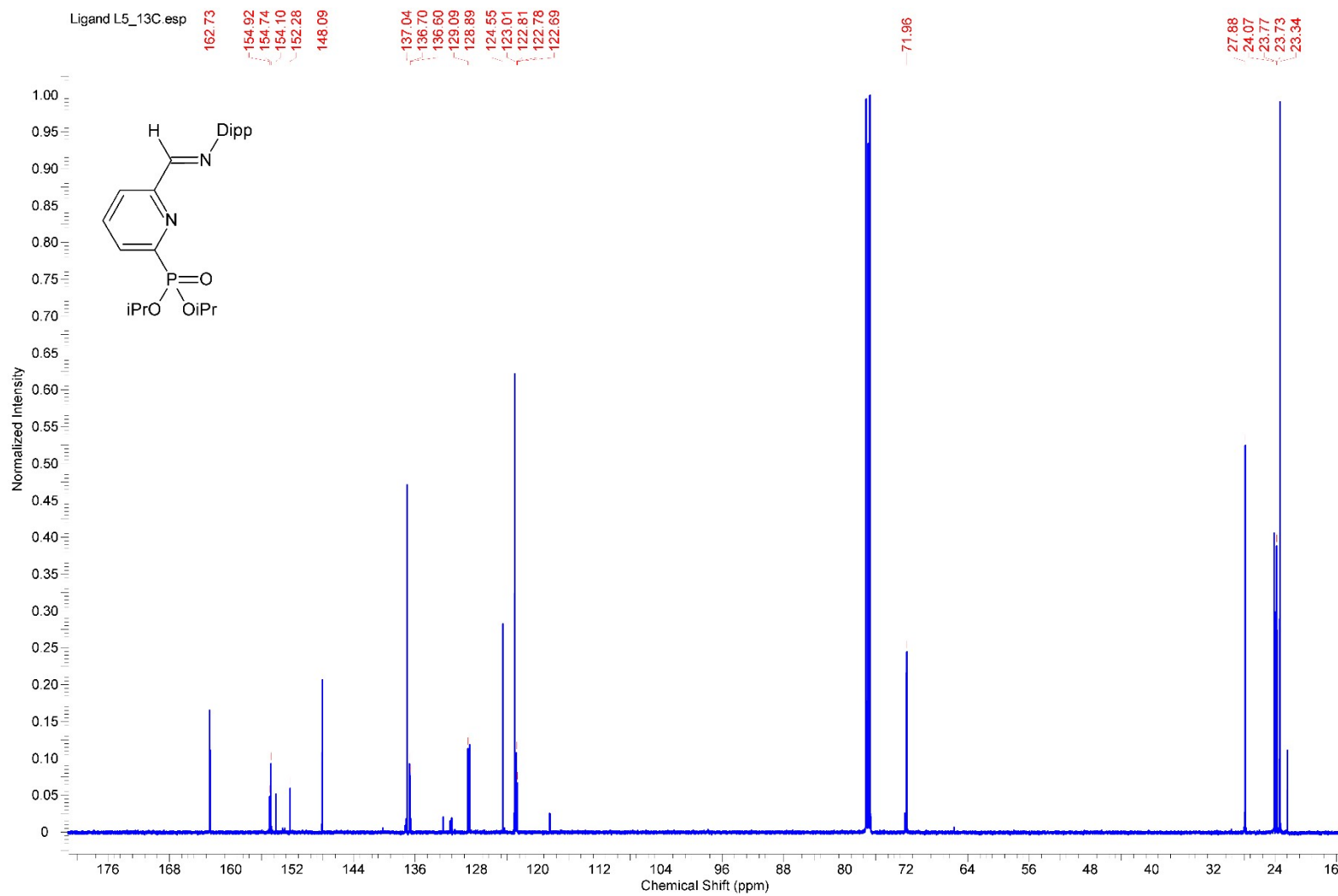


Figure S18. $^{13}\text{C}\{\text{H}\}$ NMR spectrum of \mathbf{L}^5 in CDCl_3

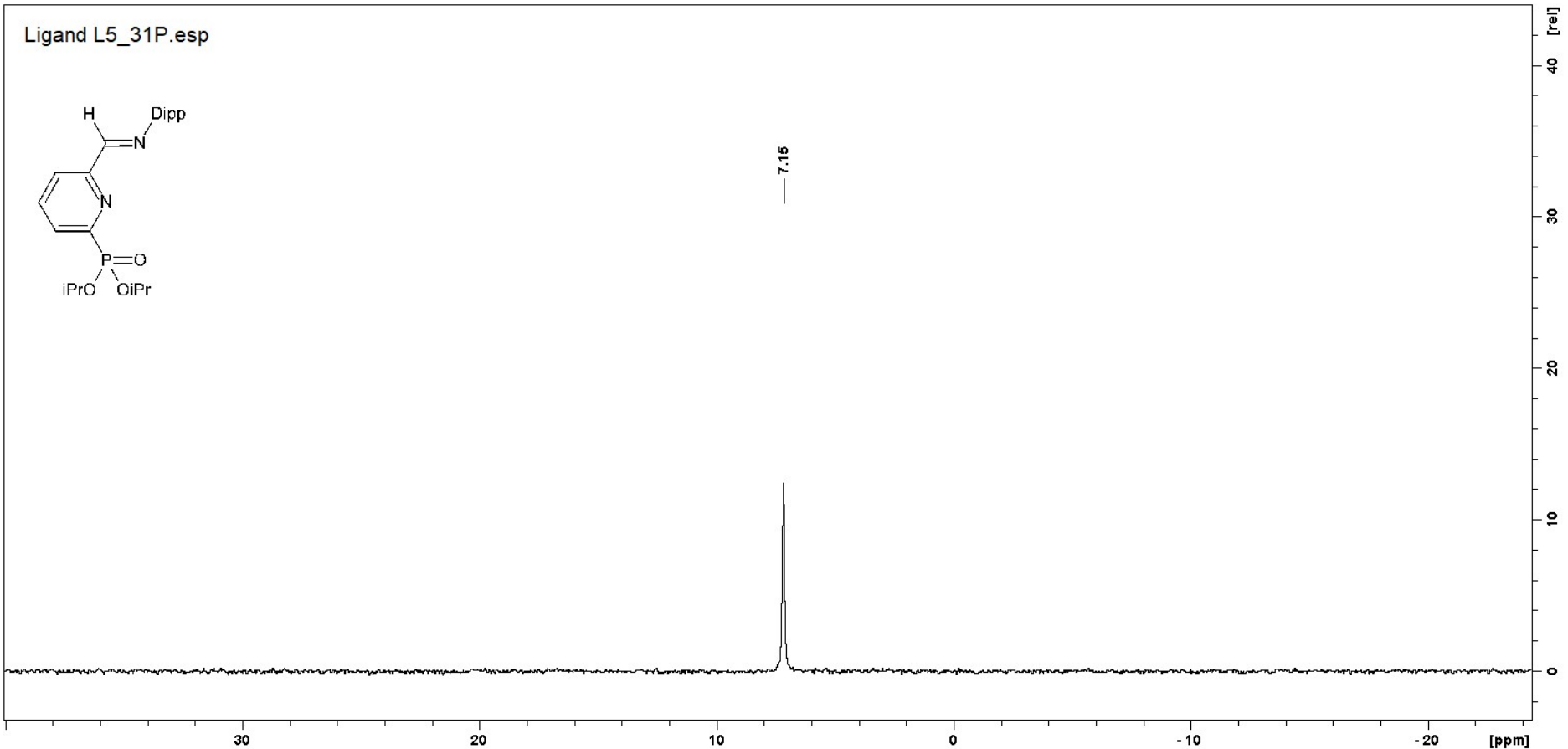


Figure S19. ^{31}P NMR spectrum of \mathbf{L}^5 in CDCl_3

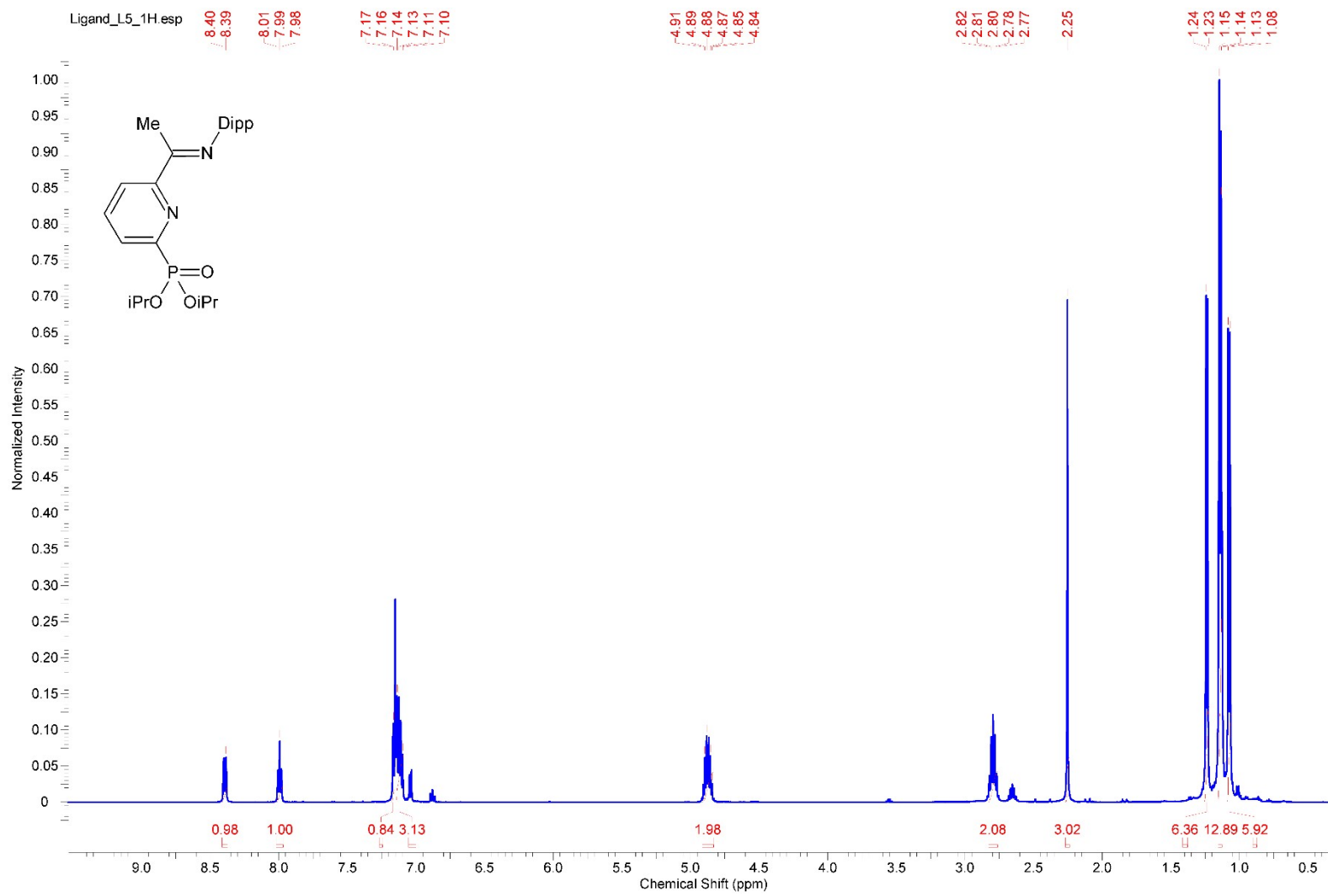


Figure S20. ^1H NMR spectrum of L^6 in CDCl_3

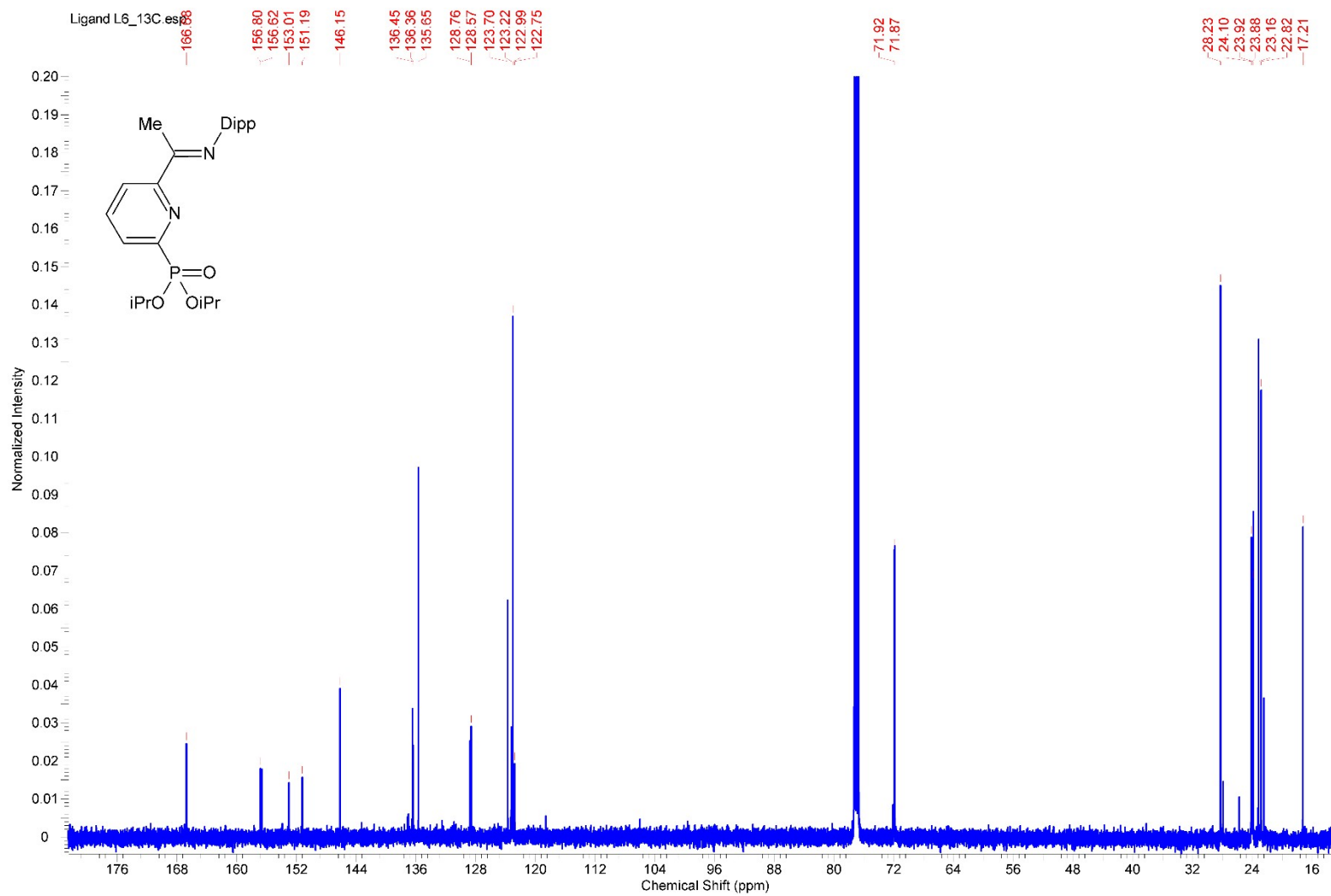


Figure S21. $^{13}\text{C}\{\text{H}\}$ NMR spectrum of L^6 in CDCl_3

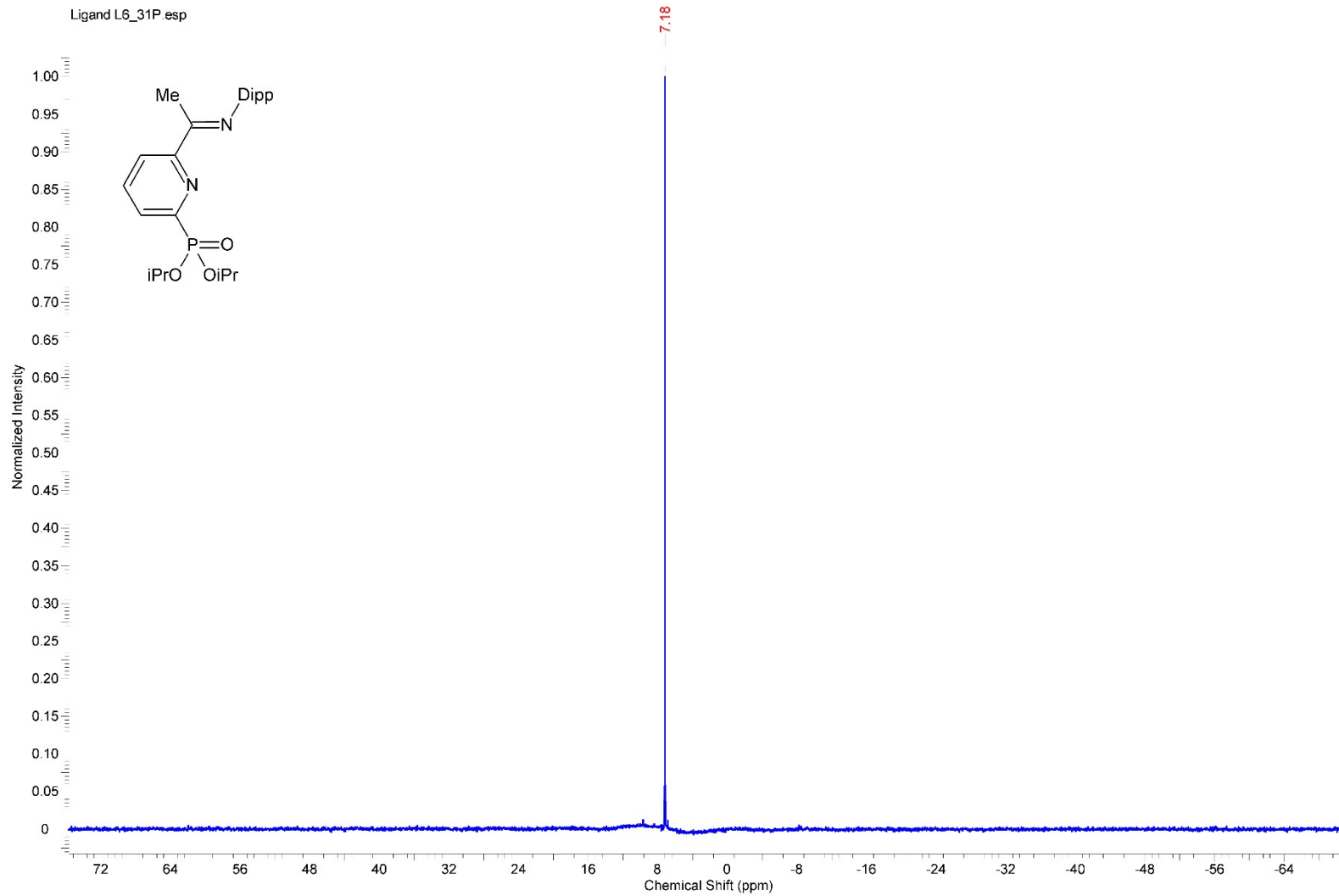


Figure S22. ^{31}P NMR spectrum of \mathbf{L}^6 in CDCl_3

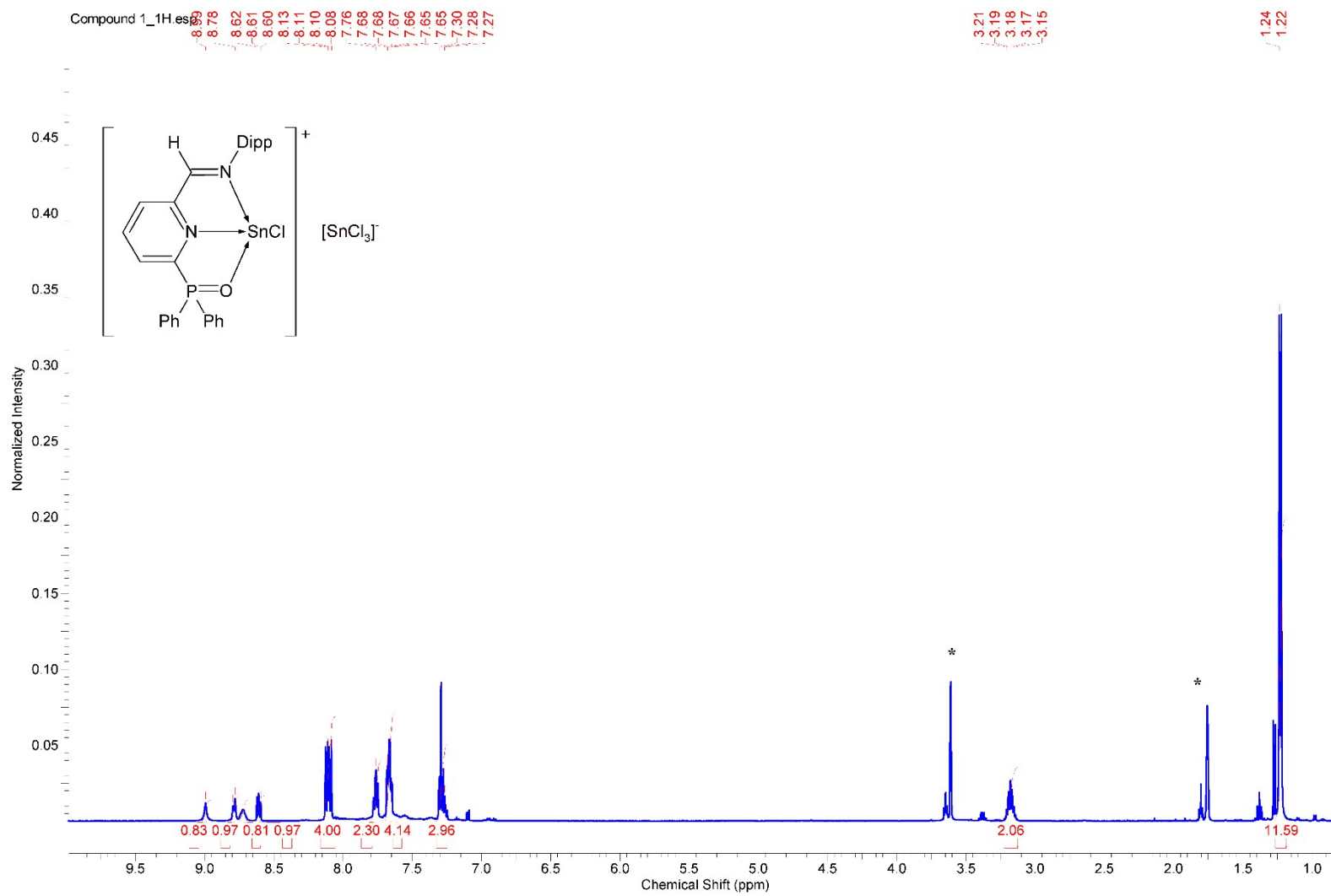


Figure S23. ^1H NMR spectrum of **1** in THF-d8 (* residual signal of THF)

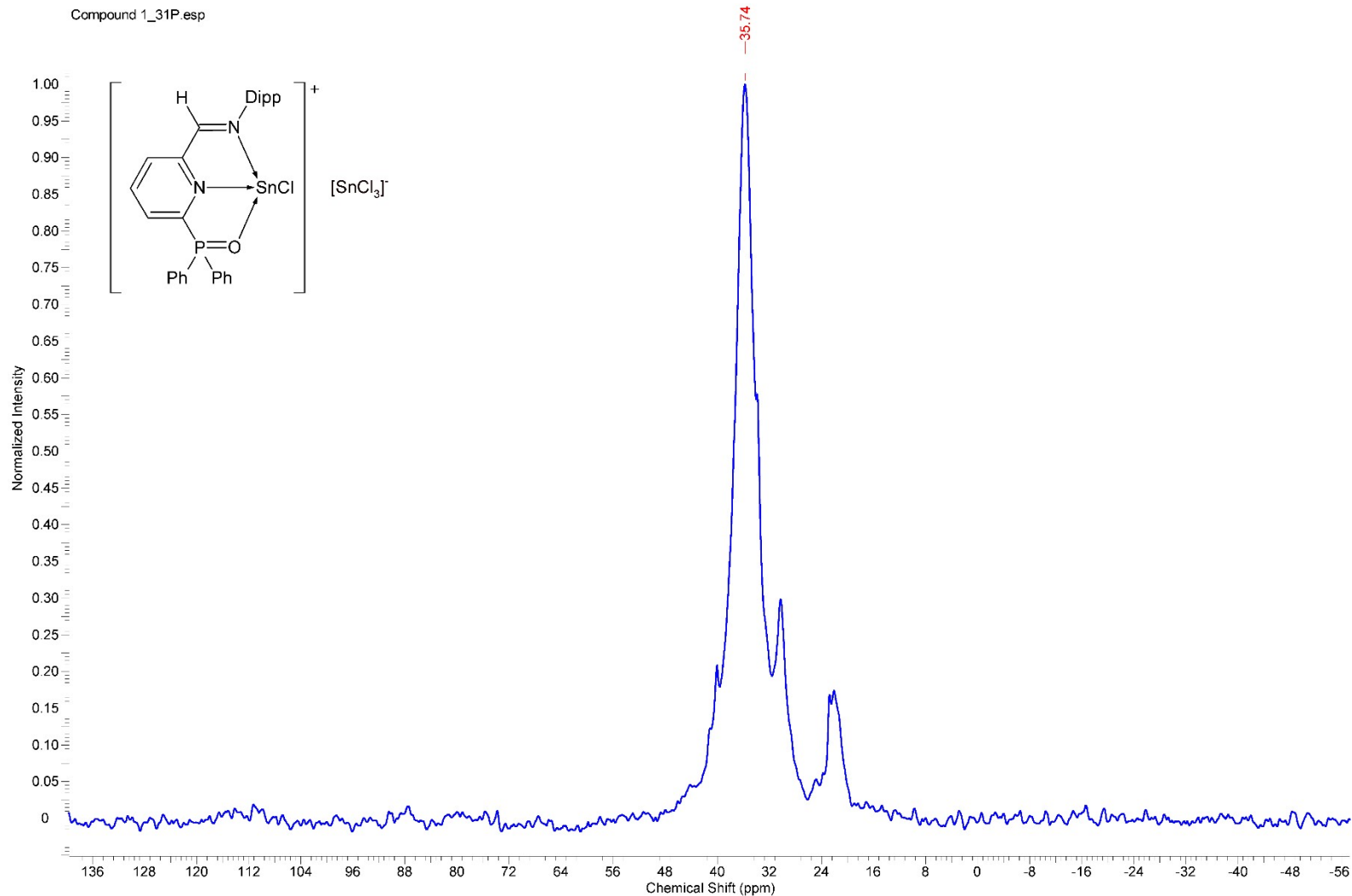


Figure S24. ^{31}P NMR spectrum of **1** in THF-d_8

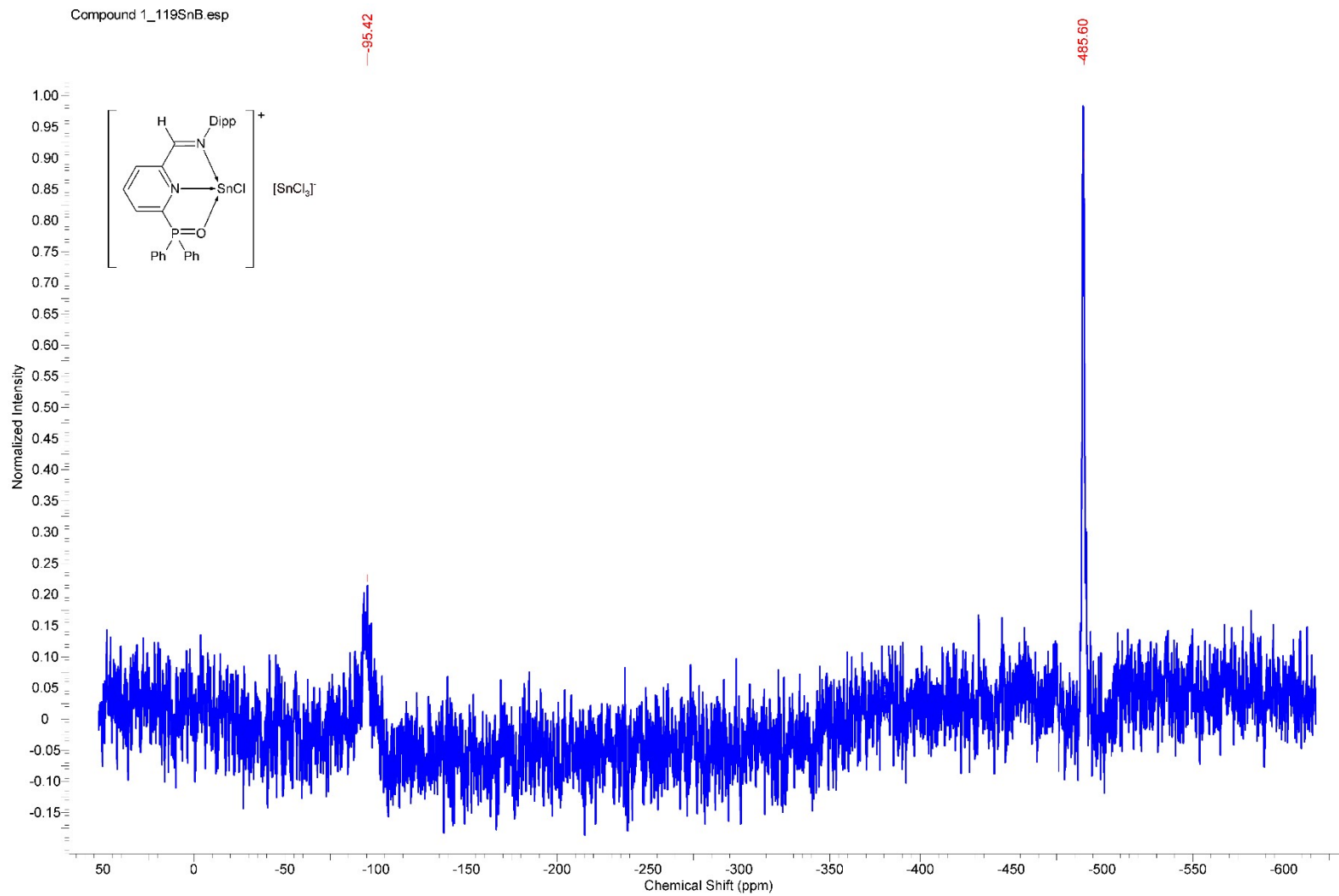


Figure S25. ^{119}Sn NMR spectrum of **1** in THF-d₈

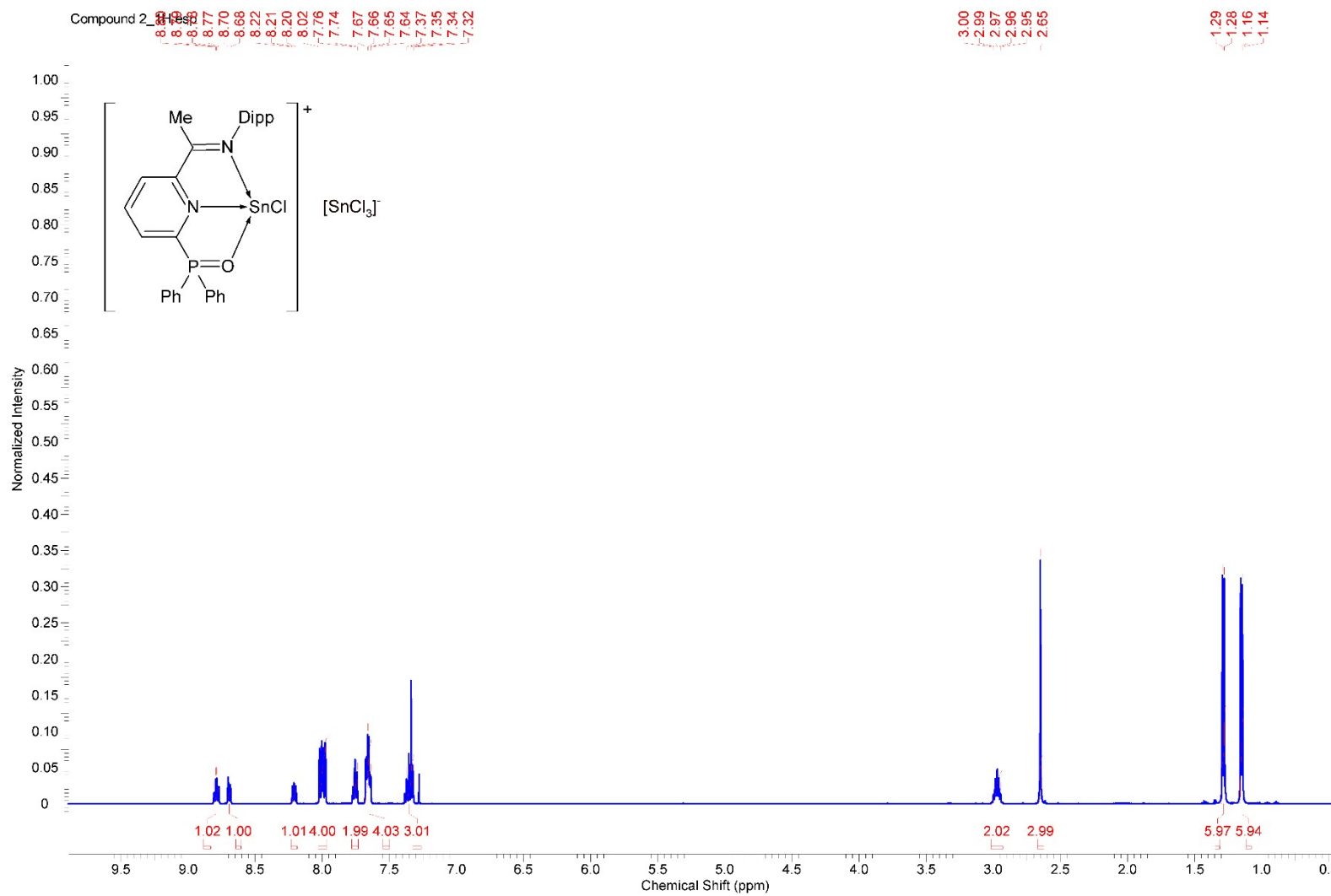


Figure S26. ^1H NMR spectrum of **2** in CDCl_3

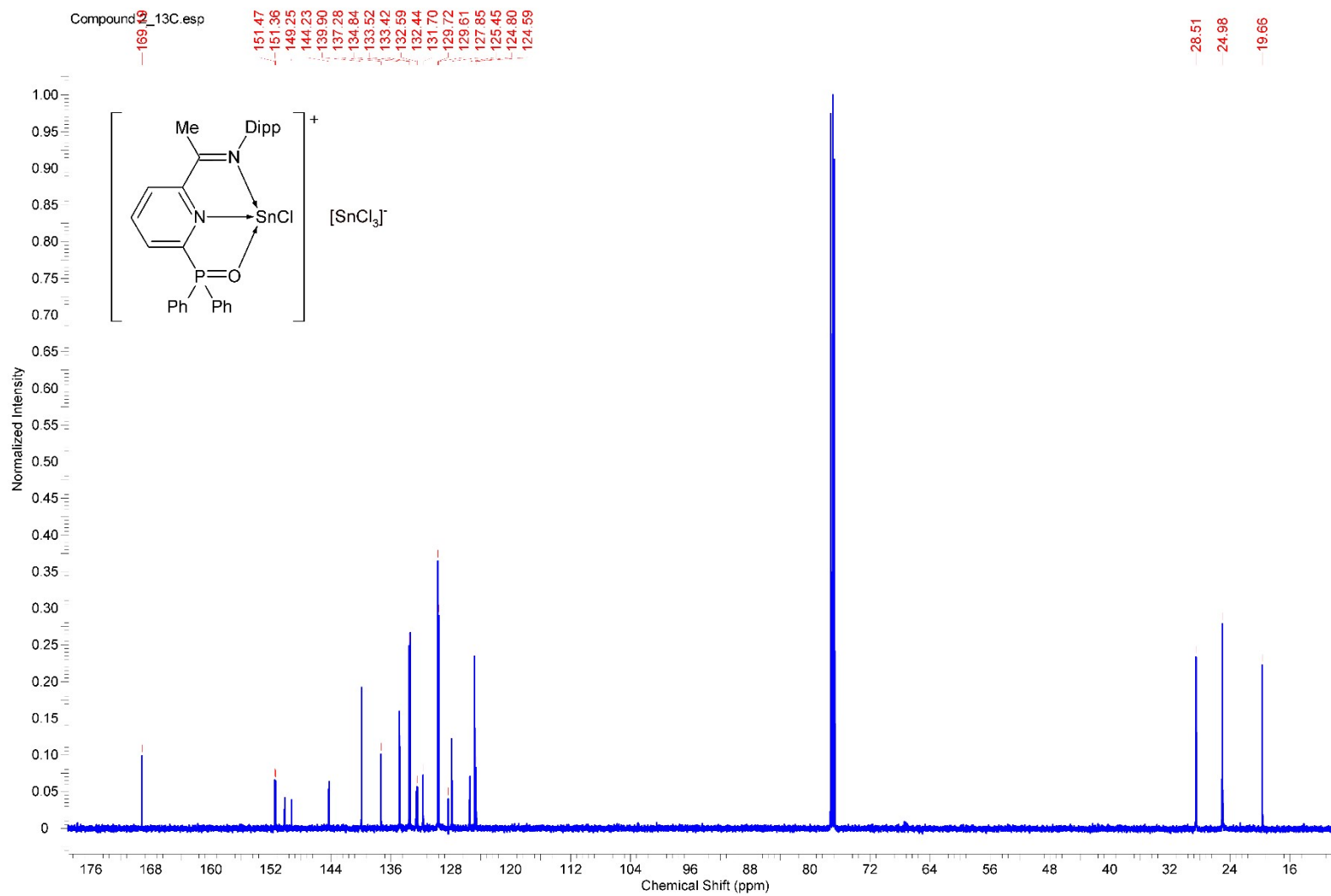


Figure S27. $^{13}\text{C}\{\text{H}\}$ NMR spectrum of **2** in CDCl_3

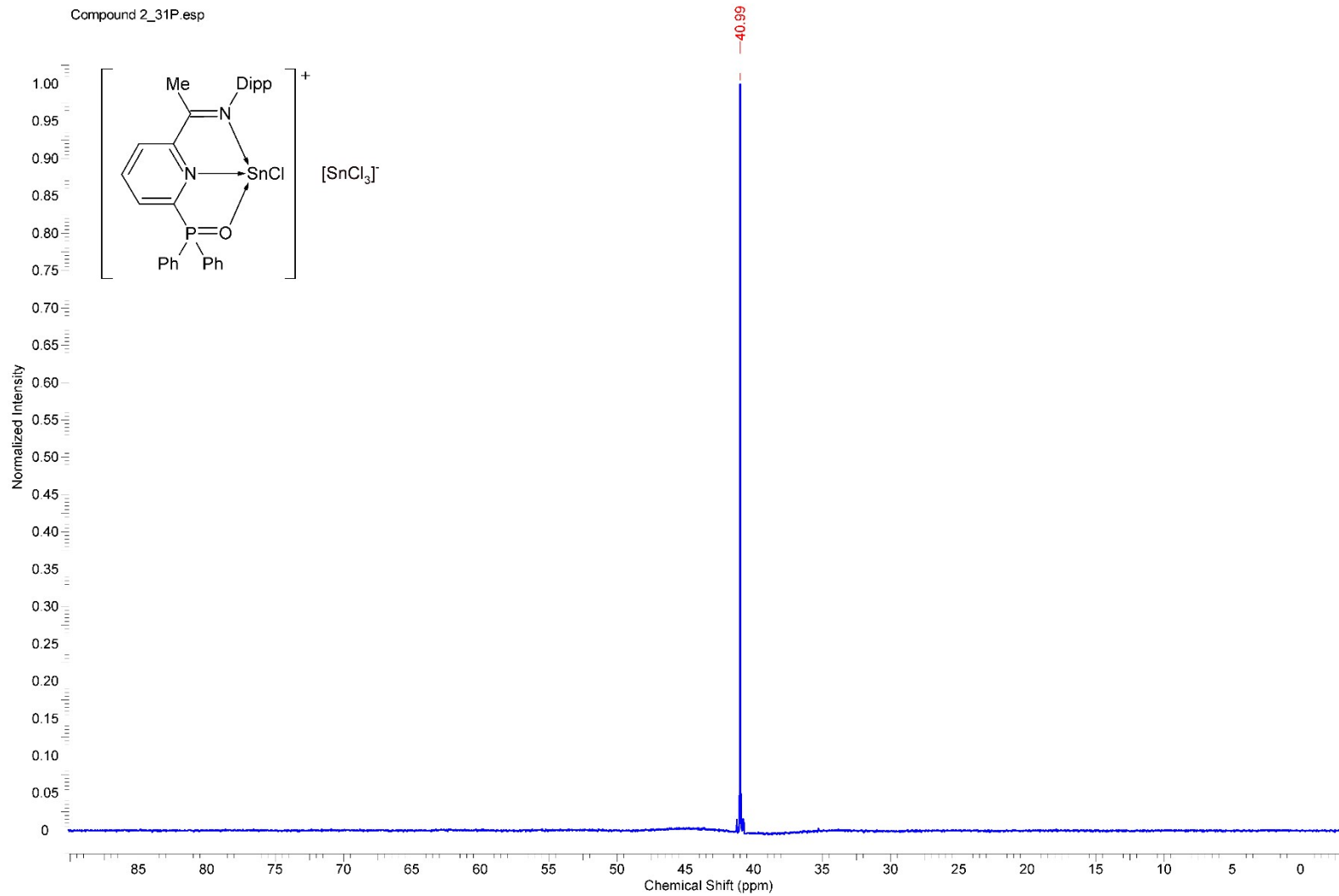


Figure S28. ^{31}P NMR spectrum of **2** in CDCl_3

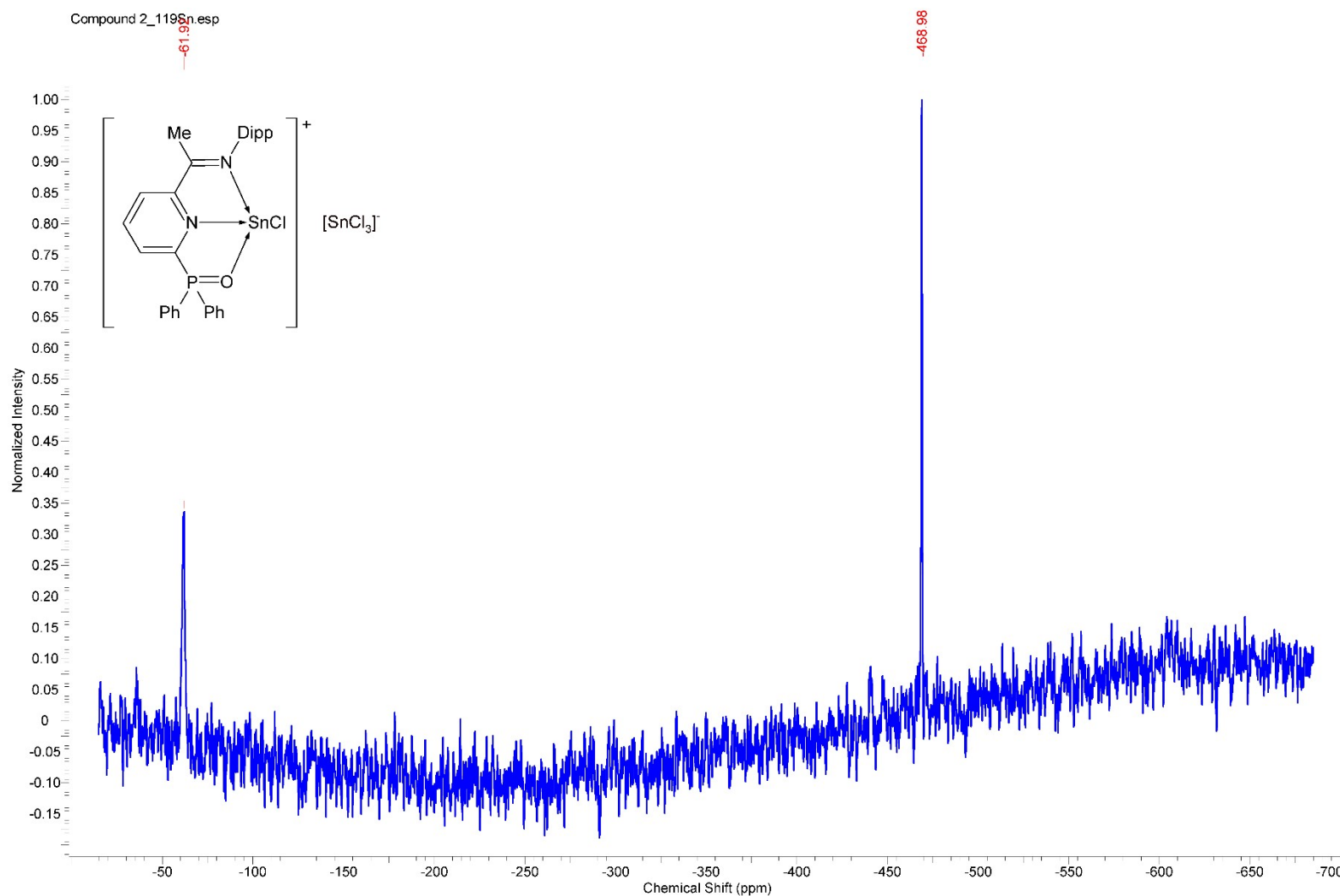


Figure S29. ^{119}Sn NMR spectrum of **2** in CDCl_3

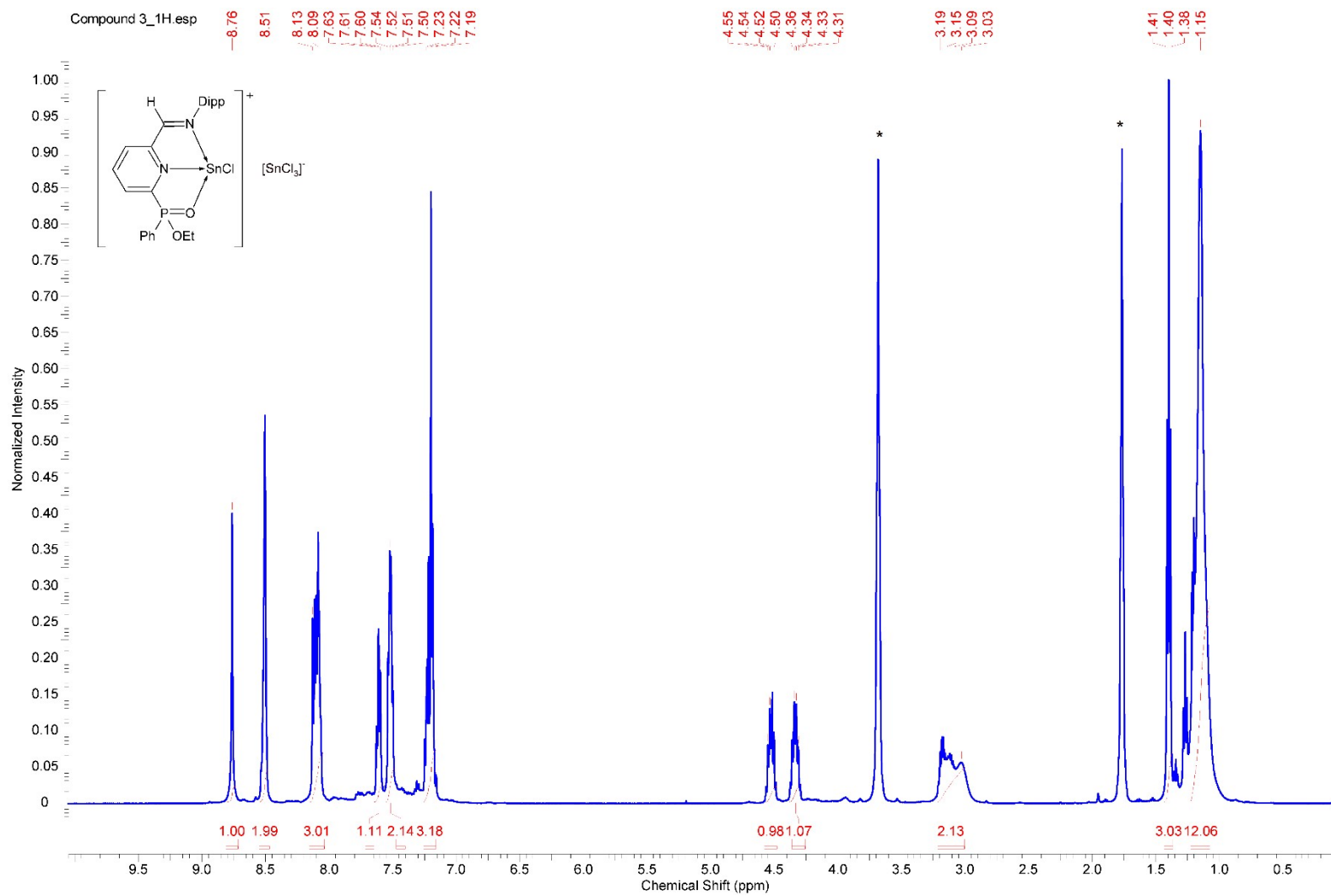


Figure S30. ^1H NMR spectrum of **3** in CDCl_3 . (* residual signal of THF).

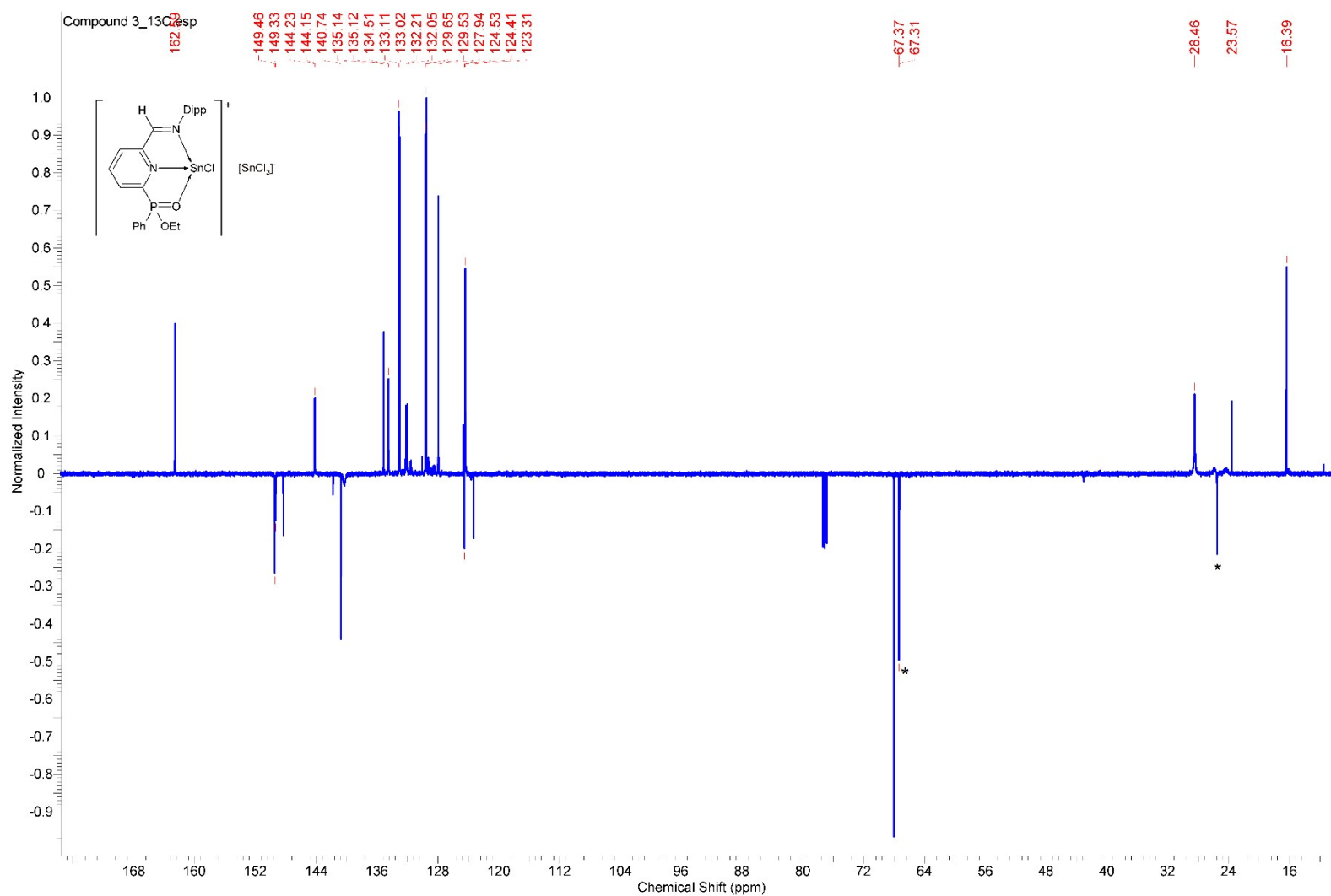


Figure S31. $^{13}\text{C}\{\text{H}\}$ APT NMR spectrum of **3** in CDCl_3 . (*) residual signal of THF)

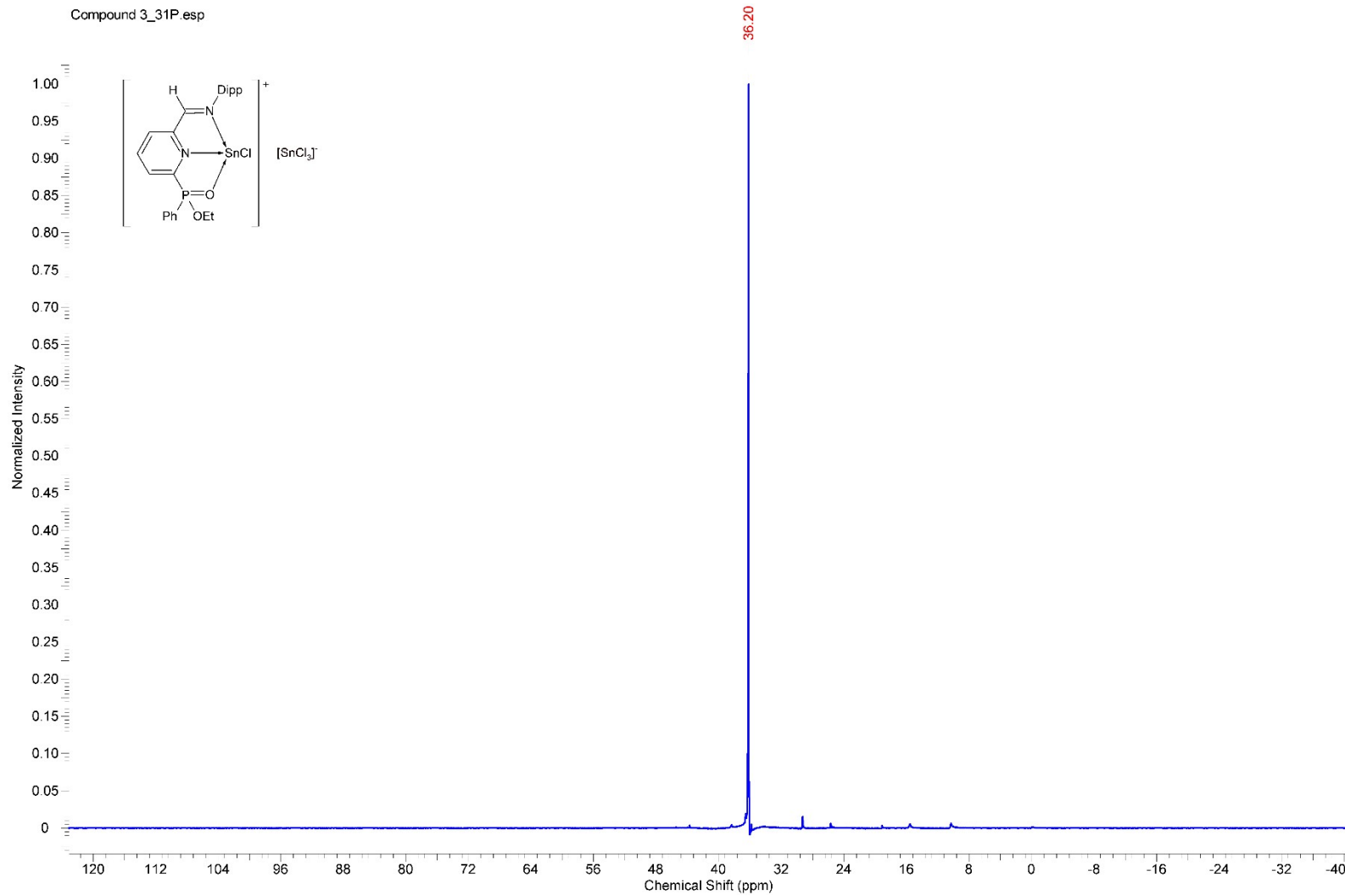


Figure S32. ^{31}P NMR spectrum of **3** in CDCl_3

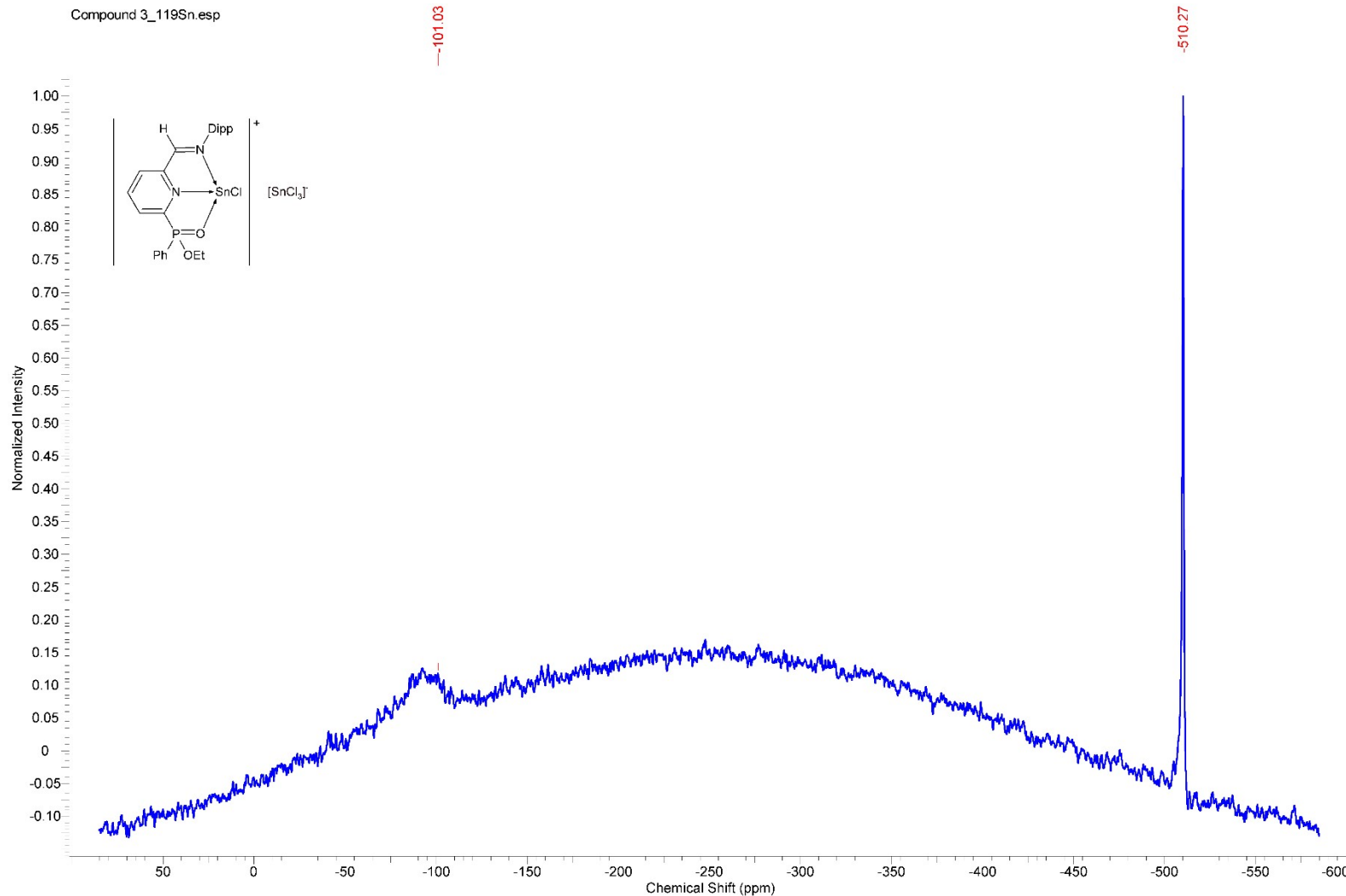


Figure S33. ^{119}Sn NMR spectrum of 3 in CDCl_3

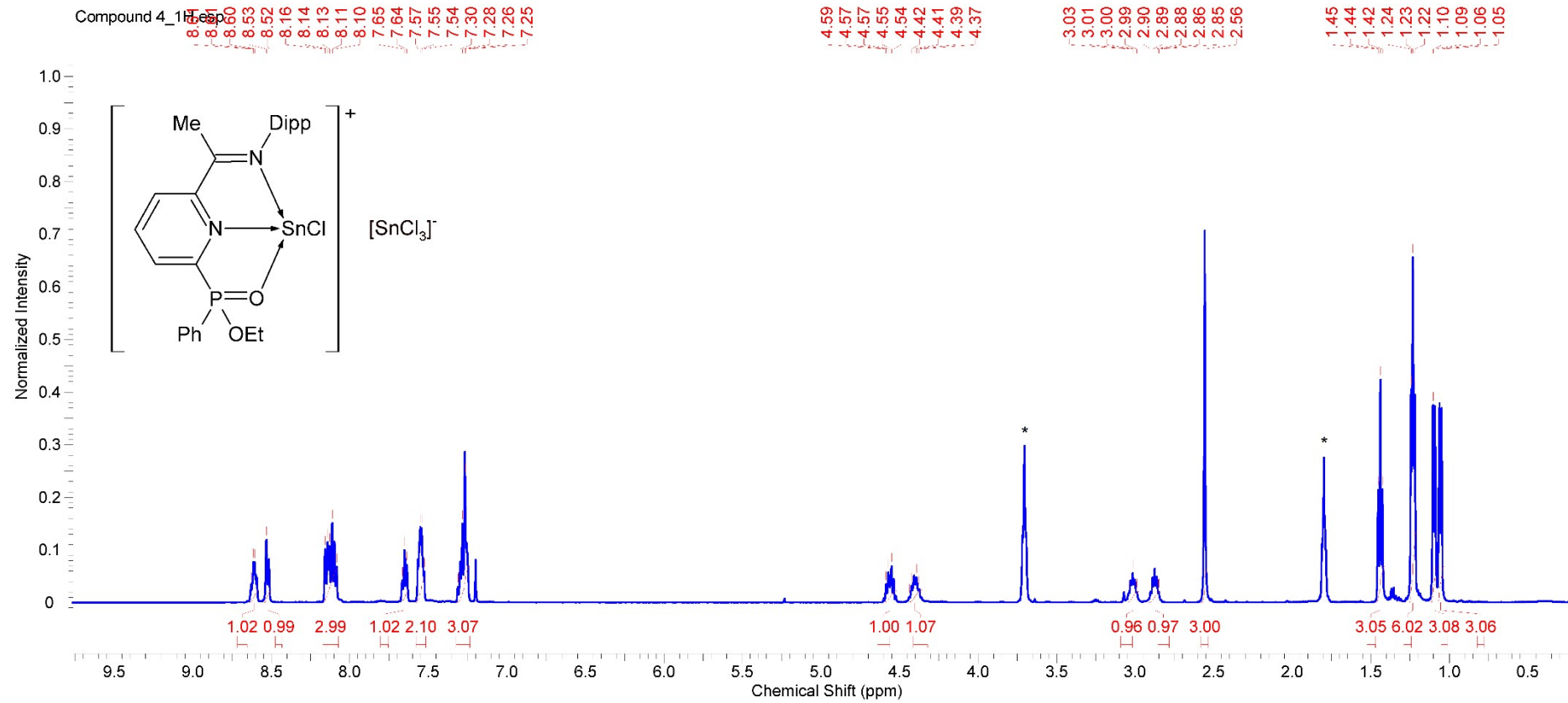


Figure S34. ^1H NMR spectrum of 4 in CDCl_3 . (* residual signal of THF)

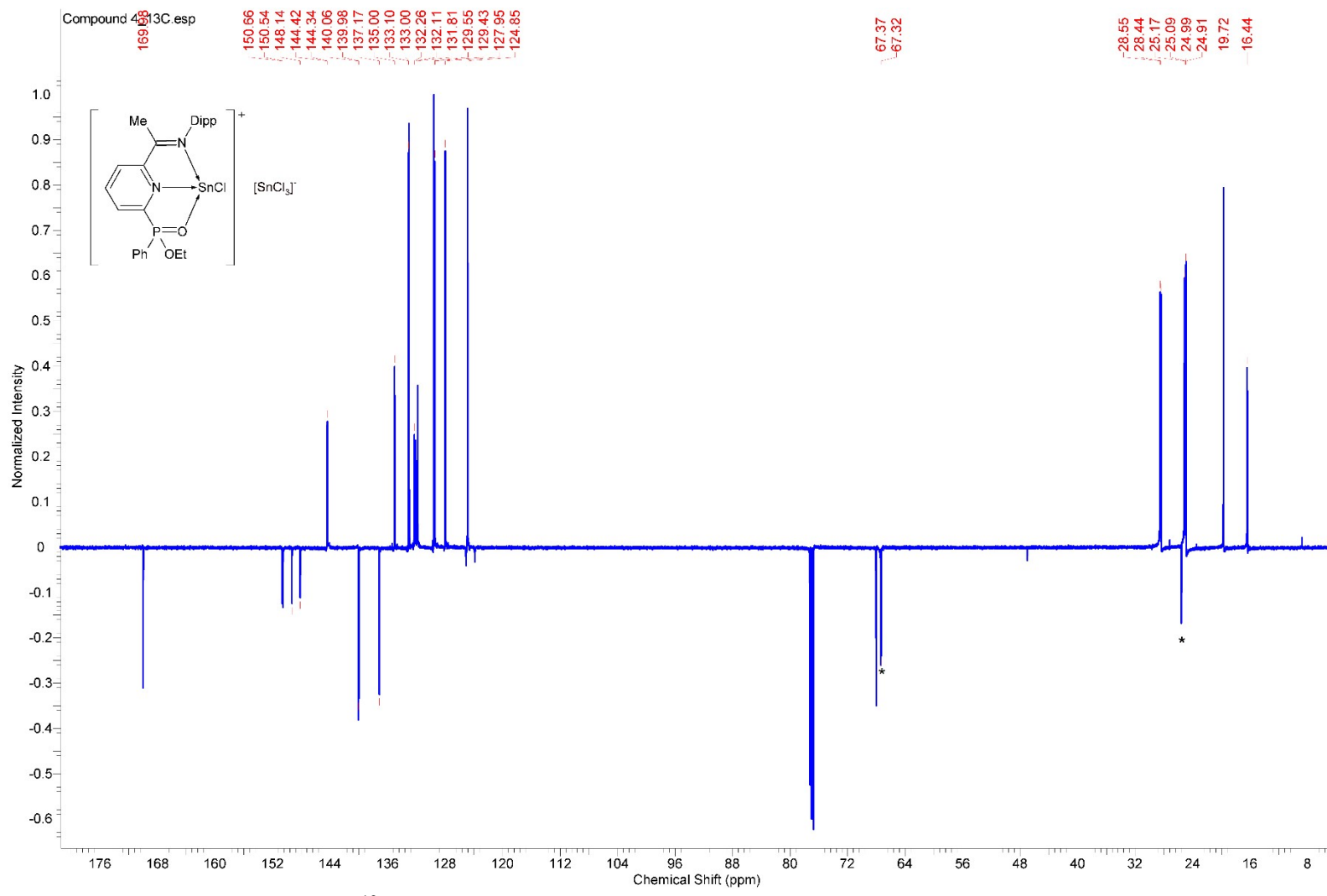


Figure S35. $^{13}\text{C}\{\text{H}\}$ APT NMR spectrum of **4** in CDCl_3 . (* residual signal of THF)

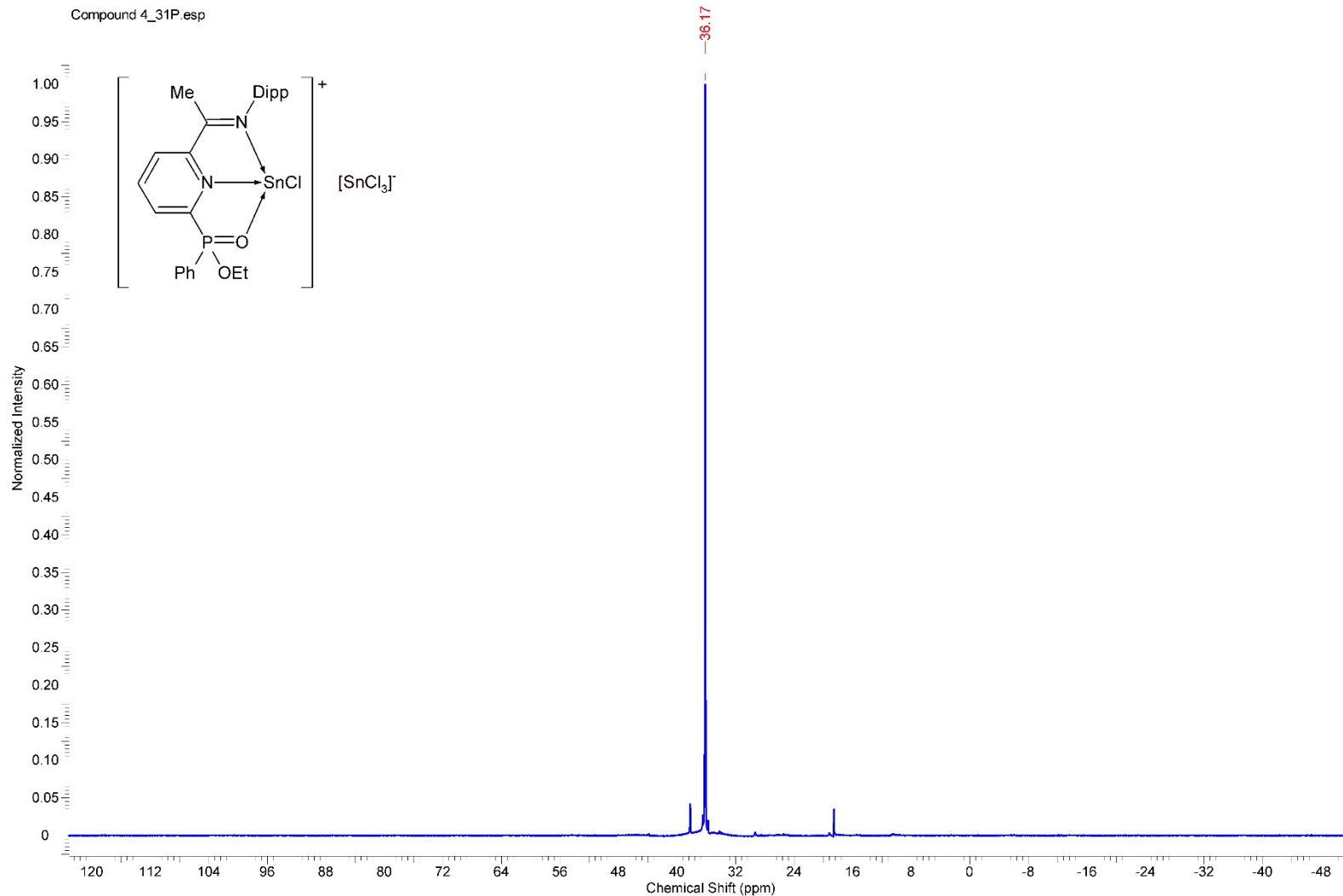


Figure S36. ^{31}P NMR spectrum of **4** in CDCl_3

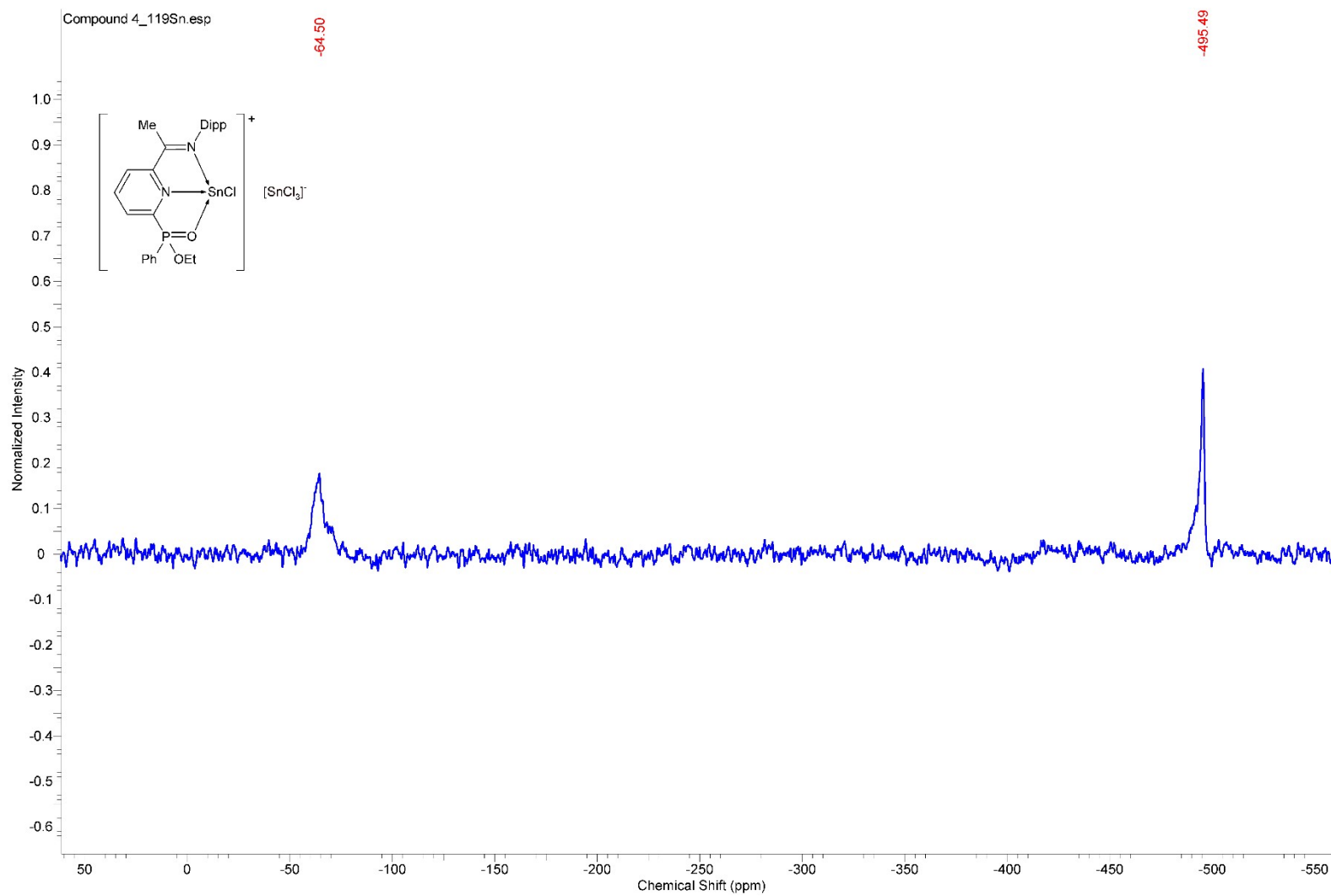


Figure S37. ^{119}Sn NMR spectrum of 4 in CDCl_3

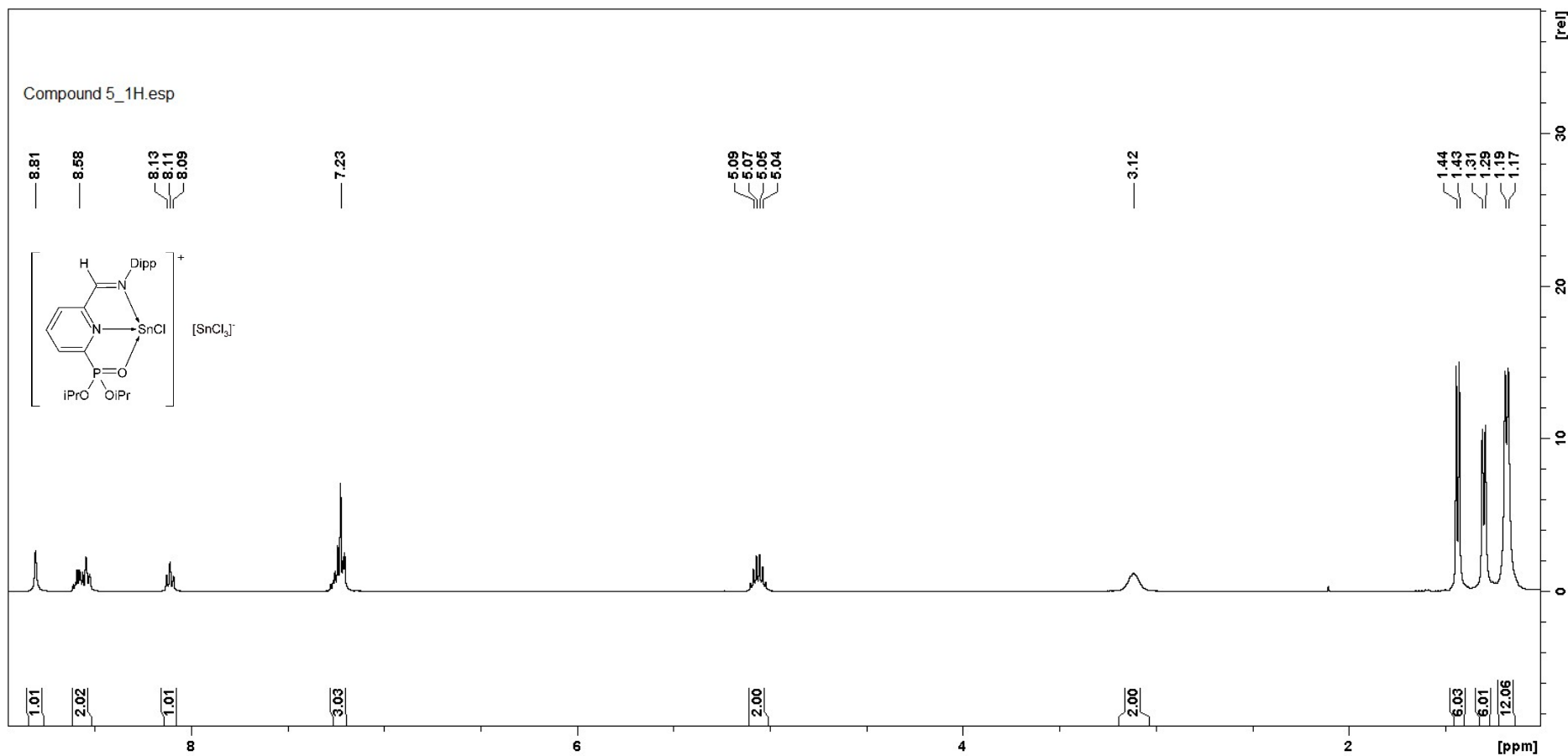


Figure S38. ^1H NMR spectrum of **5** in CDCl_3 .

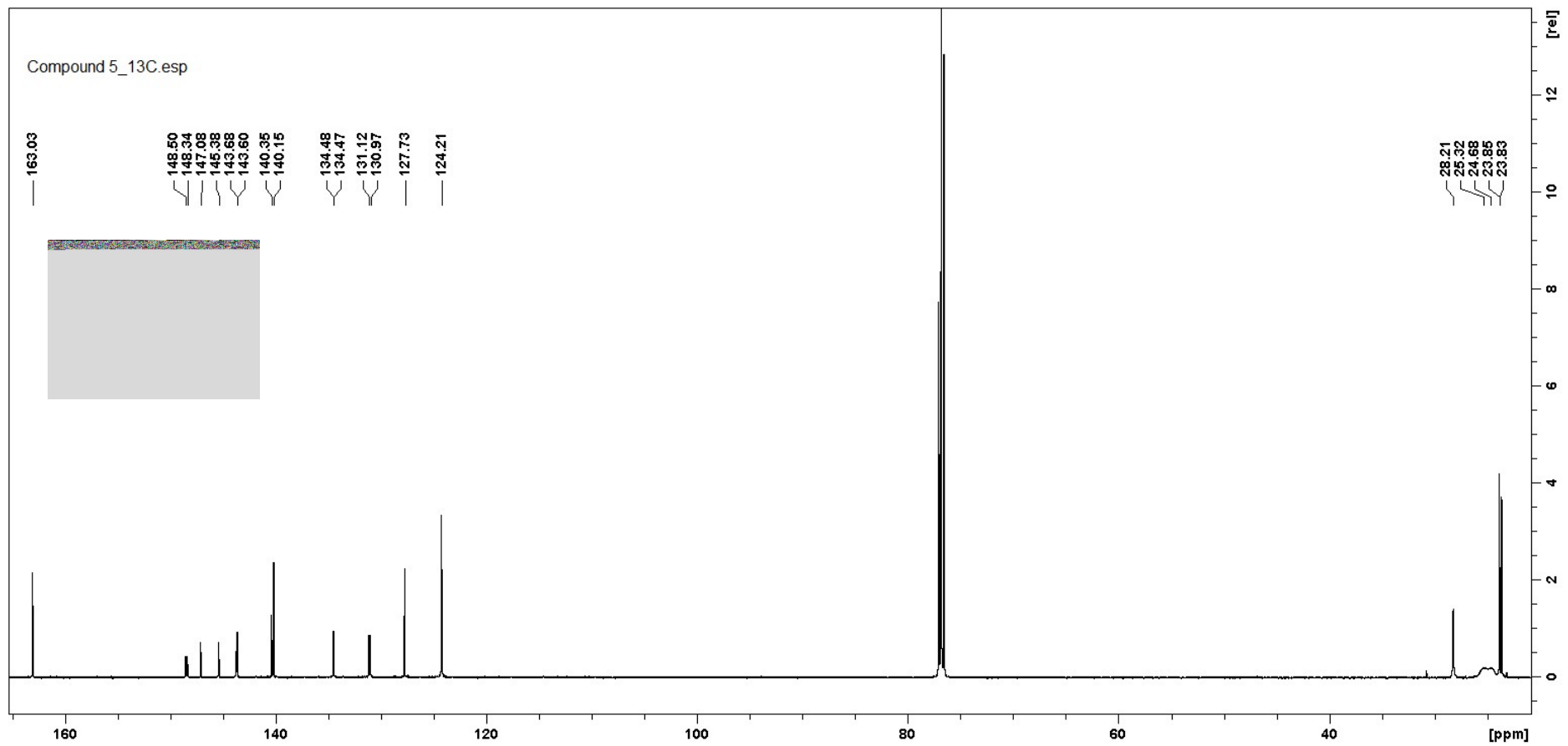


Figure S39. $^{13}\text{C}\{\text{H}\}$ NMR spectrum of **5** in CDCl_3 .

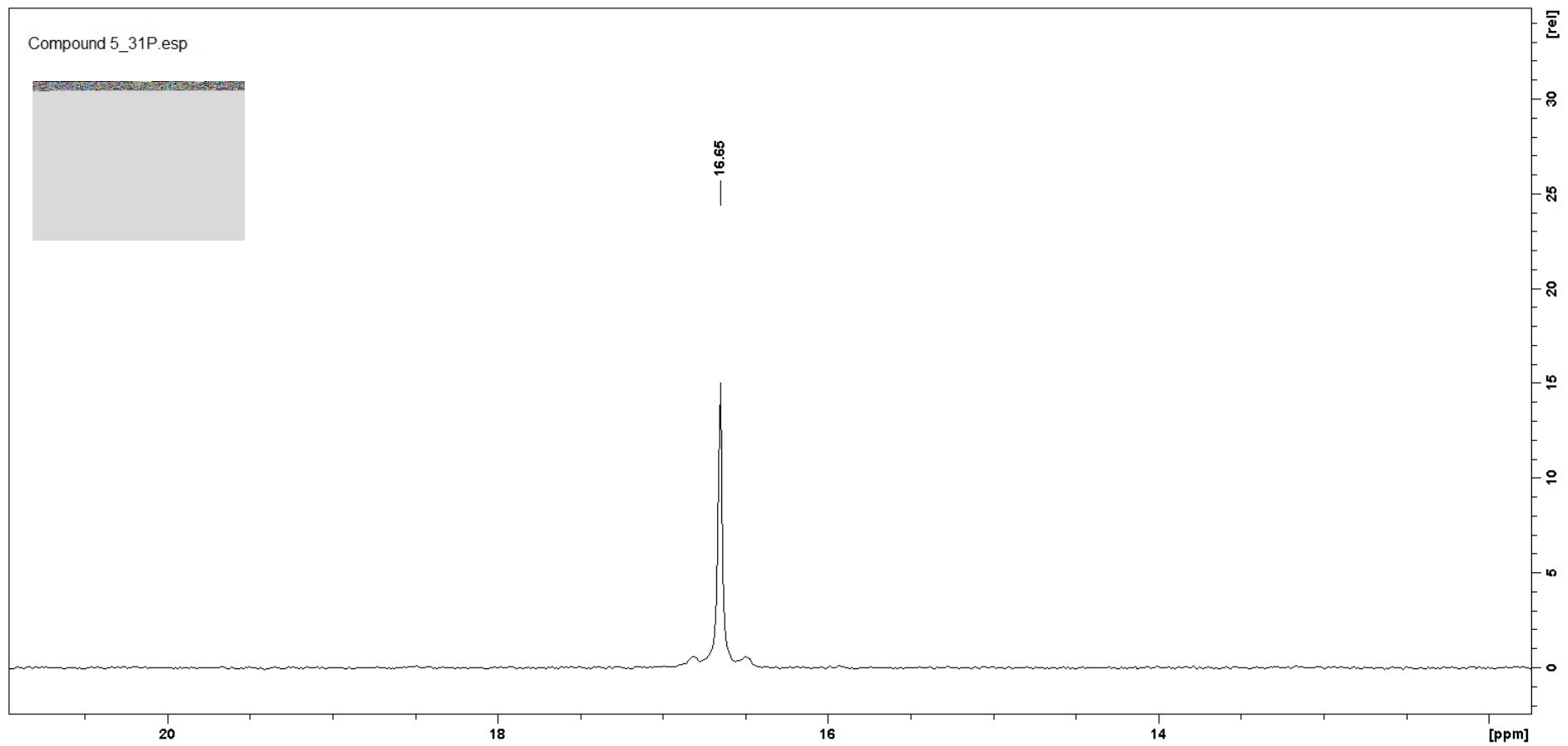


Figure S40. ^{31}P NMR spectrum of **5** in CDCl_3

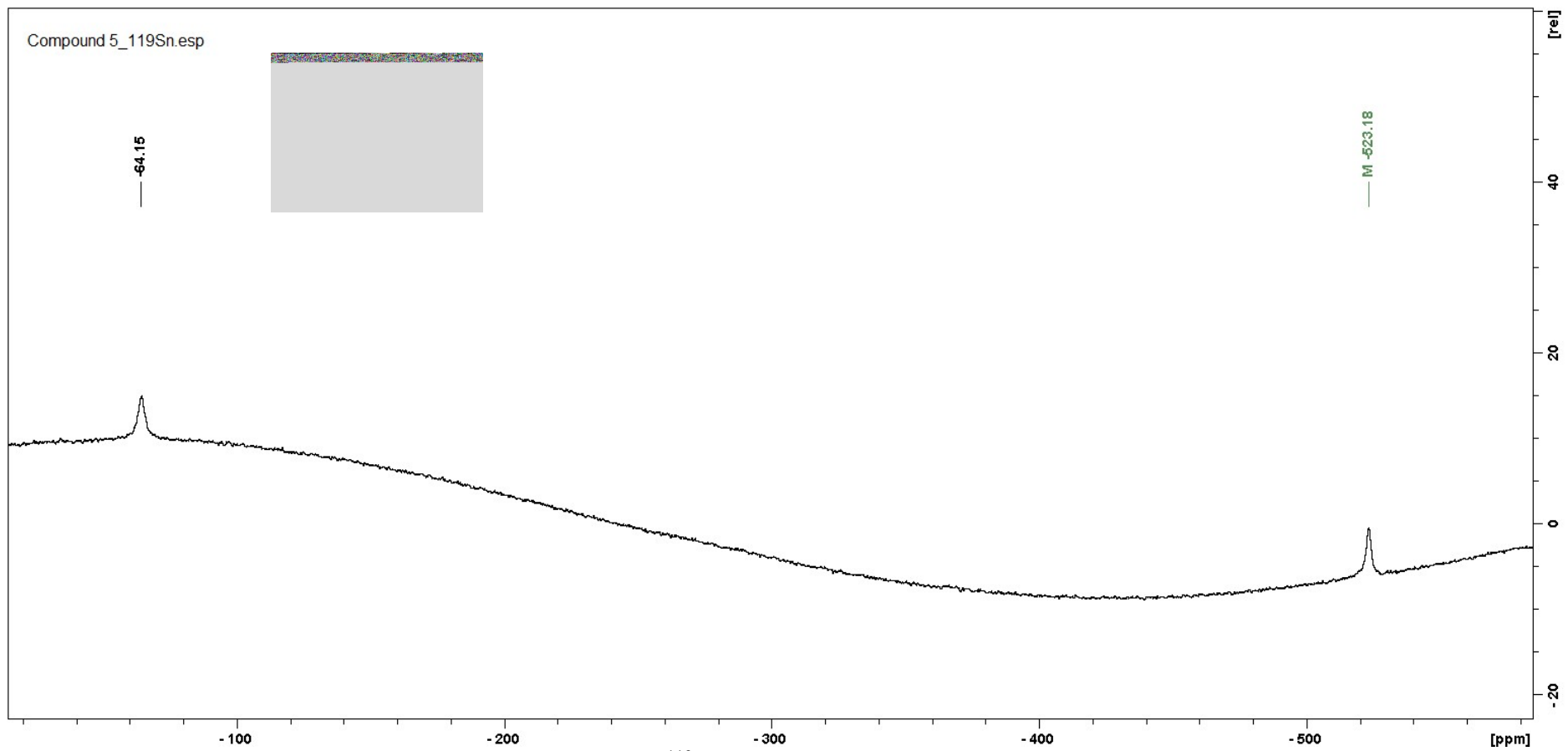


Figure S41. ^{119}Sn NMR spectrum of **5** in CDCl_3

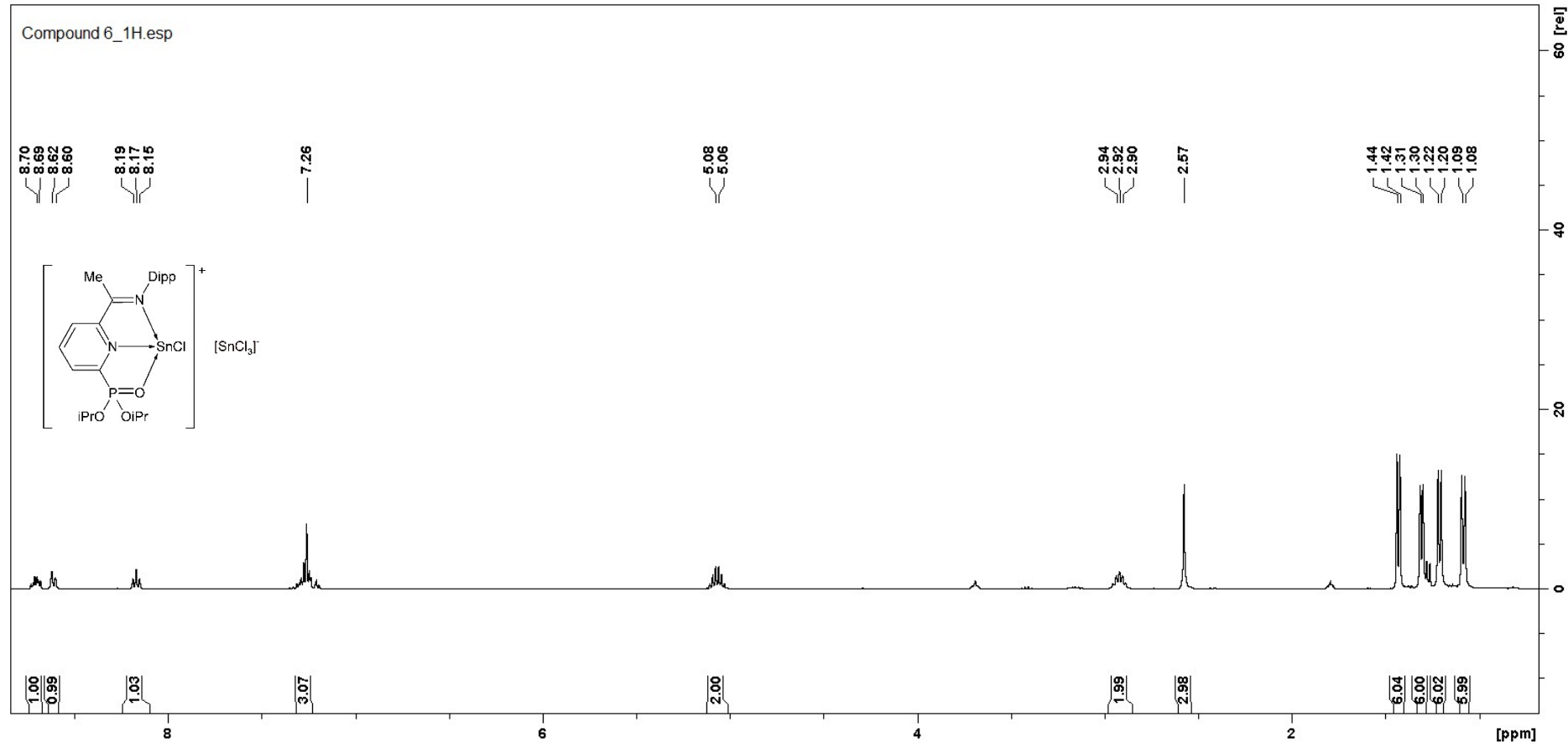


Figure S42. ^1H NMR spectrum of **6** in CDCl_3 .

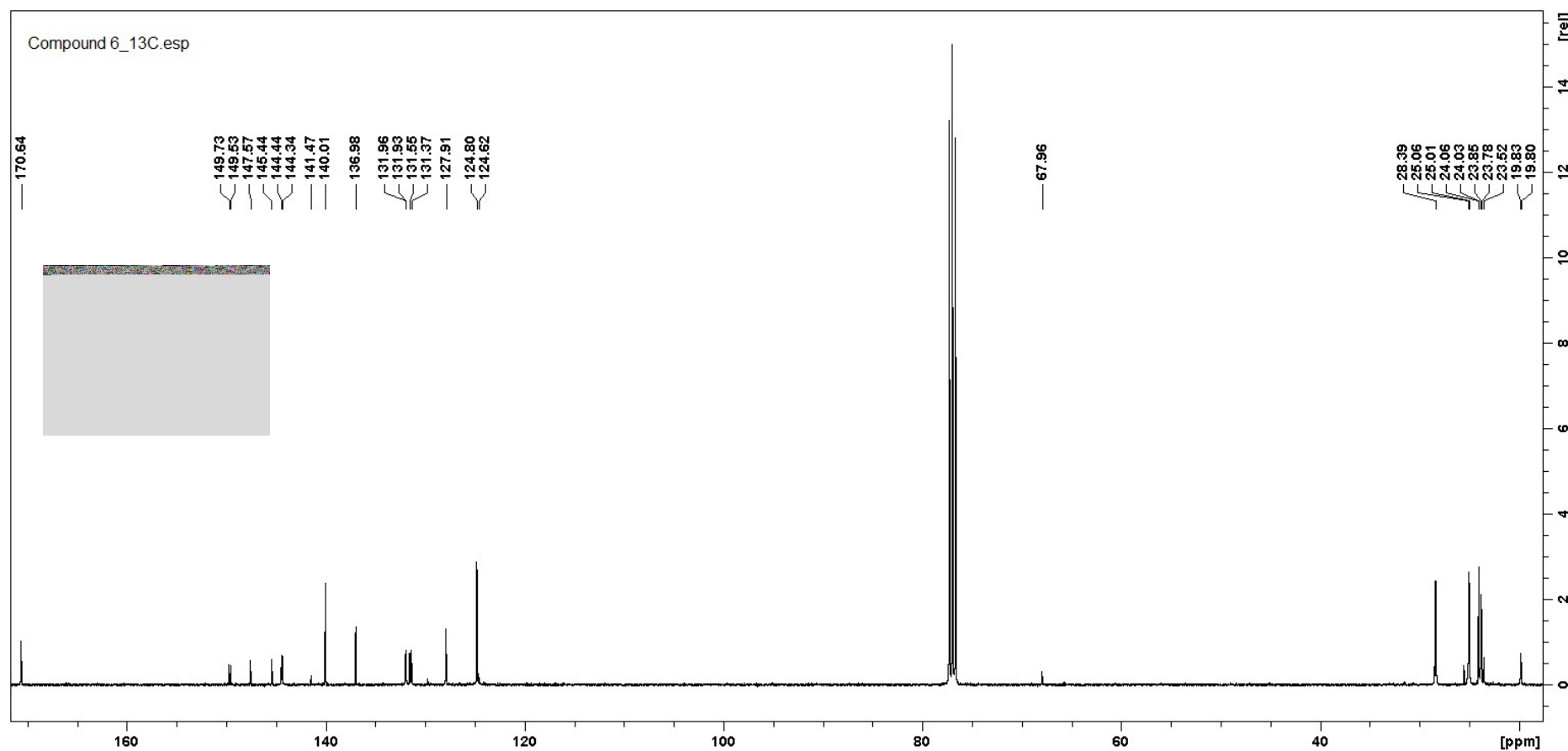


Figure S43. ¹³C NMR spectrum of 6 in CDCl_3 .

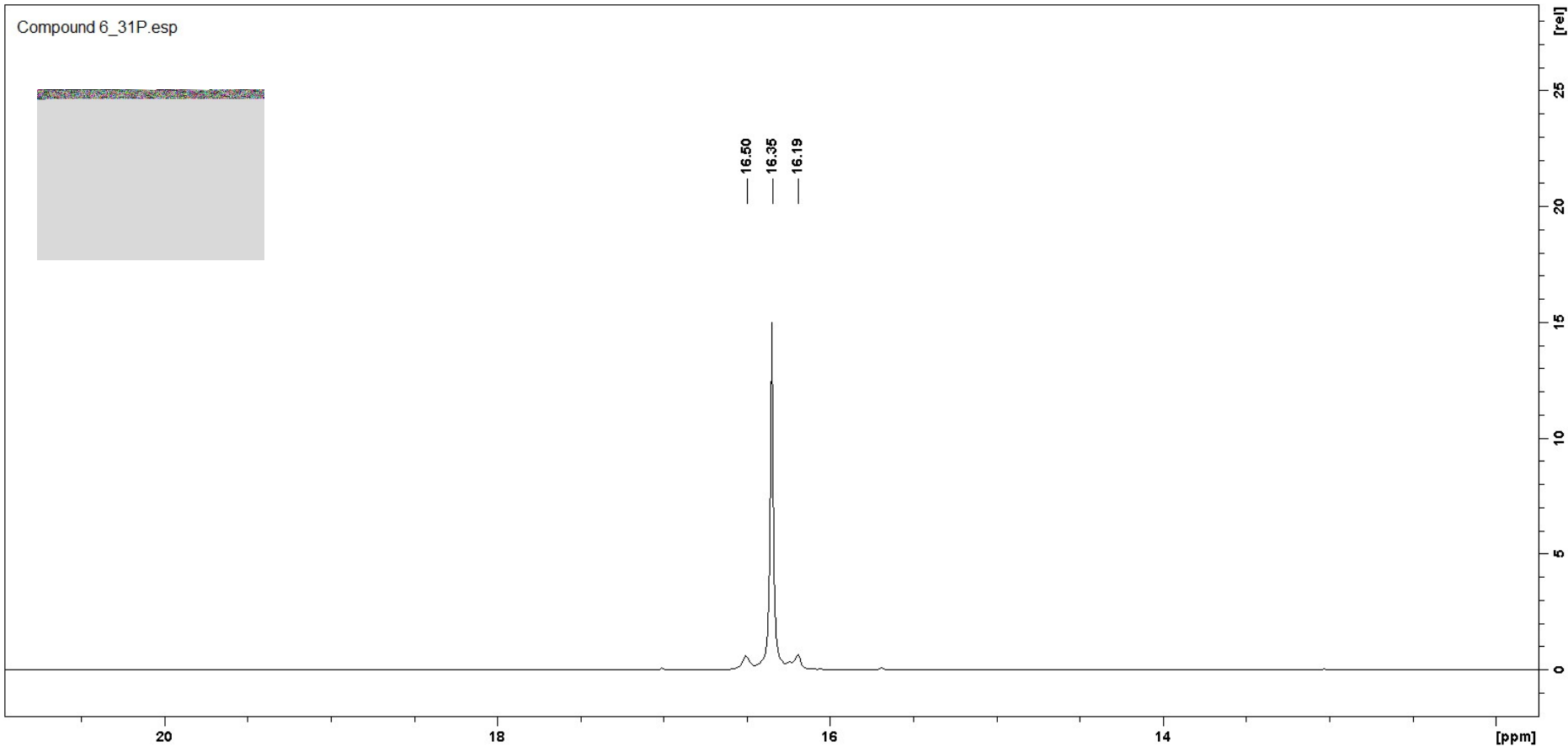


Figure S44. ^{31}P NMR spectrum of **6** in CDCl_3 .

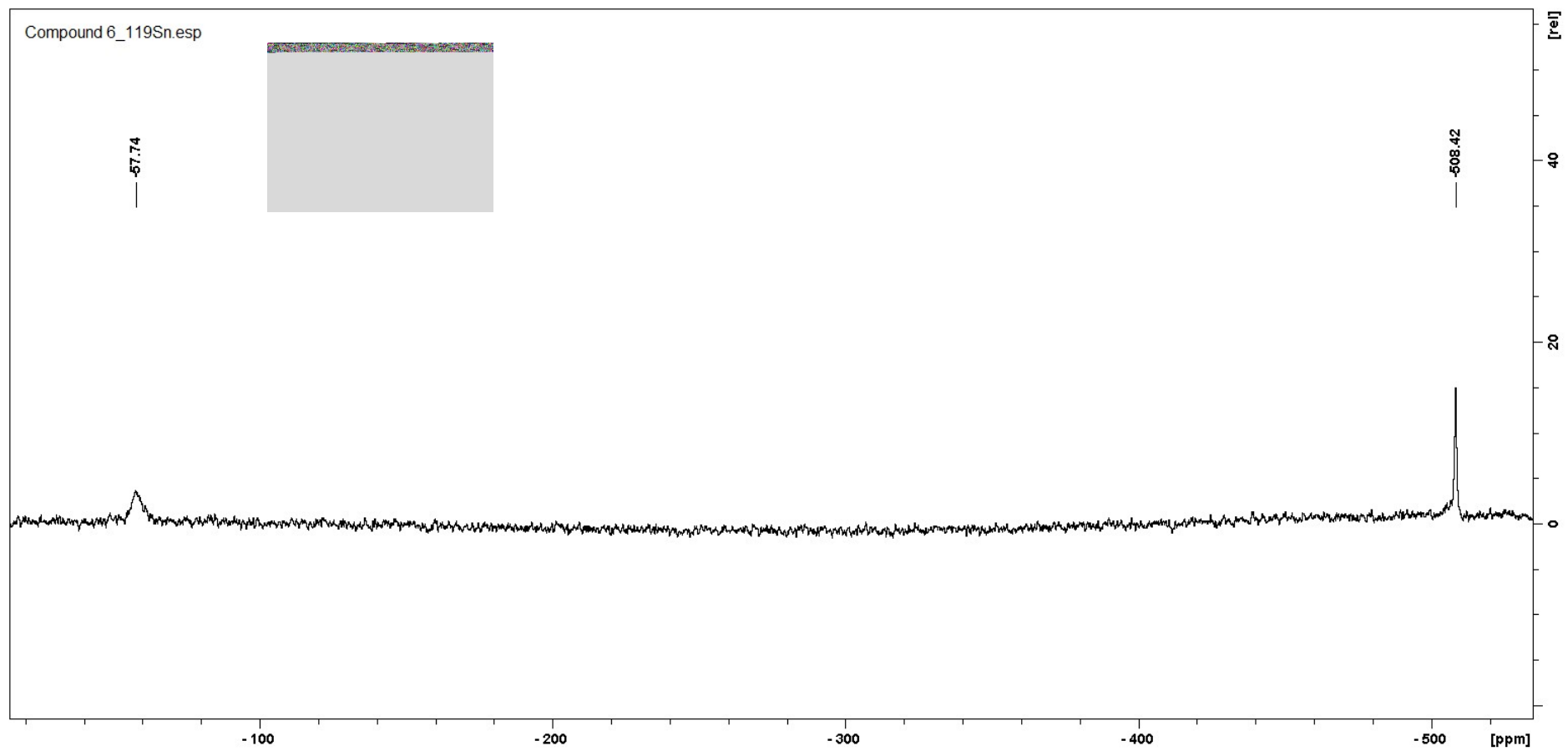


Figure S45. ^{119}Sn NMR spectrum of **6** in CDCl_3 .

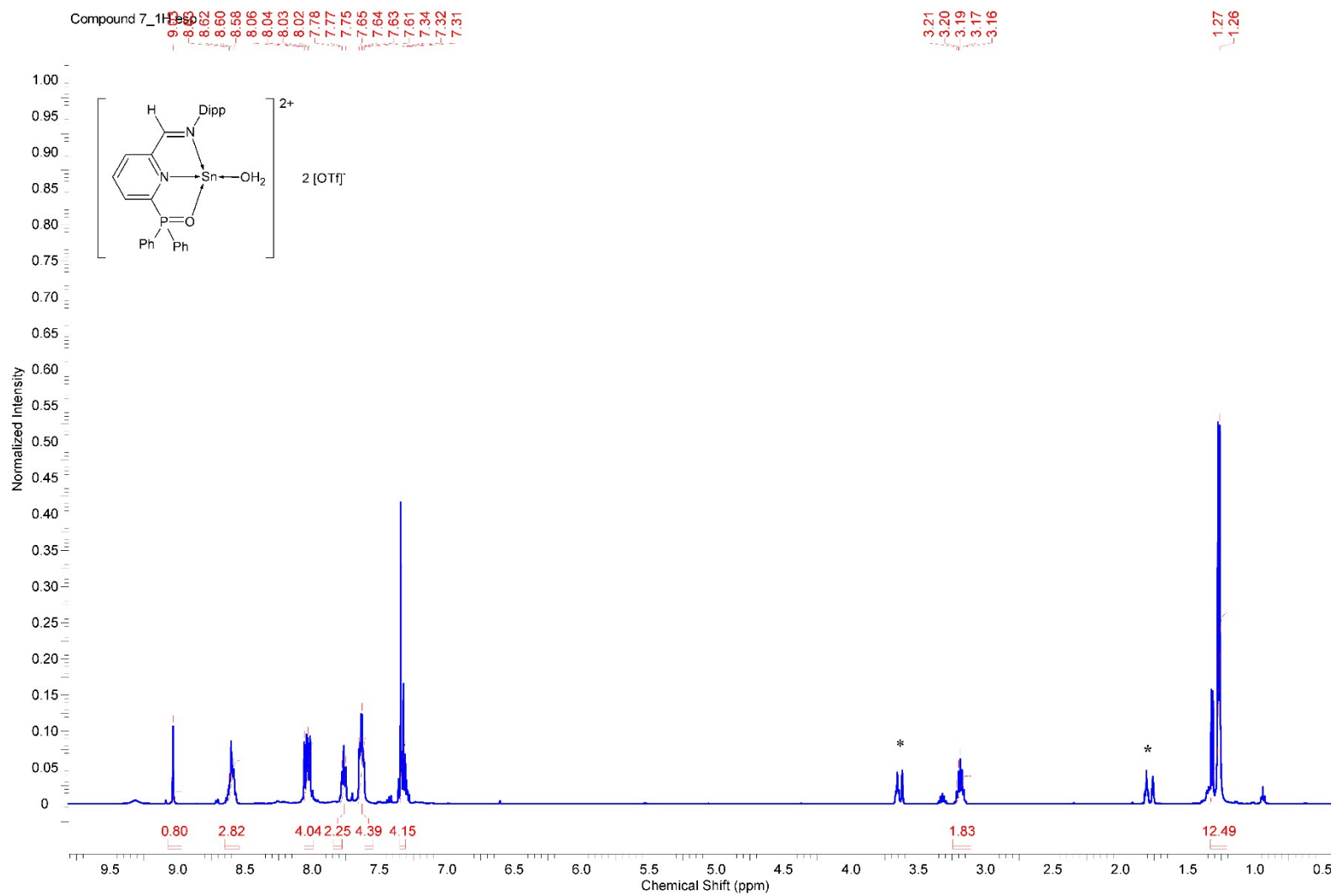


Figure S46. ^1H NMR spectrum of 7 in THF-d8. (* residual signal of THF)

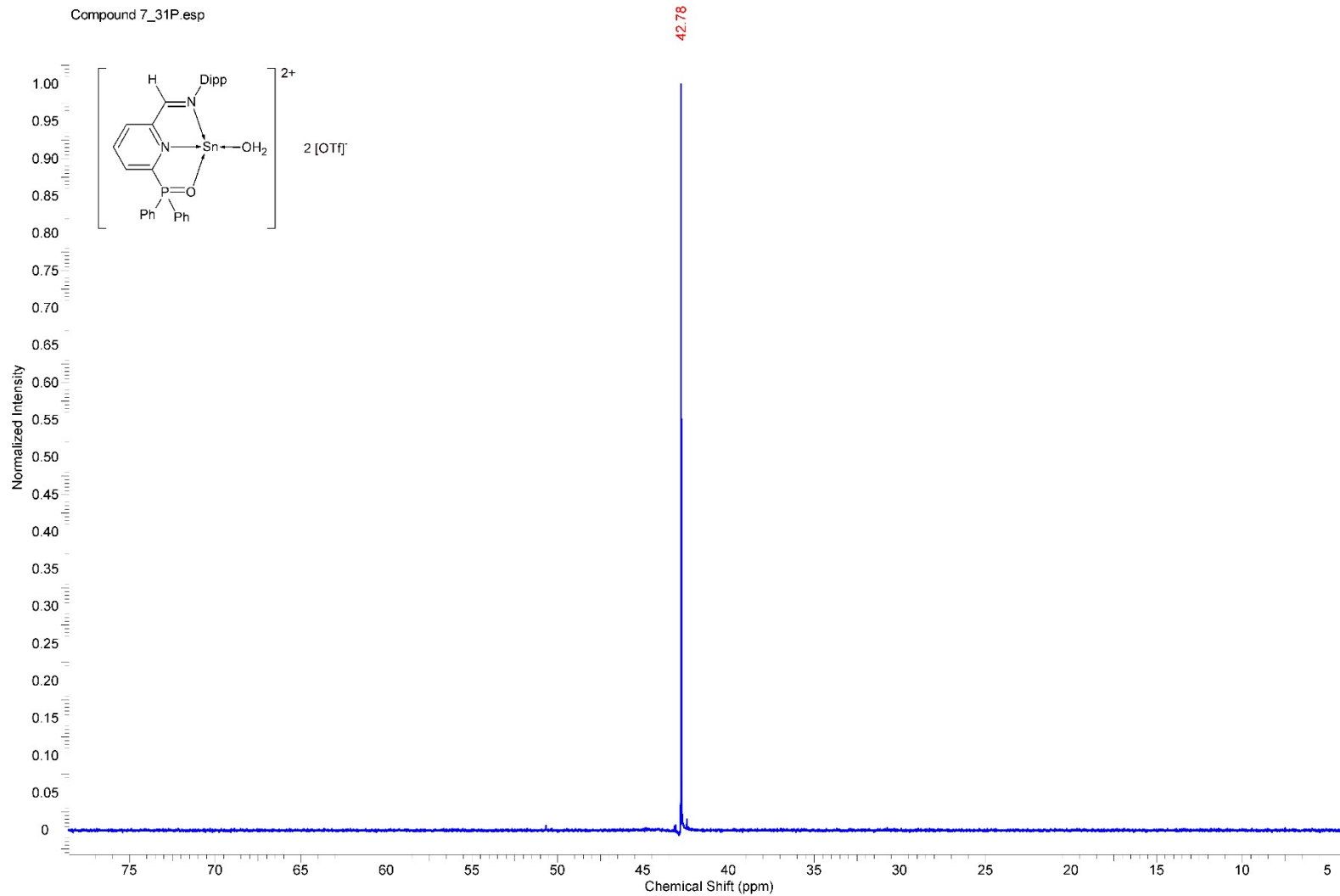


Figure S47. ^{31}P NMR spectrum of 7 in THF-d8.

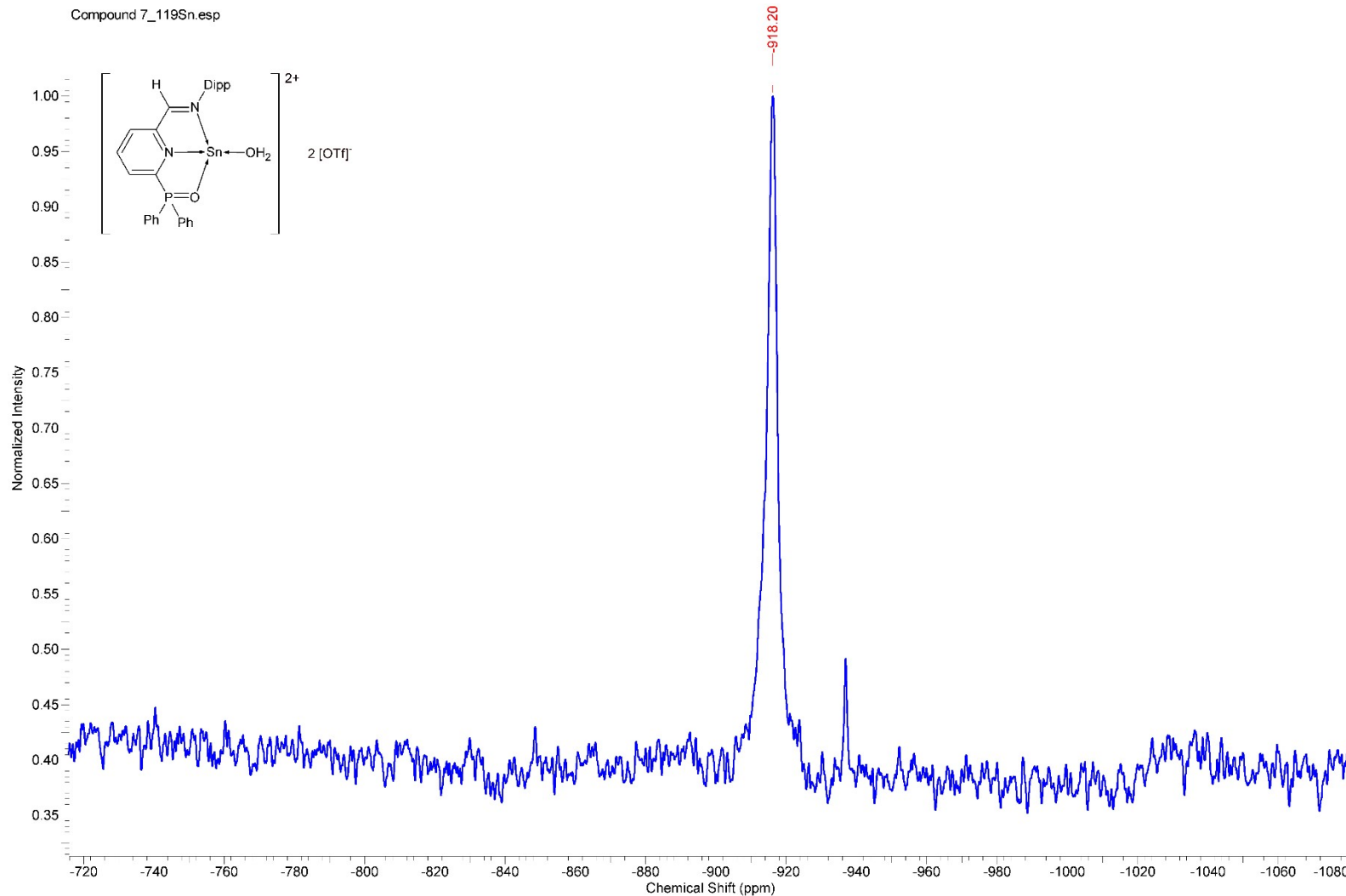


Figure S48. ^{119}Sn NMR spectrum of 7 in THF-d8.

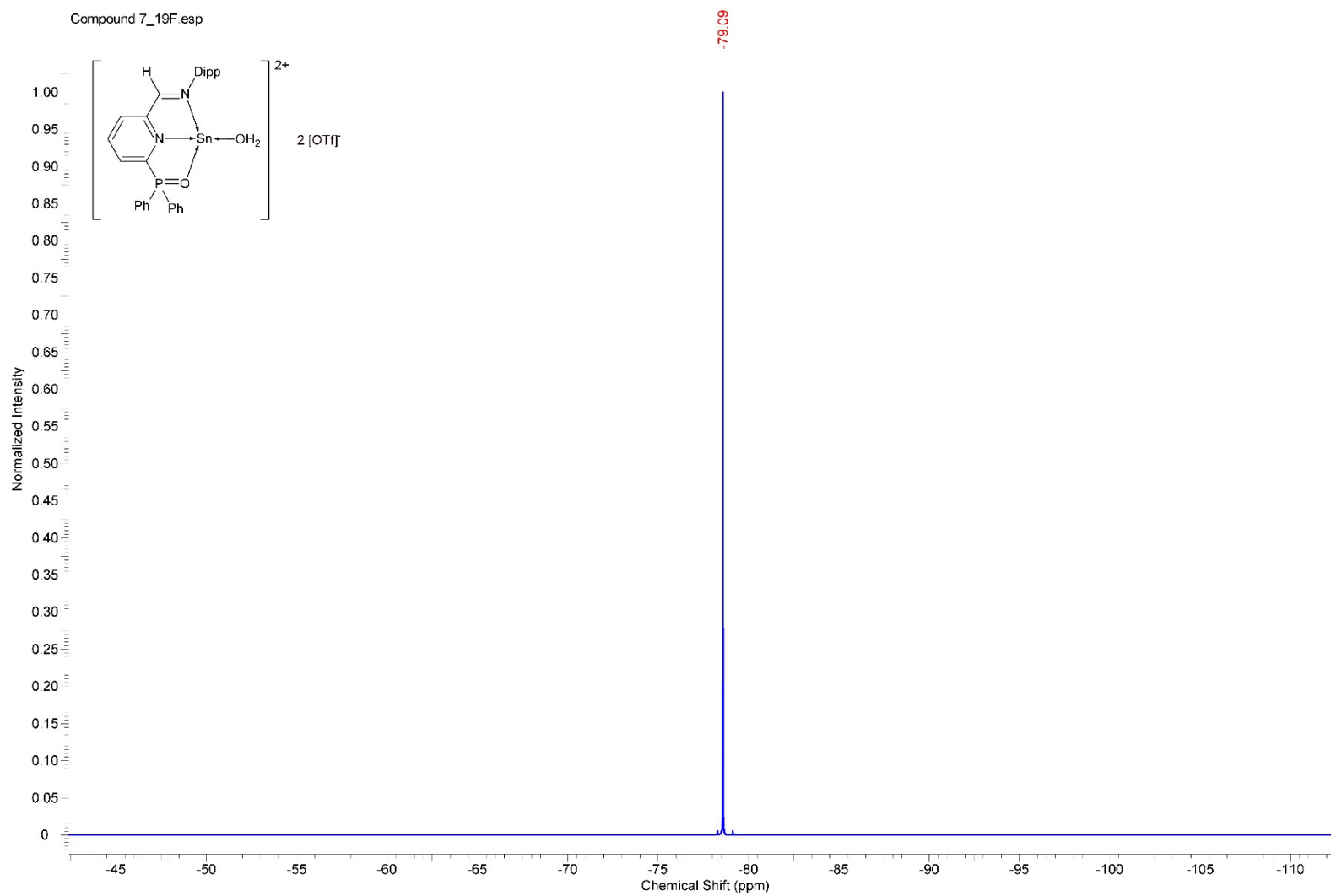


Figure S49. ¹⁹F NMR spectrum of 7 in THF-d8.

Compound 8_1H.esp

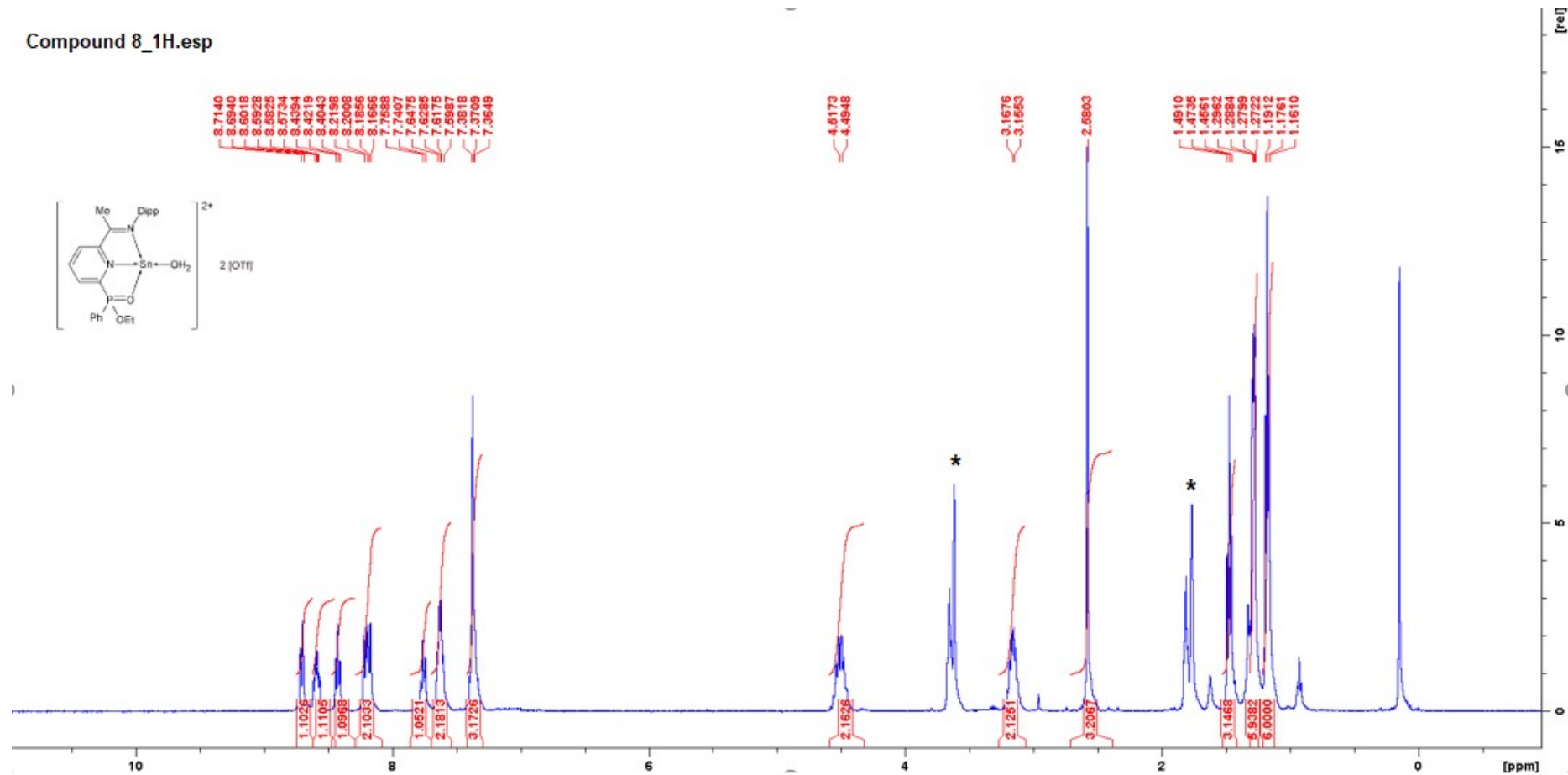


Figure S50. ¹H NMR spectrum of 8 in THF-d8. (* residual signal of THF)

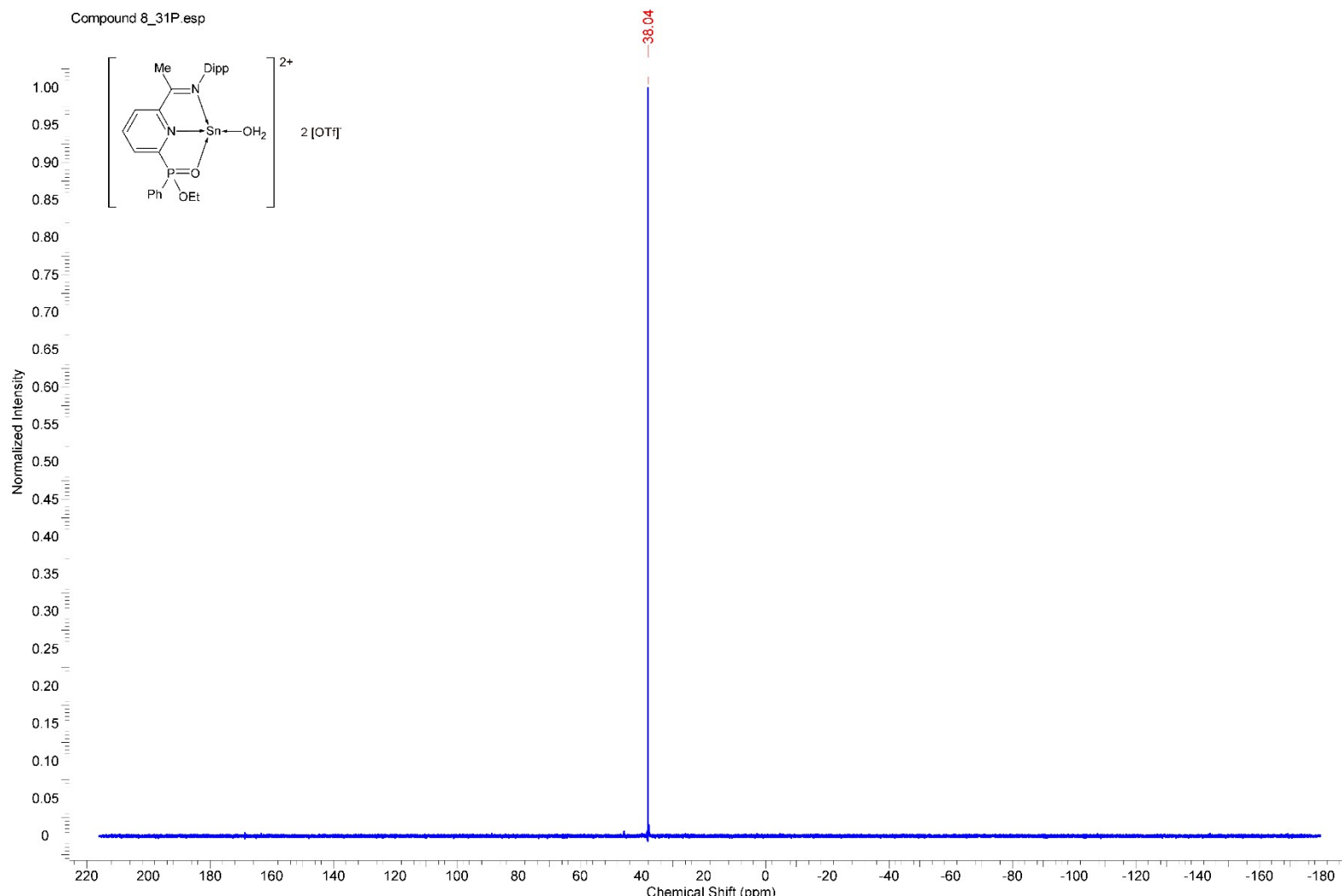


Figure S51. ^{31}P NMR spectrum of **8** in THF-d_8 .

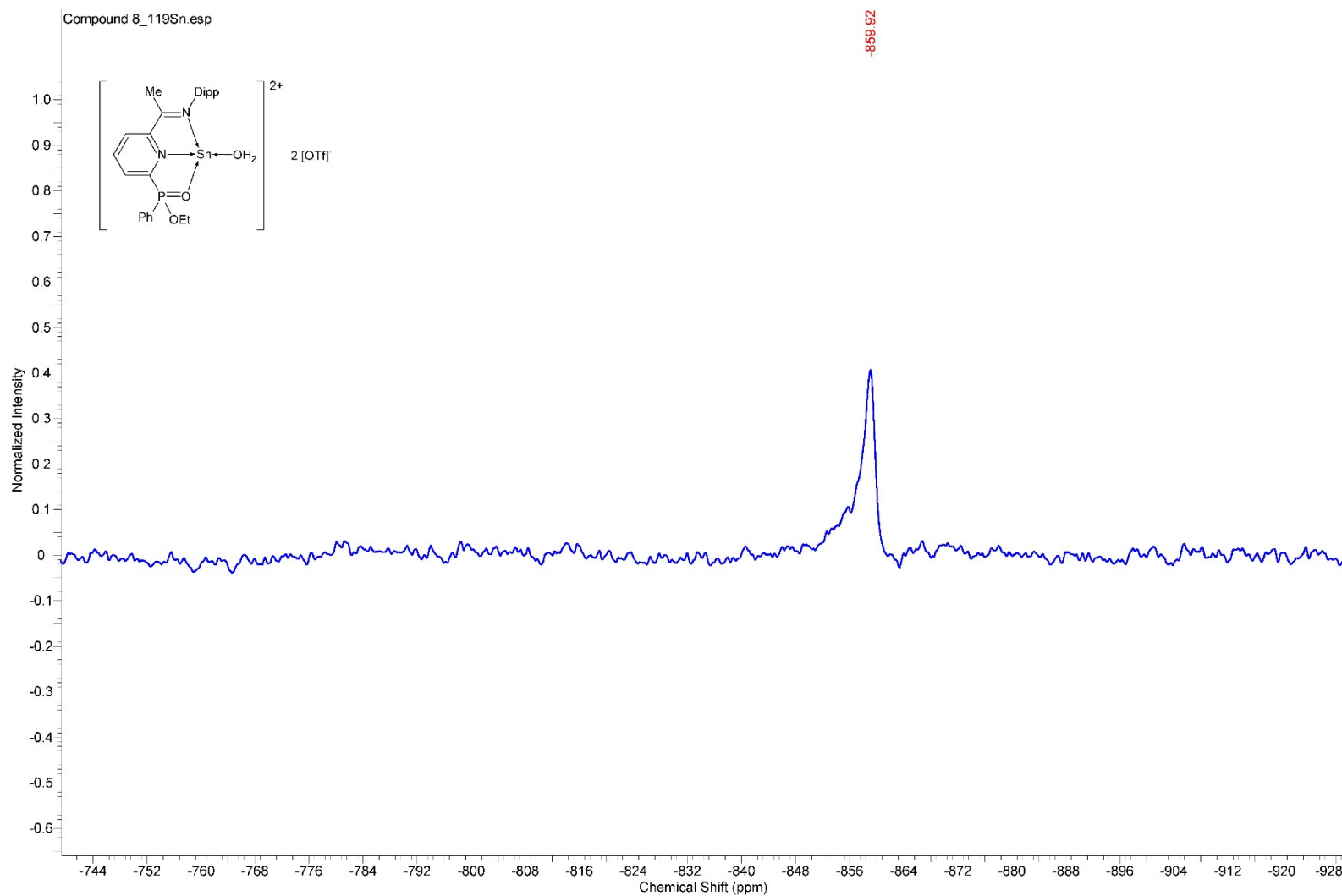


Figure S52. ^{119}Sn NMR spectrum of **8** in THF-d₈.

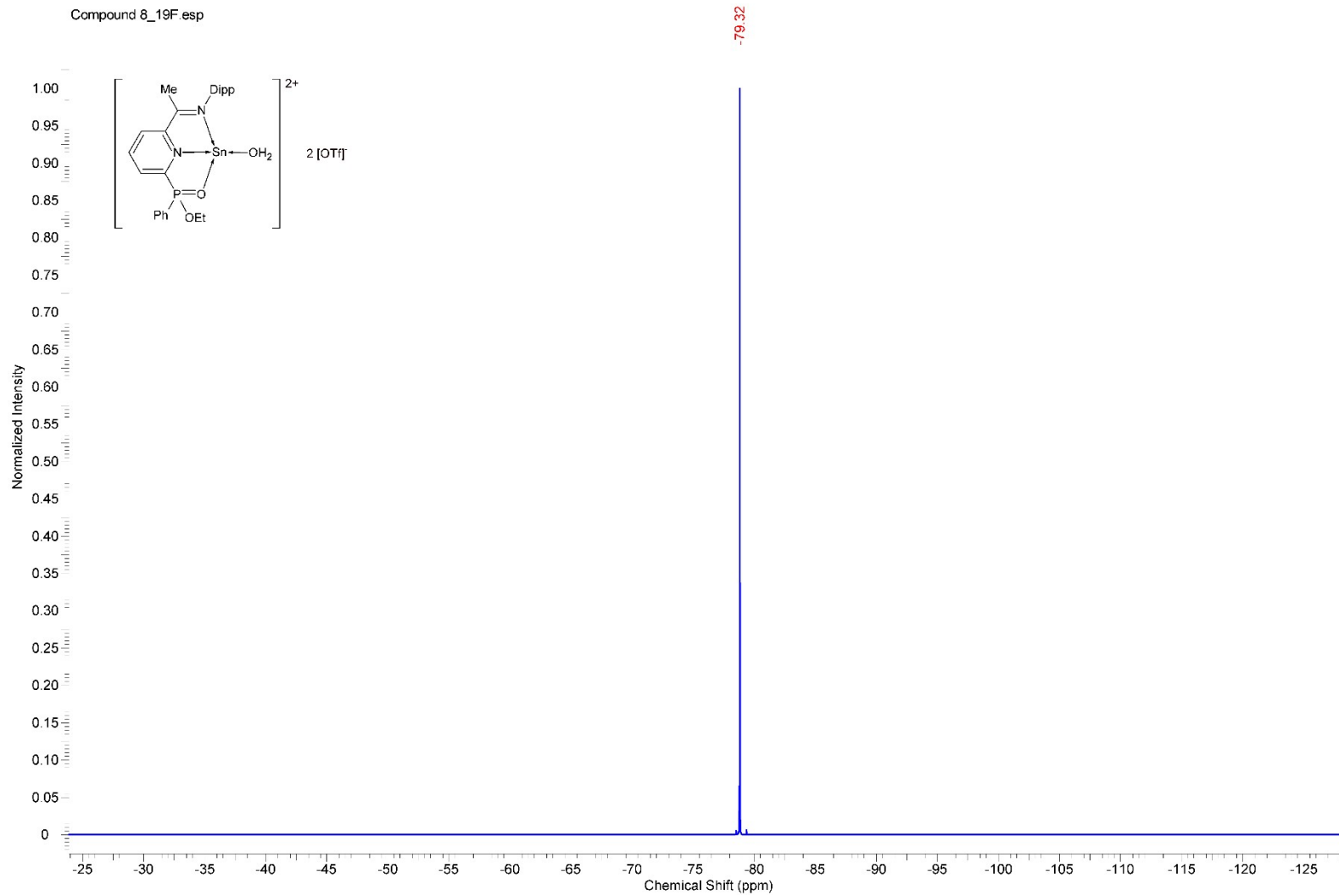


Figure S53. ¹⁹F NMR spectrum of **8** in THF-d8.

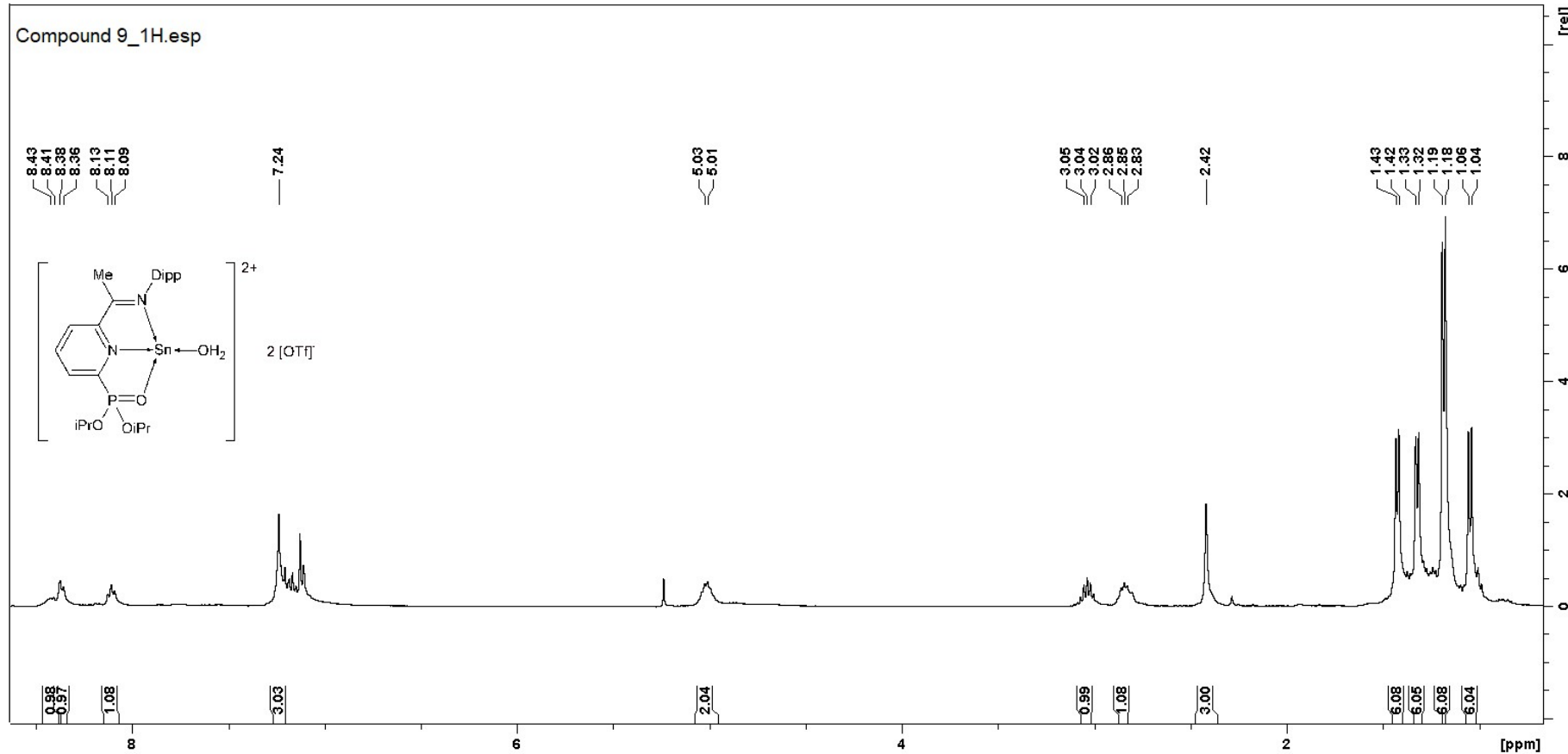


Figure S54. ^1H NMR spectrum of **9** in CDCl_3 .

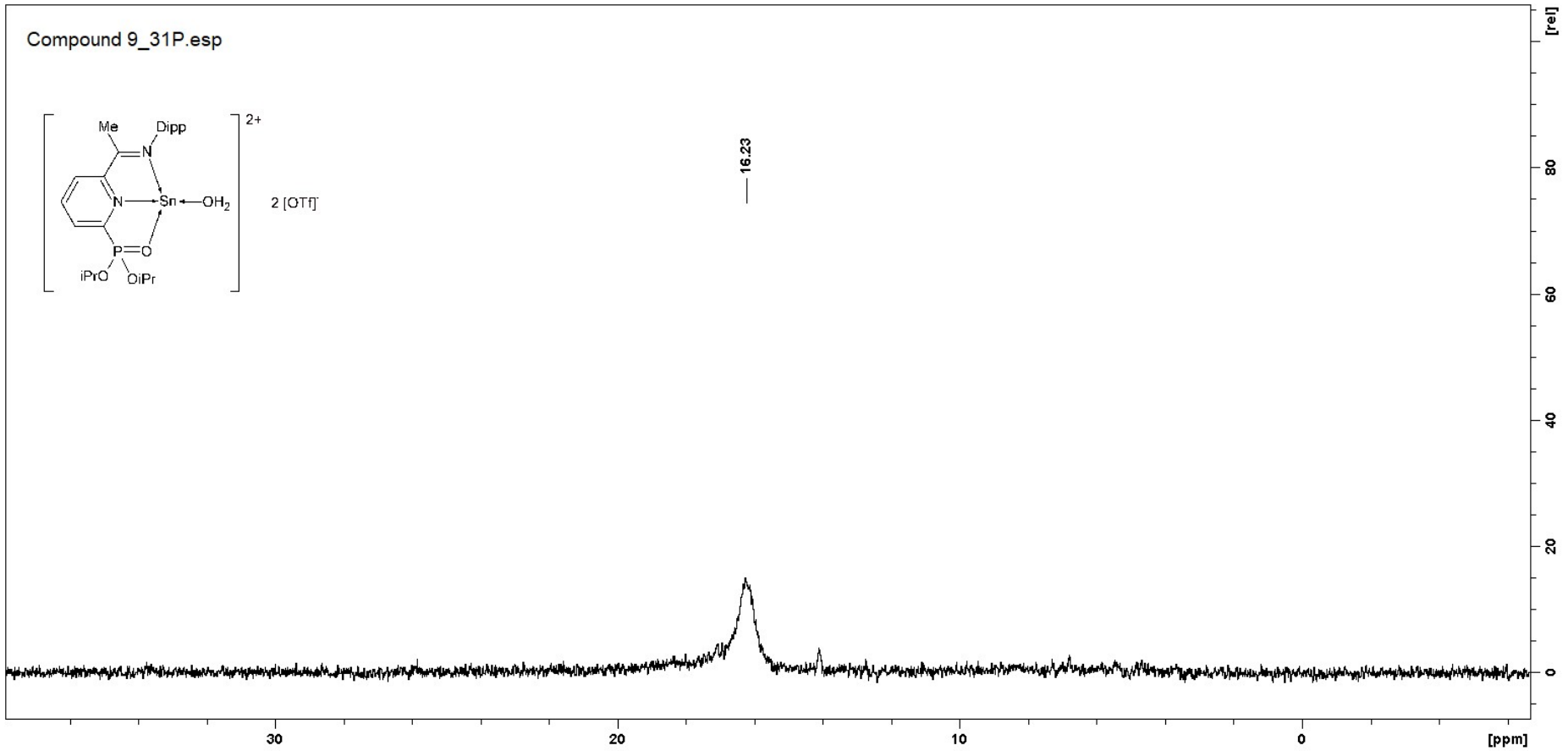


Figure S55. ^{31}P NMR spectrum of **9** in CDCl_3 .

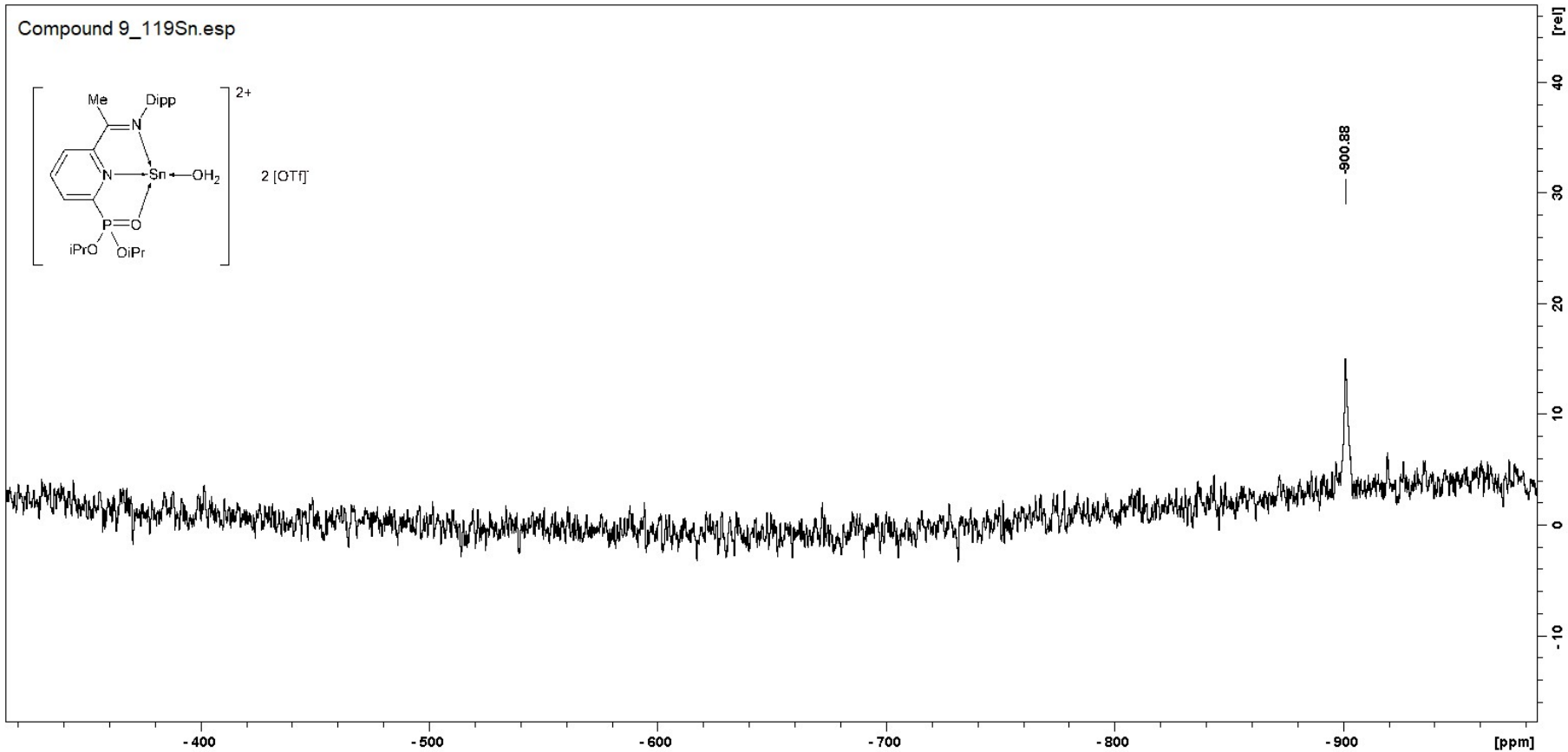


Figure S56. ^{119}Sn NMR spectrum of **9** in CDCl_3 .

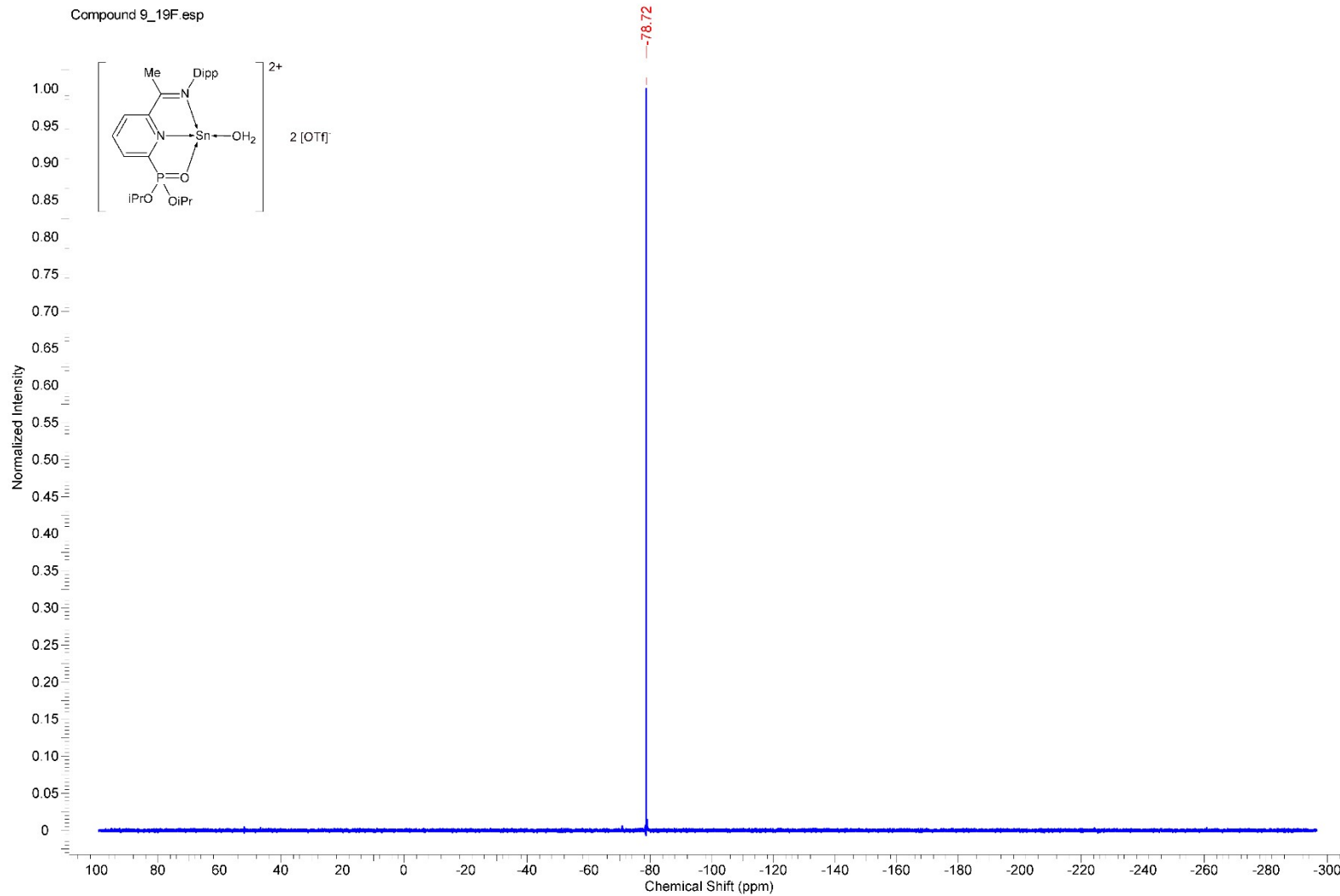


Figure S57. ¹⁹F NMR spectrum of **9** in CDCl₃.

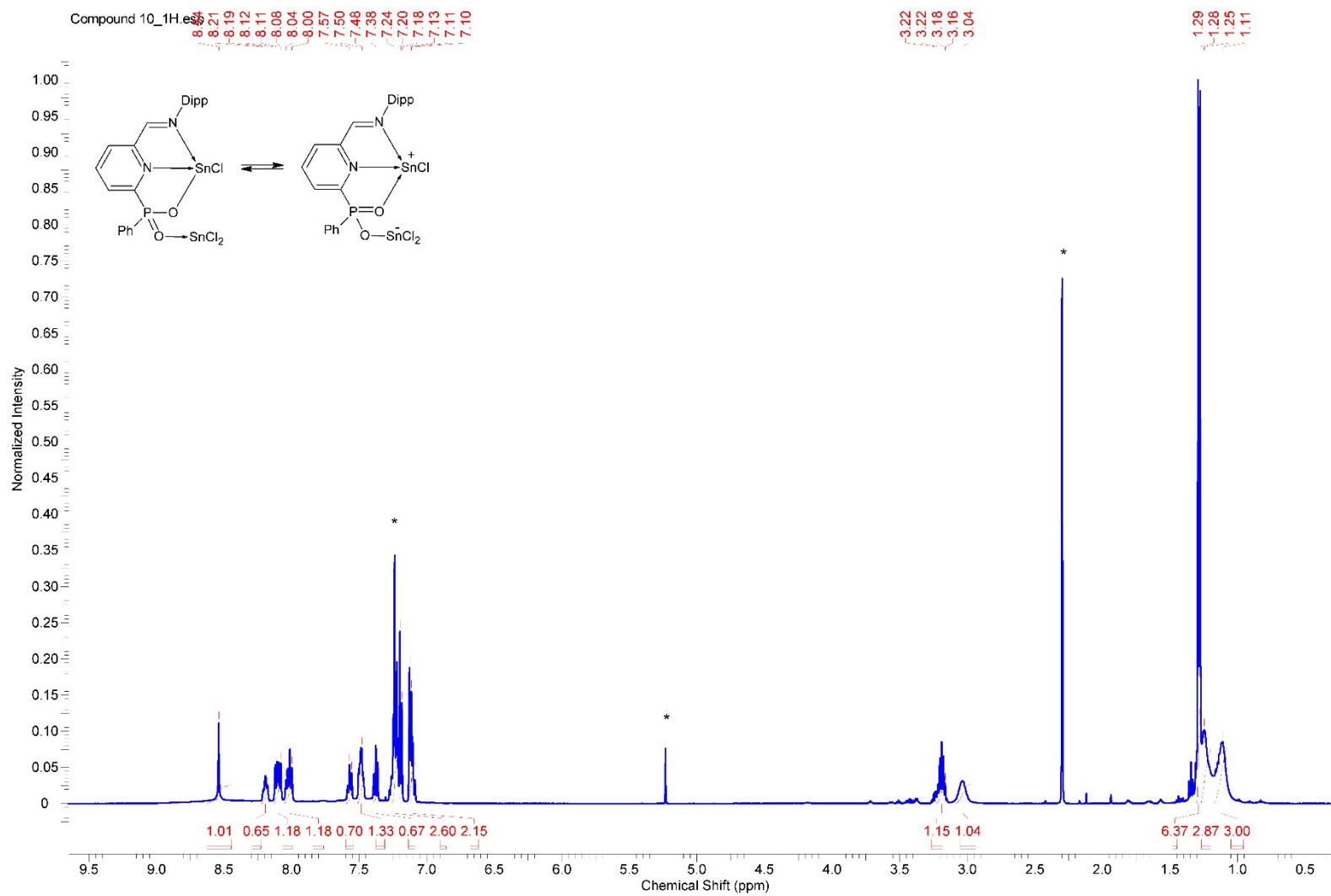


Figure S58. ¹H NMR spectrum of **10** in CDCl₃. (* residual signal of toluene and CH₂Cl₂)

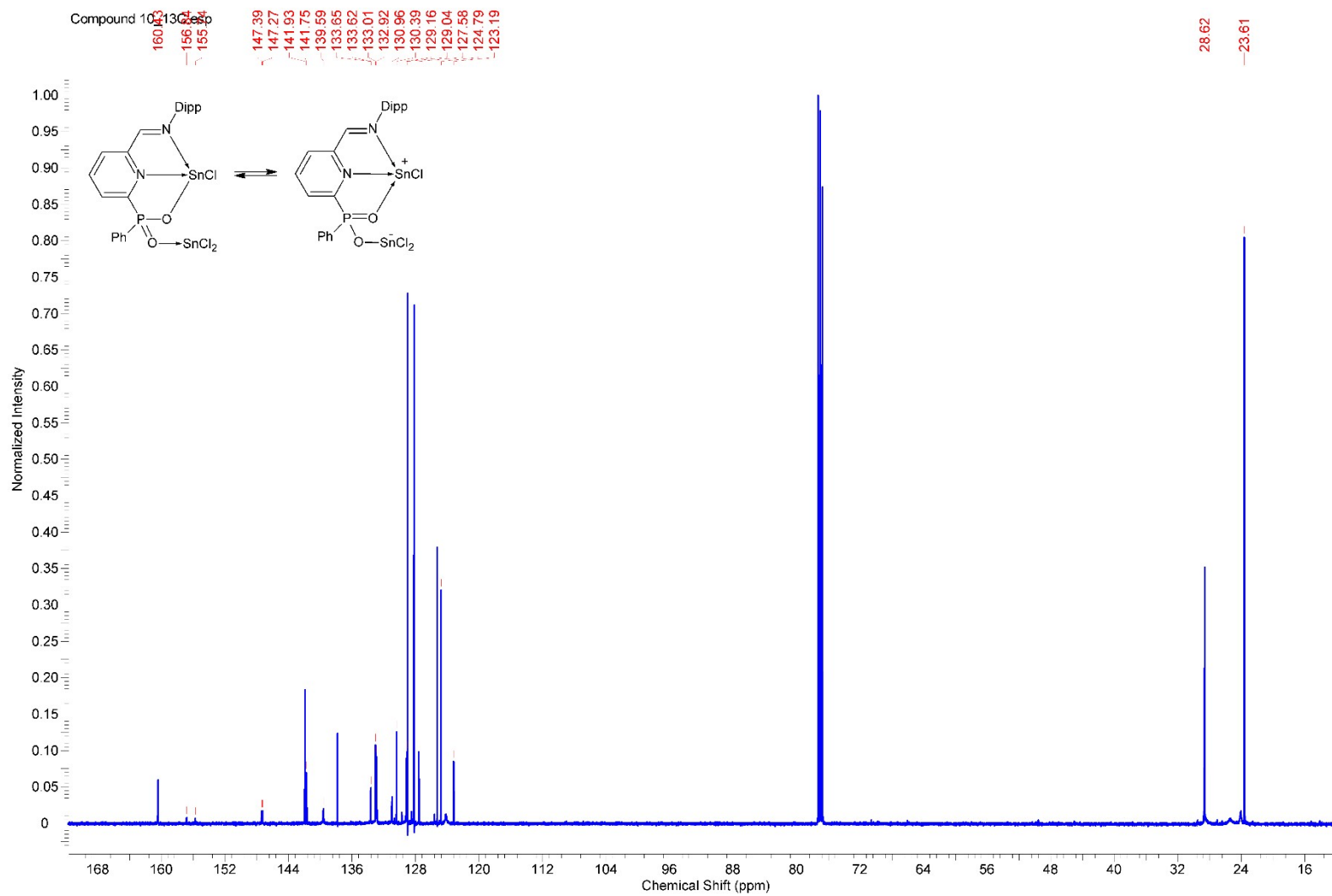


Figure S59. ¹³C NMR spectrum of **10** in CDCl₃.

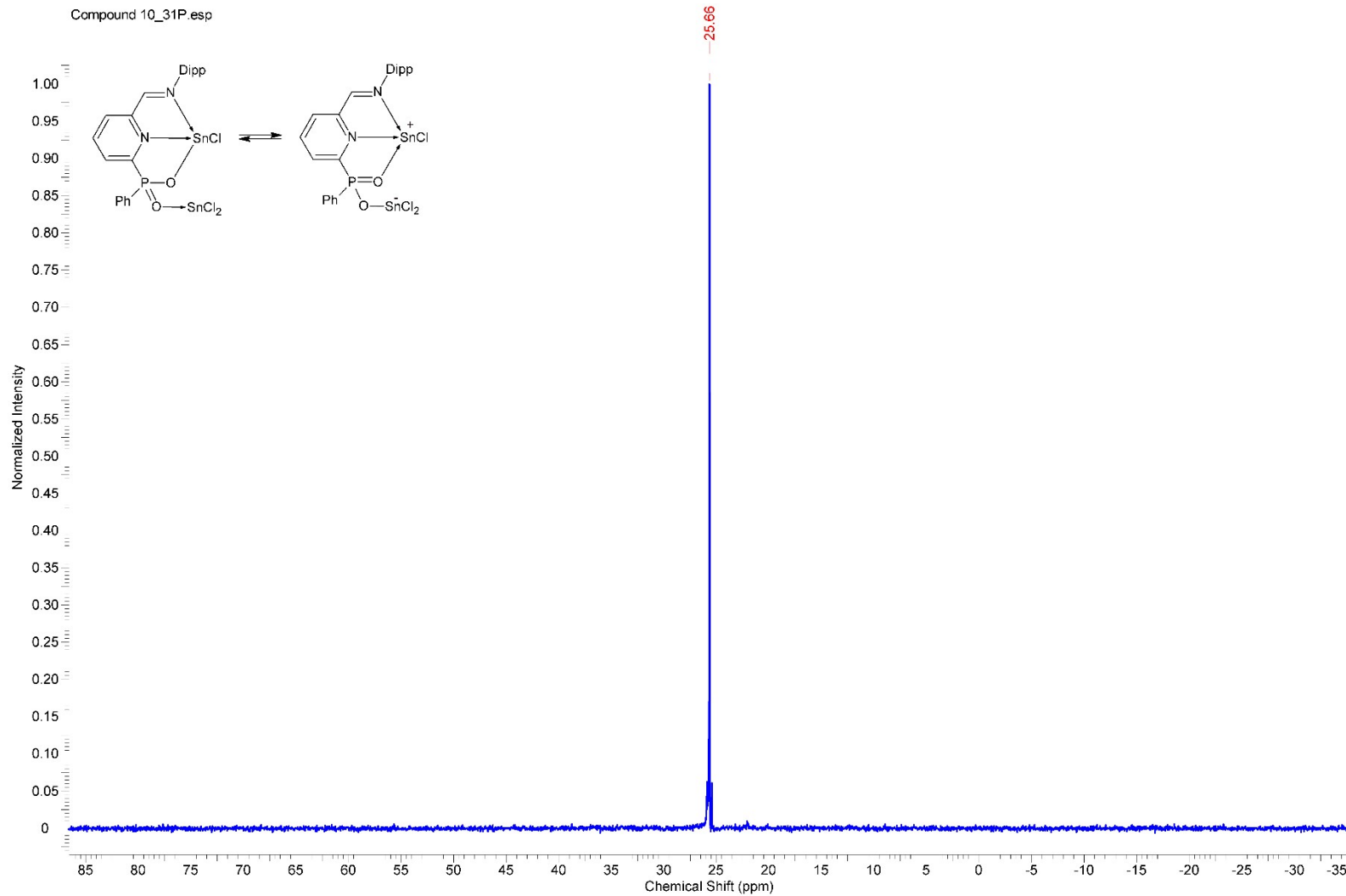


Figure S60. ^{31}P NMR spectrum of **10** in CDCl_3 .

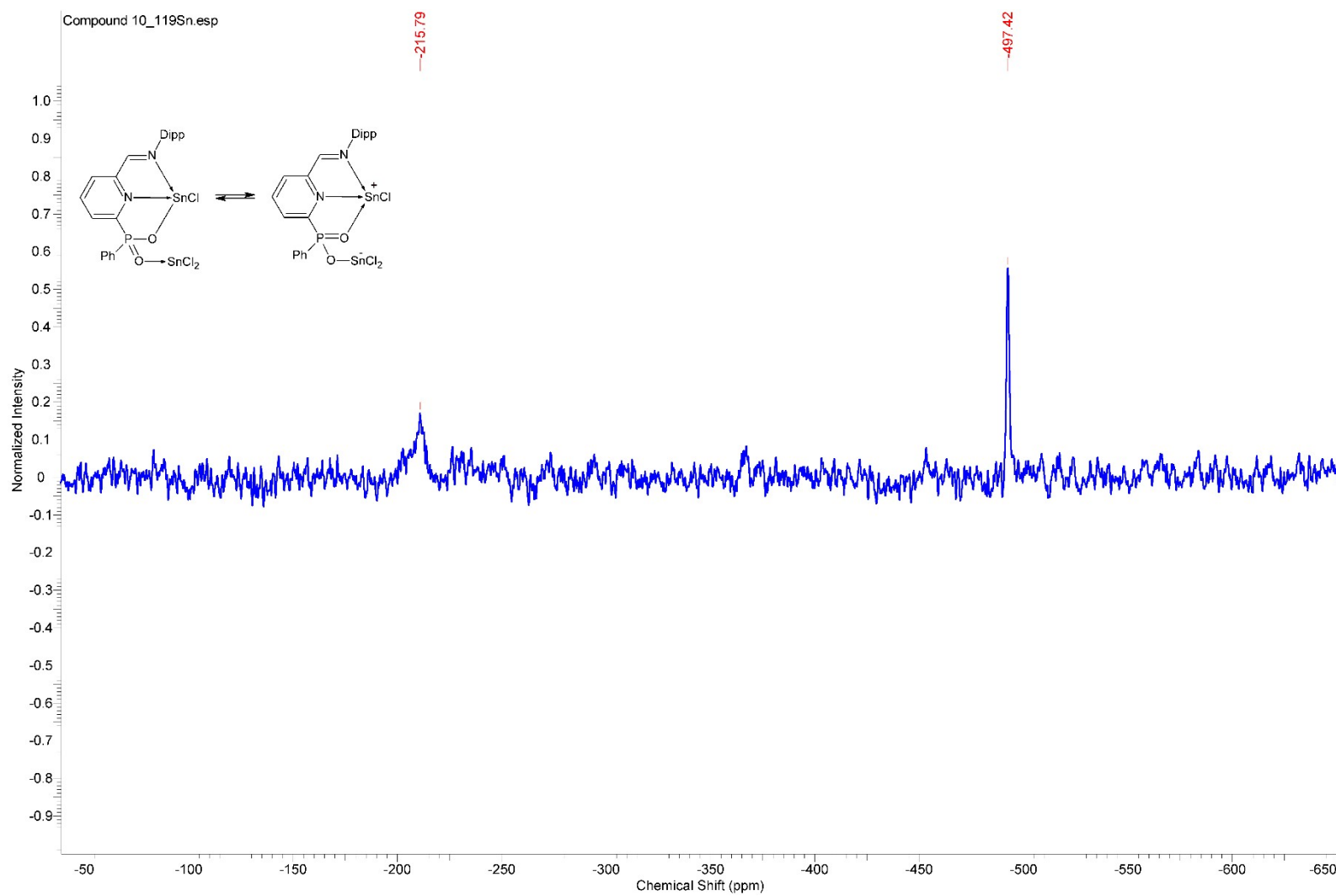


Figure S61. ^{119}Sn NMR spectrum of **10** in CDCl_3 .

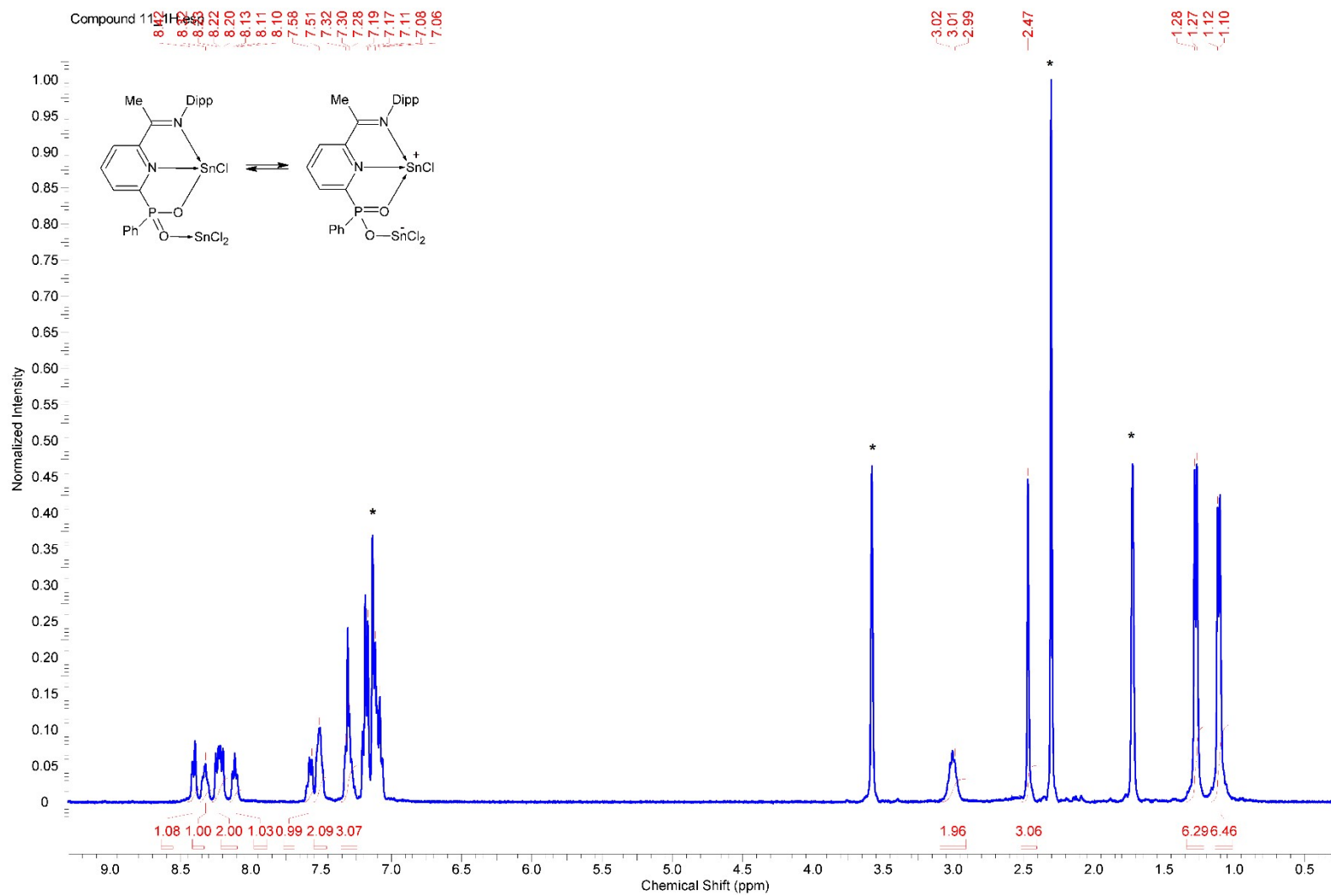


Figure S62. ^1H NMR spectrum of **11** in CDCl_3 . (*) residual signal of toluene and THF)

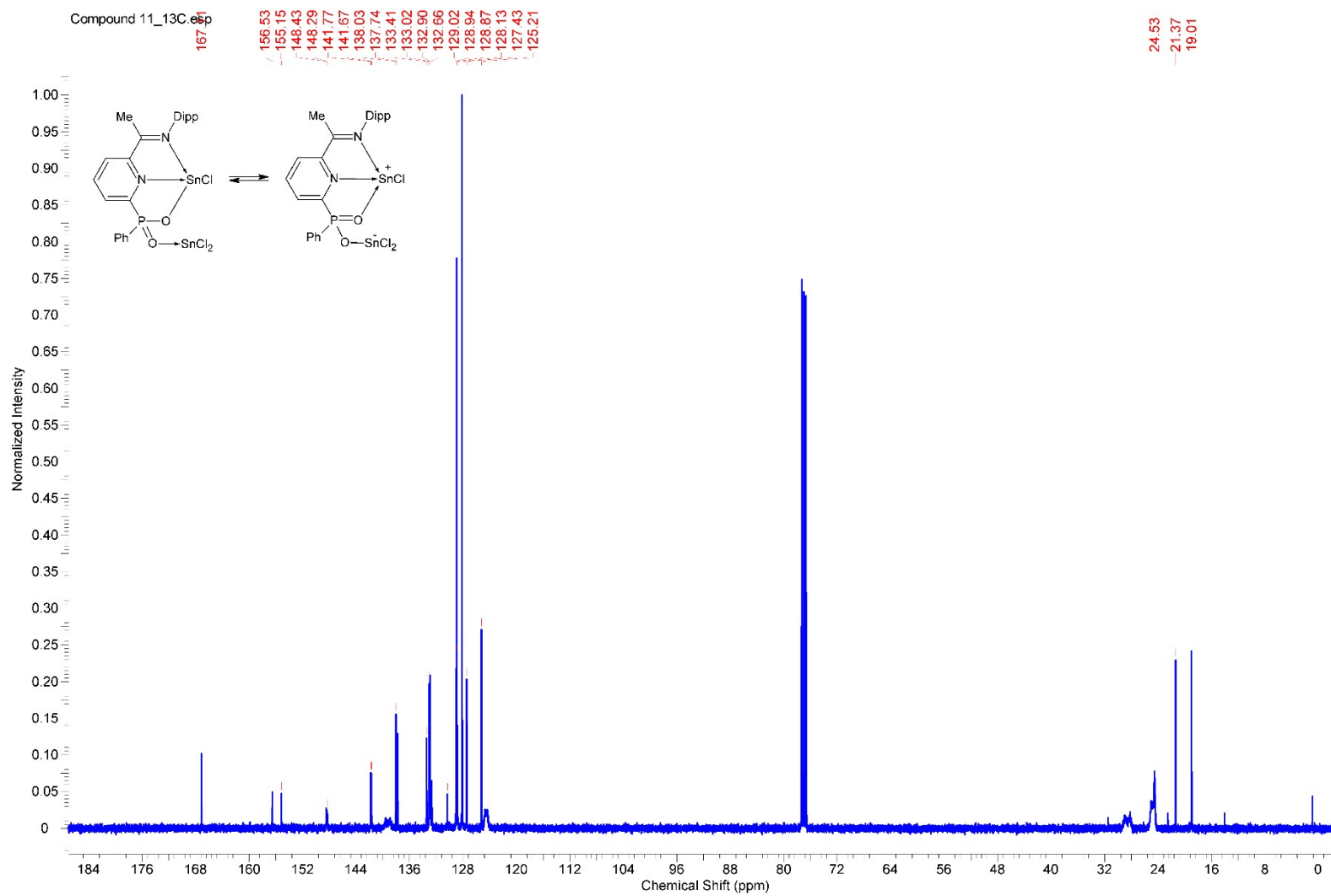


Figure S63. ^{13}C NMR spectrum of **11** in CDCl_3 .

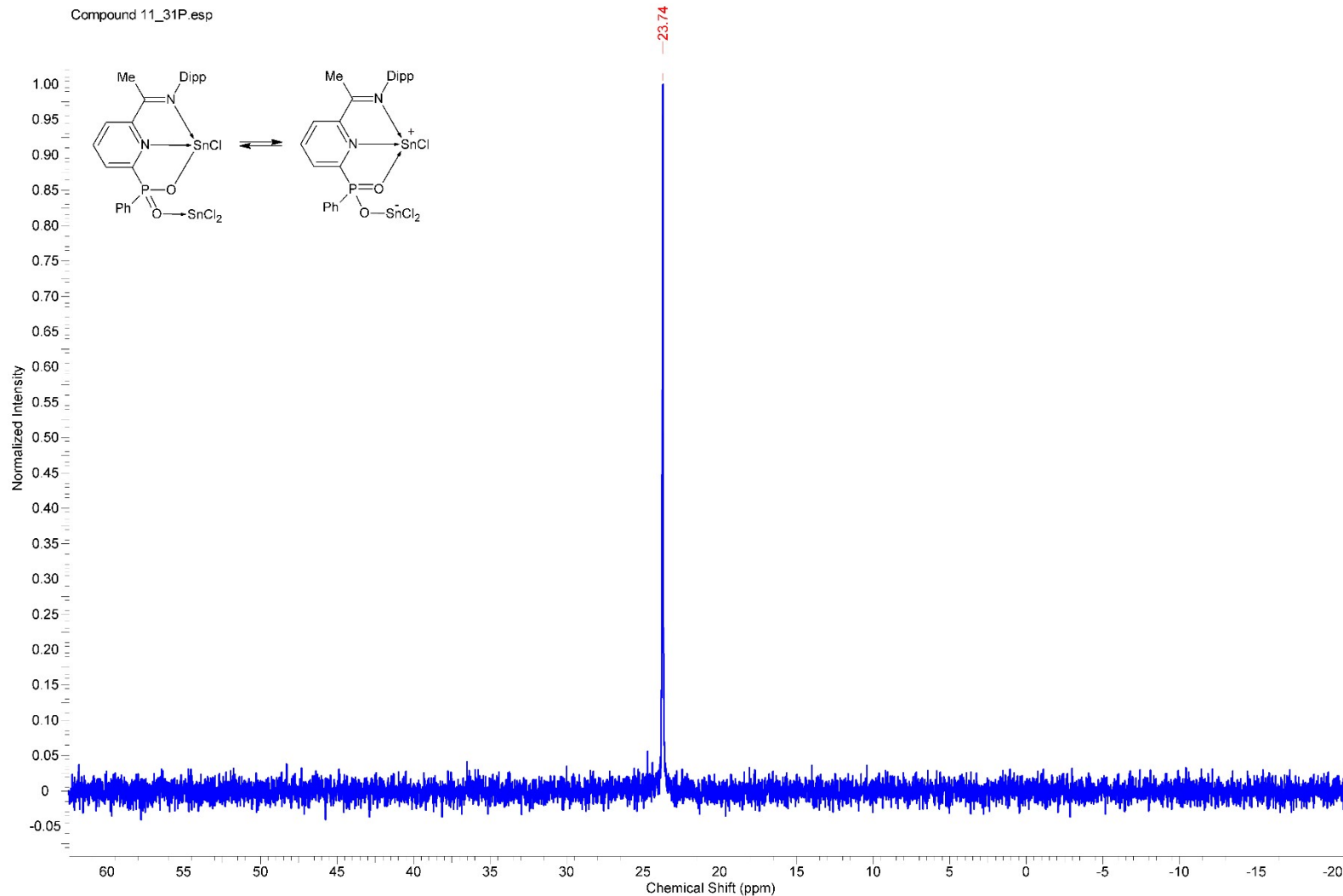


Figure S64. ^{31}P NMR spectrum of **11** in CDCl_3 .

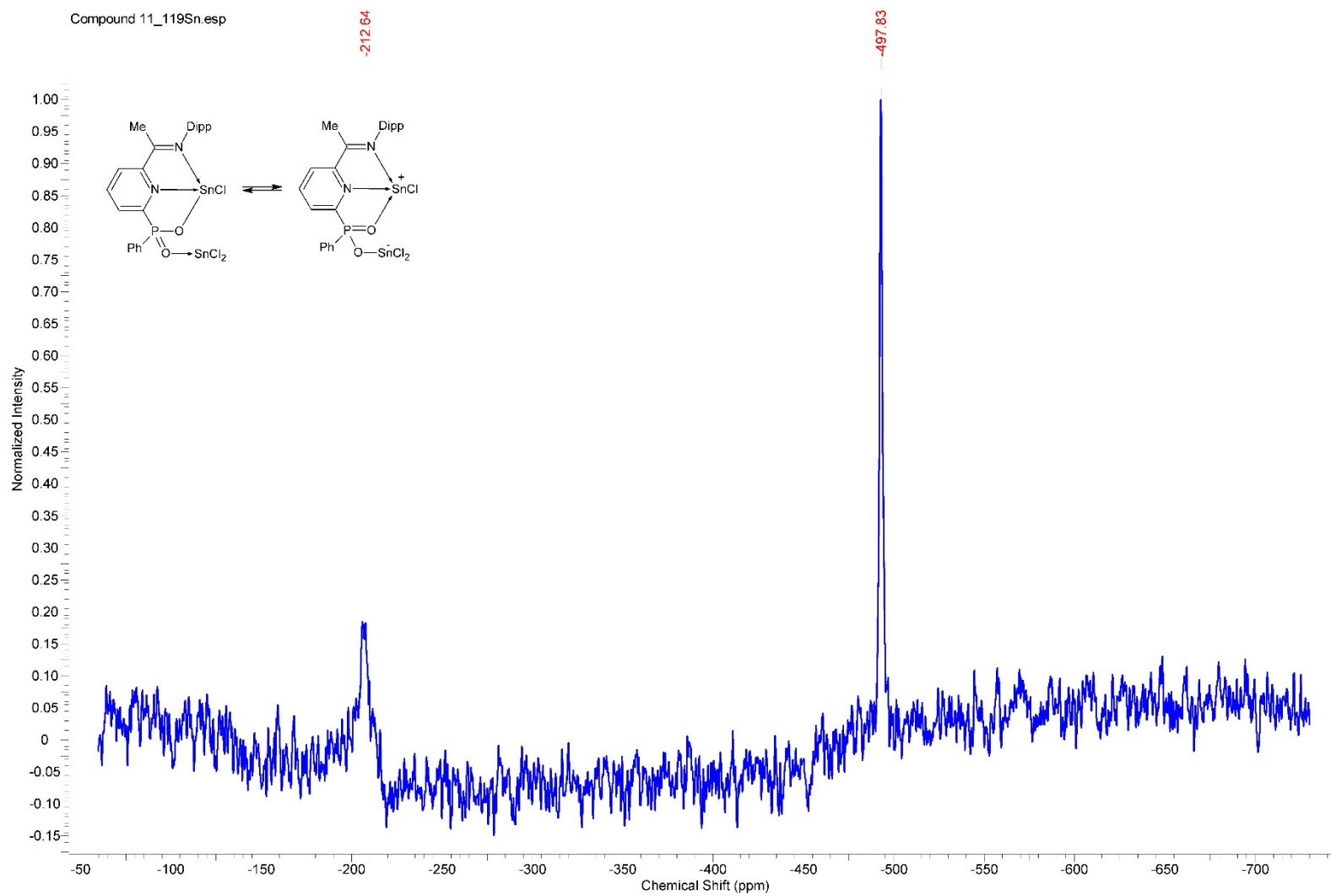


Figure S65. ^{119}Sn NMR spectrum of **11** in CDCl_3 .

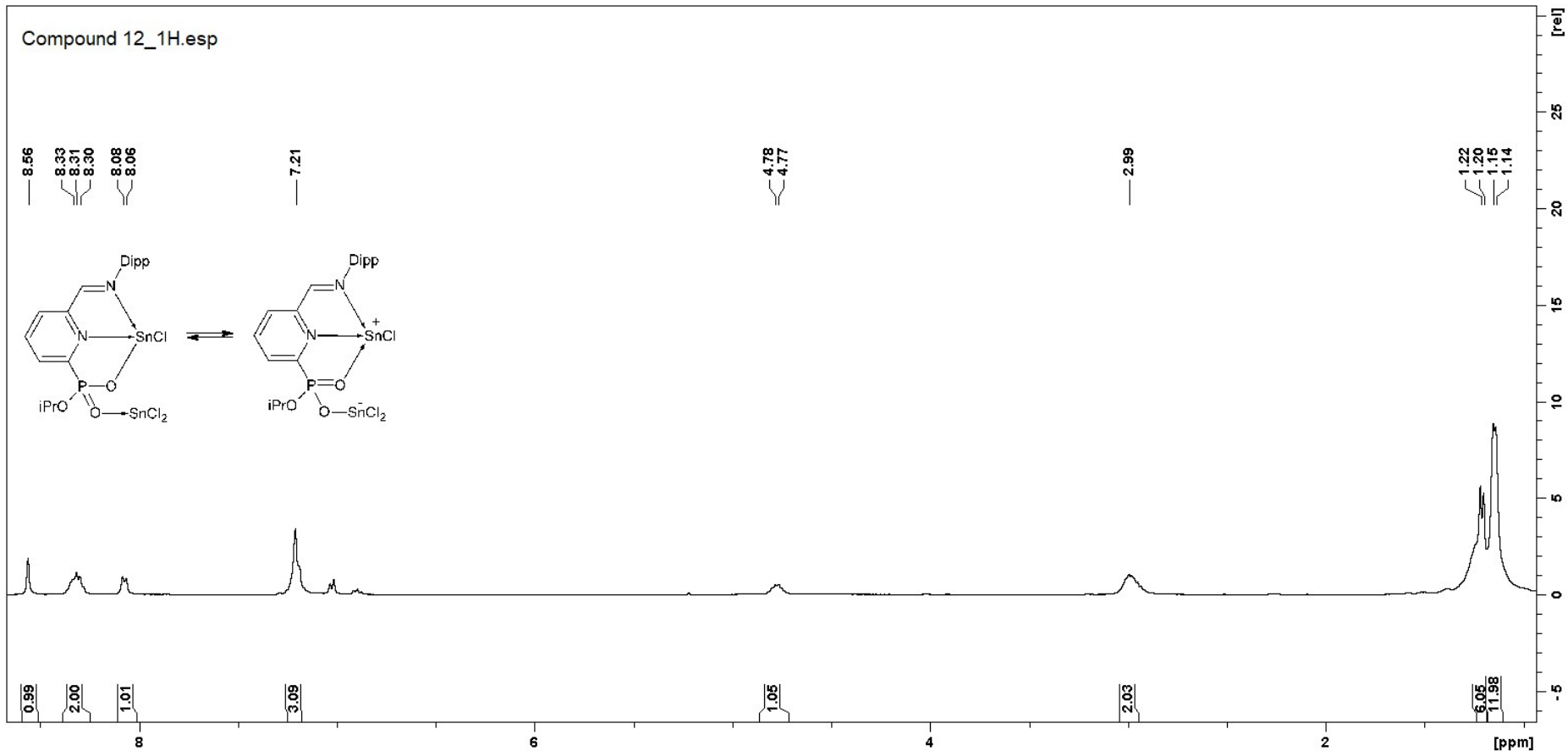


Figure S66. ^1H NMR spectrum of **12** in CDCl_3 .

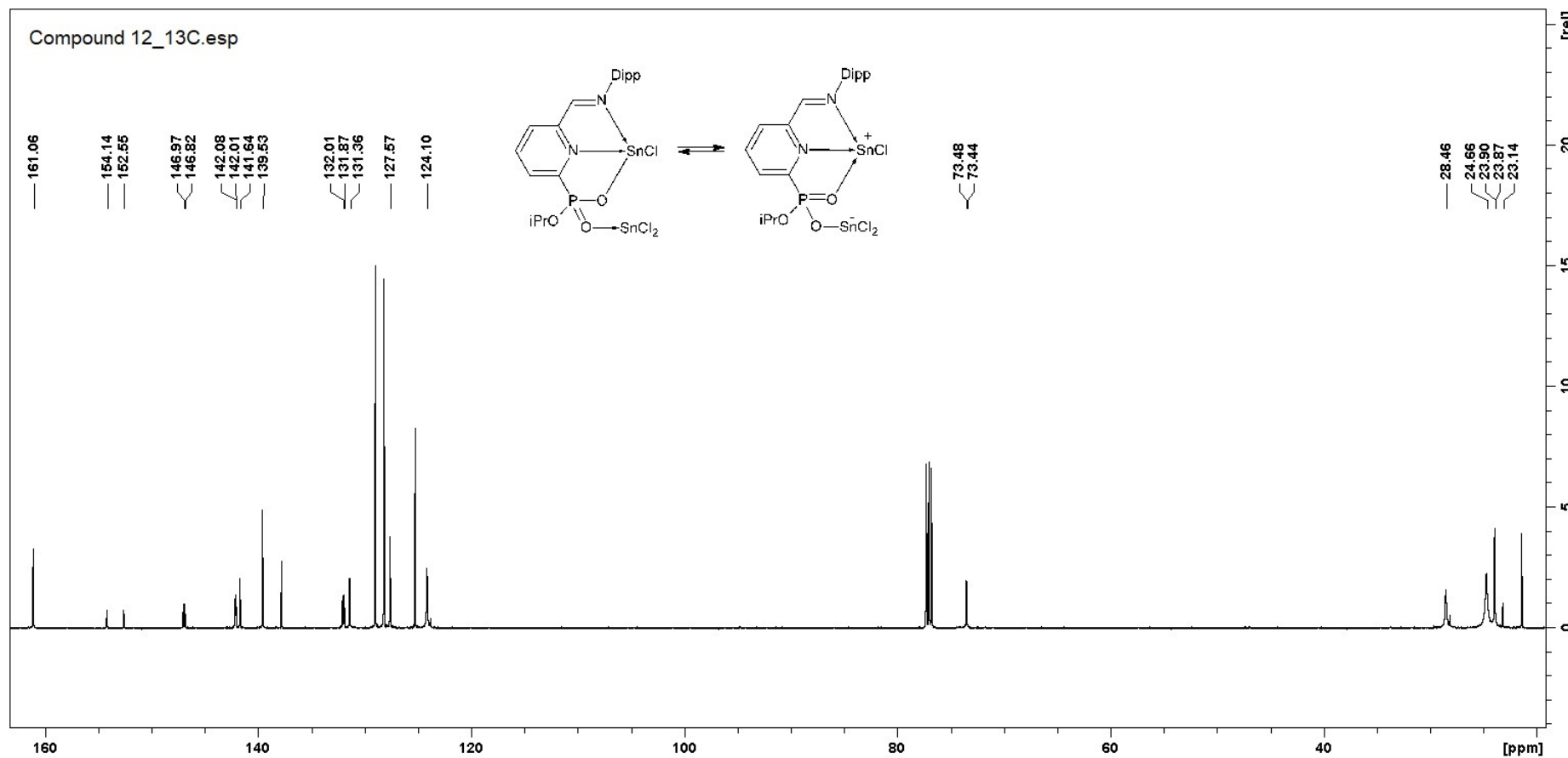


Figure S67. ^{13}C NMR spectrum of **12** in CDCl_3 .

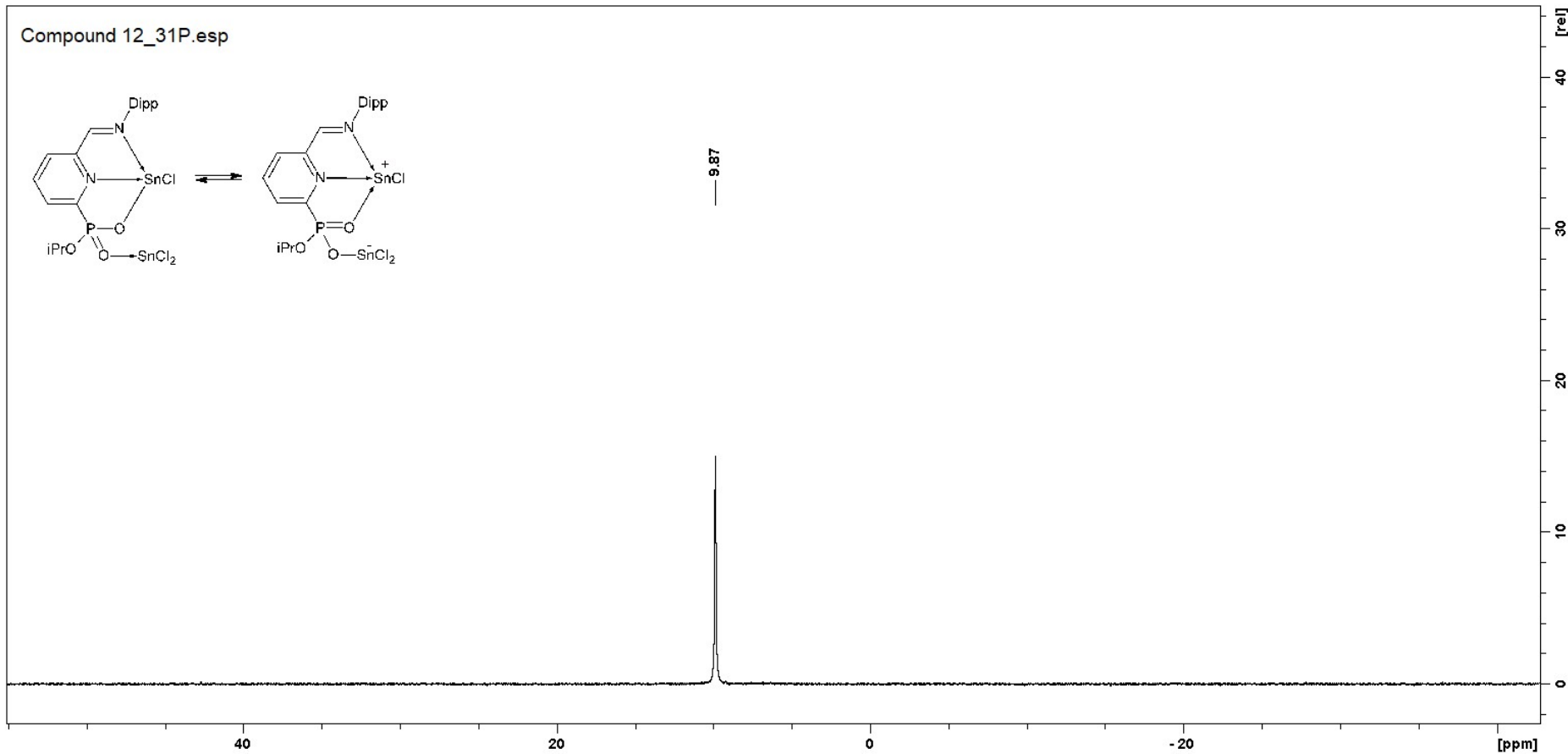


Figure S68. ^{31}P NMR spectrum of **12** in CDCl_3 .

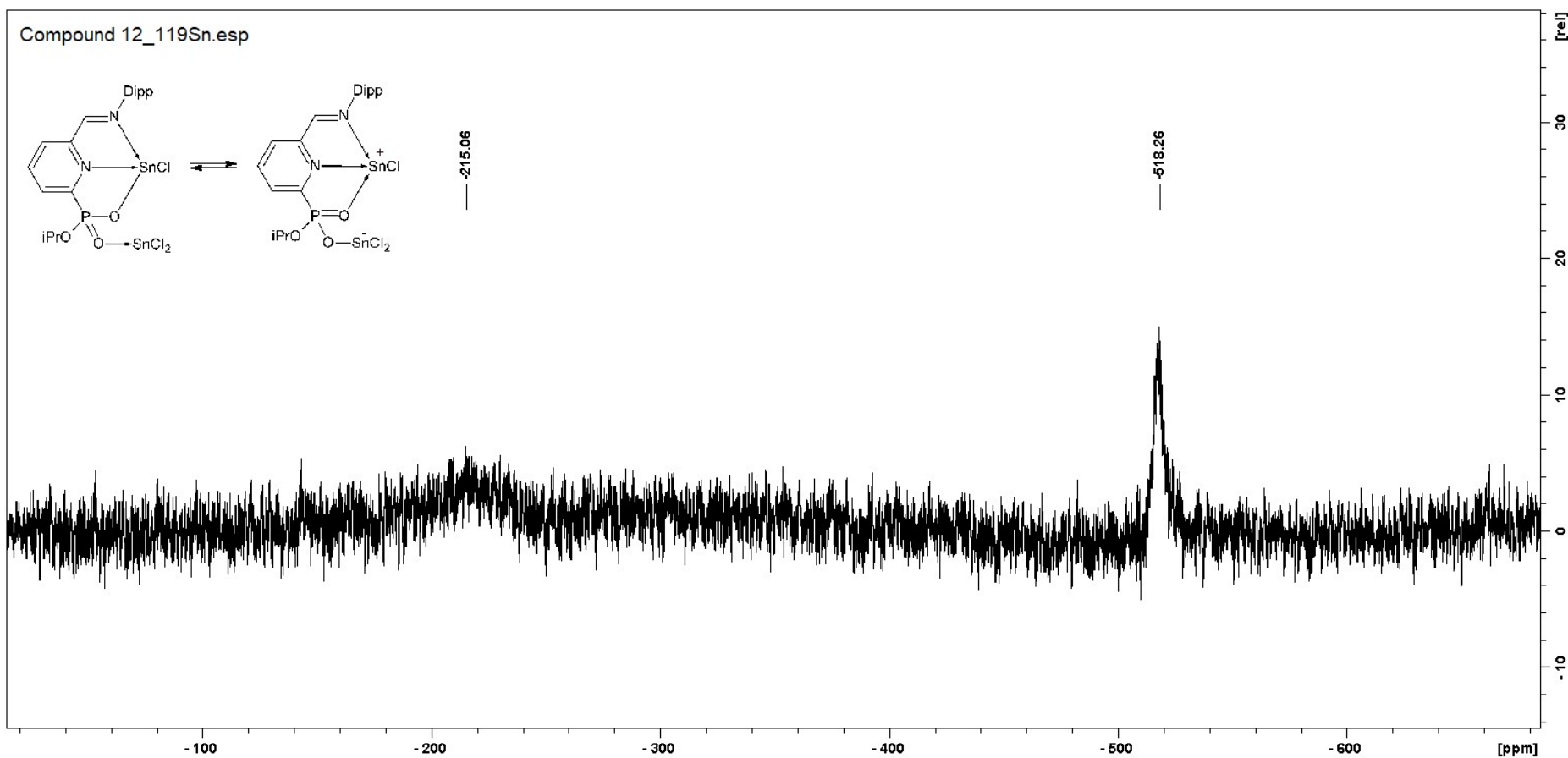


Figure S69. ¹¹⁹Sn NMR spectrum of **12** in CDCl₃.

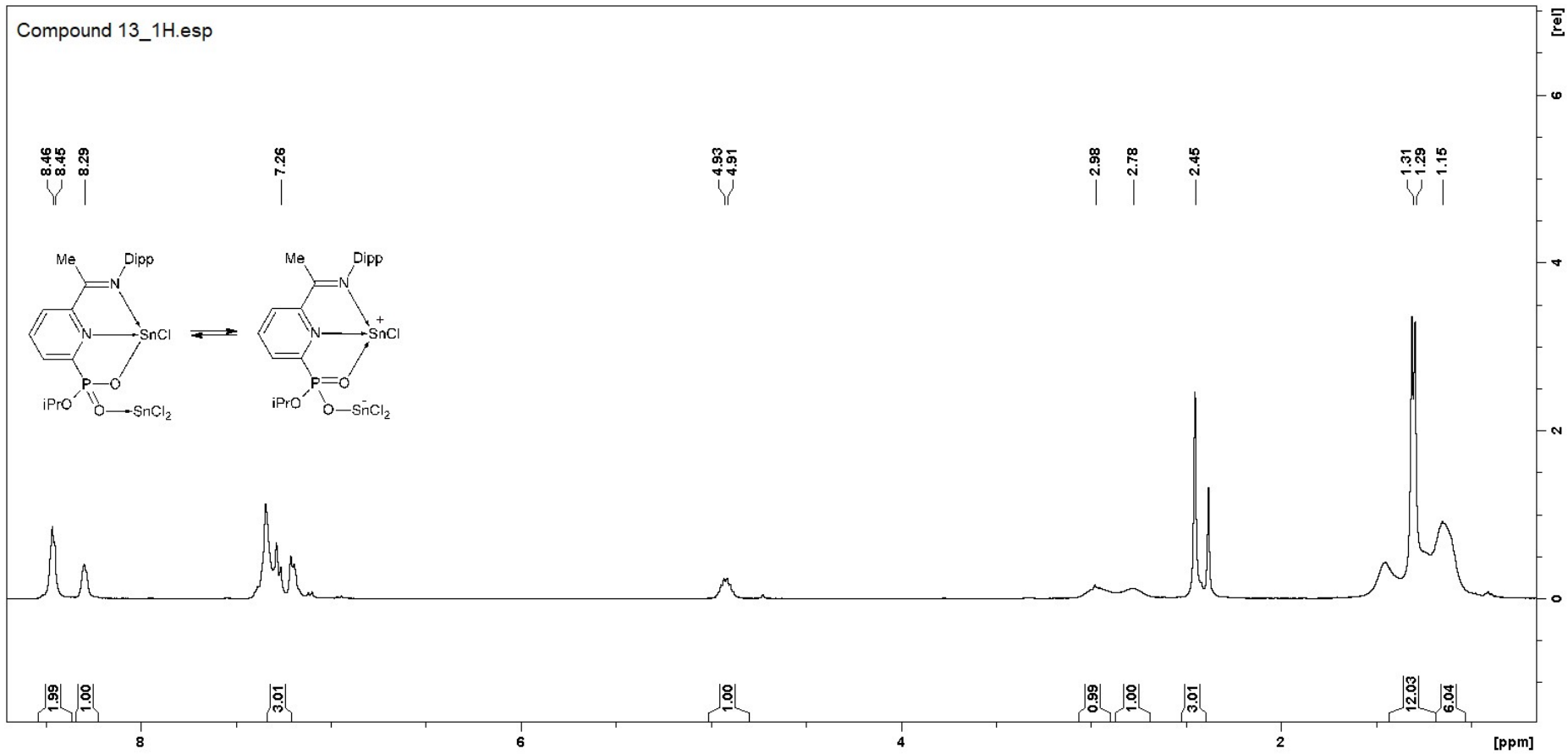


Figure S70. ^1H NMR spectrum of **13** in CDCl_3 .

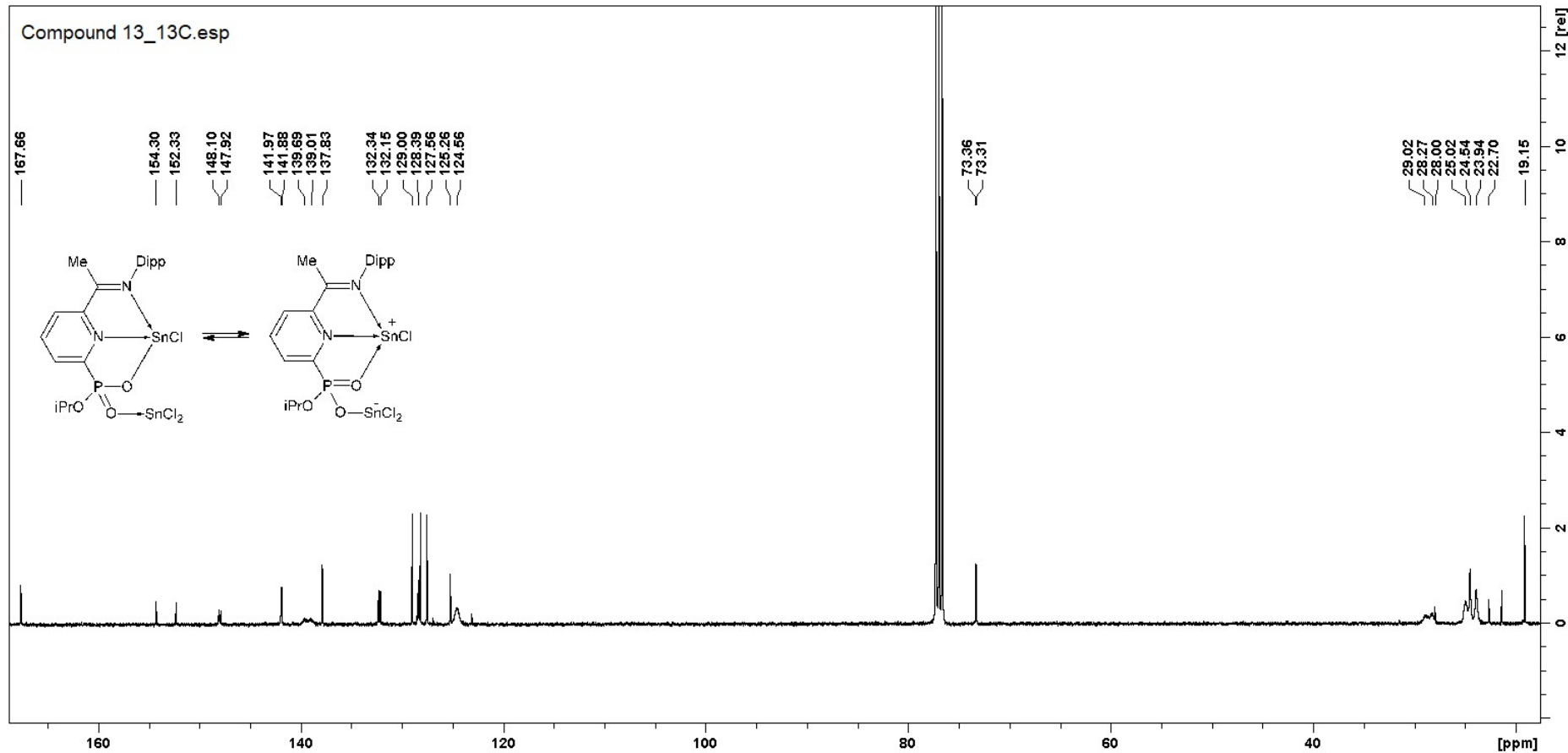


Figure S71. ^{13}C NMR spectrum of **13** in CDCl_3 .

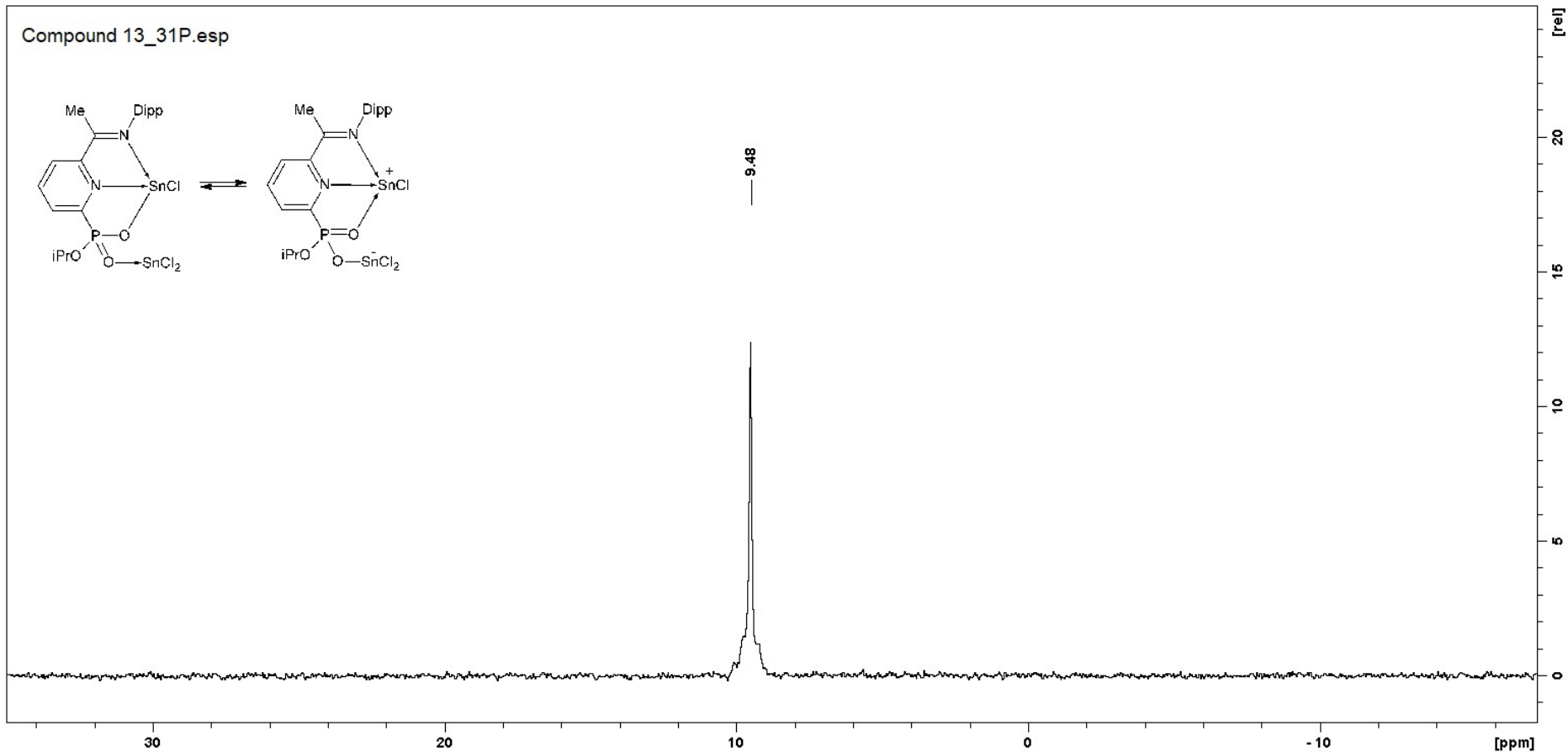


Figure S72. ^{31}P NMR spectrum of **13** in CDCl_3 .

Compound 13_119Sn.esp

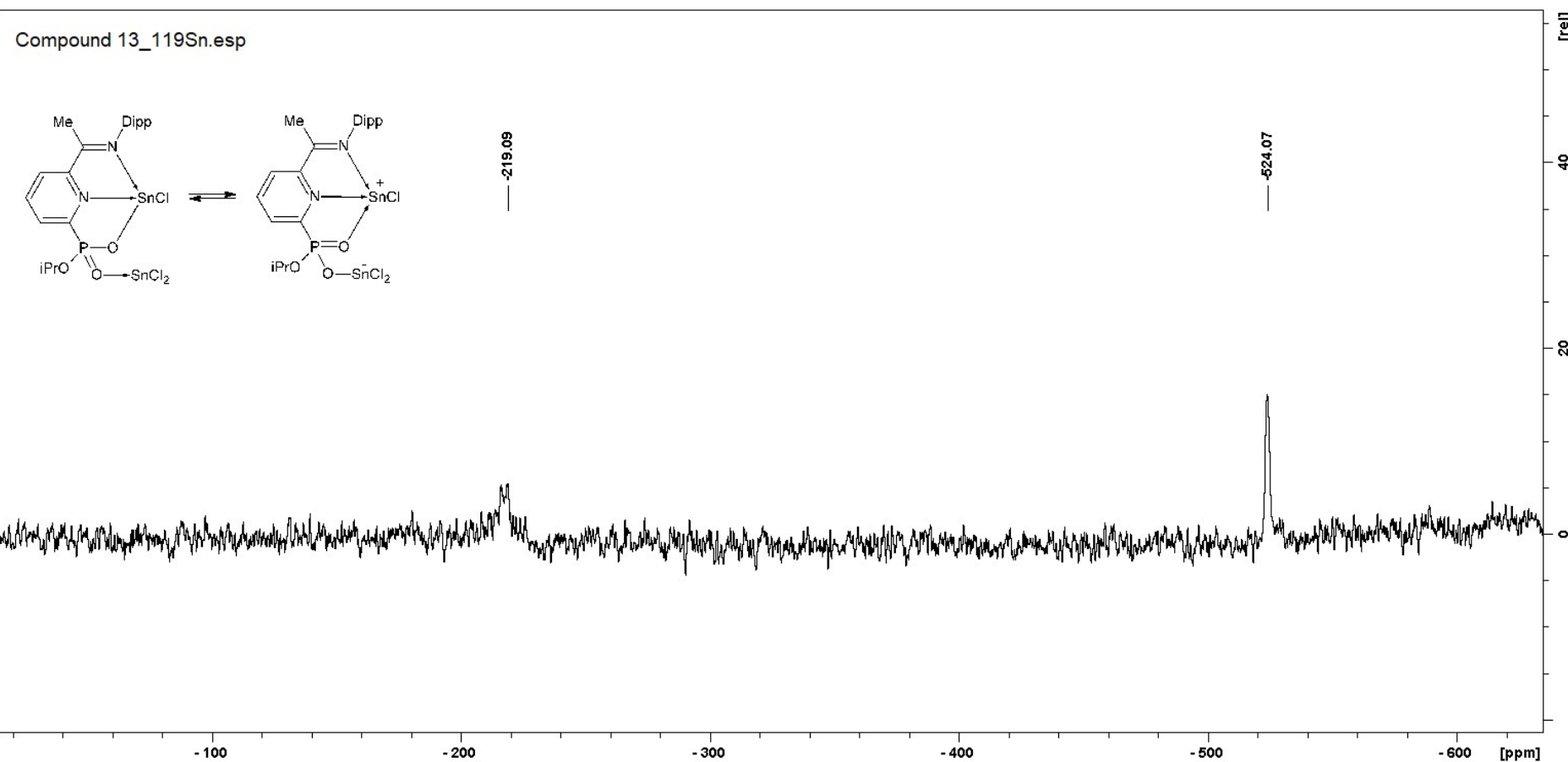


Figure S73. ^{119}Sn NMR spectrum of 13 in CDCl_3 .

References

- [S1] Gaussian 16, Revision A.03, M. J. Frisch, G. W. Trucks, H. B. Schlegel, G. E. Scuseria, M. A. Robb, J. R. Cheeseman, G. Scalmani, V. Barone, G. A. Petersson, H. Nakatsuji, X. Li, M. Caricato, A. V. Marenich, J. Bloino, B. G. Janesko, R. Gomperts, B. Mennucci, H. P. Hratchian, J. V. Ortiz, A. F. Izmaylov, J. L. Sonnenberg, D. Williams-Young, F. Ding, F. Lipparini, F. Egidi, J. Goings, B. Peng, A. Petrone, T. Henderson, D. Ranasinghe, V. G. Zakrzewski, J. Gao, N. Rega, G. Zheng, W. Liang, M. Hada, M. Ehara, K. Toyota, R. Fukuda, J. Hasegawa, M. Ishida, T. Nakajima, Y. Honda, O. Kitao, H. Nakai, T. Vreven, K. Throssell, J. A. Montgomery, Jr., J. E. Peralta, F. Ogliaro, M. J. Bearpark, J. J. Heyd, E. N. Brothers, K. N. Kudin, V. N. Staroverov, T. A. Keith, R. Kobayashi, J. Normand, K. Raghavachari, A. P. Rendell, J. C. Burant, S. S. Iyengar, J. Tomasi, M. Cossi, J. M. Millam, M. Klene, C. Adamo, R. Cammi, J. W. Ochterski, R. L. Martin, K. Morokuma, O. Farkas, J. B. Foresman, and D. J. Fox, Gaussian, Inc., Wallingford CT, 2016.
- [S2] Y. Zhao and D. G. Truhlar, *Theor. Chem. Acc.*, 2008, **120**, 215.
- [S3] (a) T. H. Dunning, *J. Chem. Phys.*, 1989, **90**, 1007; (b) D. E. Woon and T. H. Dunning, *J. Chem. Phys.*, 1993, **98**, 1358.
- [S4] (a) B. Metz, H. Stoll and M. Dolg, *J. Chem. Phys.*, 2000, **113**, 2563; (b) K. A. Peterson, *J. Chem. Phys.*, 2003, **119**, 11099.
- [S5] A. V. Marenich, C. J. Cramer and D. G. Truhlar, *J. Phys. Chem. B*, 2009, **113**, 6378.
- [S6] (a) J. P. Foster and F. Weinhold, *J. Am. Chem. Soc.*, 1980, **102**, 7211; (b) F. Weinhold, *J. Comput. Chem.*, 2012, **33**, 2363, and references therein; (c) C. R. Landis and F. Weinhold, in *The Chemical Bond: Fundamental Aspects of Chemical Bonding*, ed. G. Frenking and S. Shaik, Wiley-VCH, Weinheim, 2014, ch. 3, pp. 91-120.
- [S7] K. B. Wiberg, *Tetrahedron*, 1968, **24**, 1083.
- [S8] NBO 7.0, E. D. Glendening, J. K. Badenhoop, A. E. Reed, J. E. Carpenter, J. A. Bohmann, C. M. Morales, P. Karafiloglou, C. R. Landis, and F. Weinhold, Theoretical Chemistry Institute, University of Wisconsin, Madison, 2018.
- [S9] (a) T. Ziegler and A. Rauk, *Theor. Chim. Acta*, 1977, **46**, 1; (b) T. Ziegler and A. Rauk, *Inorg. Chem.*, 1979, **18**, 1558; (c) T. Ziegler and A. Rauk, *Inorg. Chem.*, 1979, **18**, 1755; (d) F. M. Bickelhaupt and E. J. Baerends, in *Reviews in Computational Chemistry*, ed. K. B. Lipkowitz and D. B. Boyd, Wiley, New York, 2000, vol. 15, ch. 1, pp. 1-86.
- [S10] (a) E. van Lenthe, E. J. Baerends and J. G. Snijders, *J. Chem. Phys.*, 1993, **99**, 4597; (b) E. van Lenthe, E. J. Baerends and J. G. Snijders, *J. Chem. Phys.*, 1994, **101**, 9783; (c) E. van Lenthe, A. E. Ehlers and E. J. Baerends, *J. Chem. Phys.*, 1999, **110**, 8943.
- [S11] (a) E. van Lenthe and E. J. Baerends, *J. Comput. Chem.*, 2003, **24**, 1142; (b) D. P. Chong, E. van Lenthe, S. J. A. van Gisbergen and E. J. Baerends, *J. Comput. Chem.*, 2004, **25**, 1030; (c) D. P. Chong, *Mol. Phys.*, 2005, **103**, 749.
- [S12] (a) G. te Velde, F. M. Bickelhaupt, E. J. Baerends, C. Fonseca Guerra, S. J. A. van Gisbergen, J. G. Snijders and T. Ziegler, Chemistry with ADF, *J. Comput. Chem.*, 2001, **22**, 931; (b) AMS/ADF 2020.1, SCM, Theoretical Chemistry, Vrije Universiteit, Amsterdam, The Netherlands, <http://www.scm.com>.
- [S13] (a) A. Poater, B. Cosenza, A. Correa, S. Giudice, F. Ragone, V. Scarano and L. Cavallo, *Eur. J. Inorg. Chem.*, 2009, 1759; (b) L. Falivene, Z. Cao, A. Petta, L. Serra, A. Poater, R. Oliva, V. Scarano and L. Cavallo, *Nat. Chem.*, 2019, **11**, 872.
- [S14] Y. Zhao and D. G. Truhlar, *J. Phys. Chem. A*, 2005, **109**, 5656.
- [S15] (a) B. Metz, H. Stoll and M. Dolg, *J. Chem. Phys.*, 2000, **113**, 2563; (b) F. Weigend, F. Furche and R. Ahlrichs, *J. Chem. Phys.*, 2003, **119**, 12753; (c) F. Weigend and R.

Ahlichhs, *Phys. Chem. Chem. Phys.*, 2005, **7**, 3297; (d) F. Weigend, *Phys. Chem. Chem. Phys.*, 2006, **8**, 1057.

- [S16] P. Erdmann, J. Leitner, J. Schwarz and L. Greb, *ChemPhysChem*, 2020, **21**, 987.